

# Proximal Interacting Particle Langevin Algorithms

Paula Cordero Encinar<sup>1</sup>, Francesca R. Crucinio<sup>2</sup>, and O. Deniz Akyildiz<sup>1</sup>

<sup>1</sup>Imperial College London

<sup>2</sup>King's College London

October 21, 2024

## Abstract

We introduce a class of algorithms, termed Proximal Interacting Particle Langevin Algorithms (PIPLA), for inference and learning in latent variable models whose joint probability density is non-differentiable. Leveraging proximal Markov chain Monte Carlo (MCMC) techniques and the recently introduced interacting particle Langevin algorithm (IPLA), we propose several variants within the novel proximal IPLA family, tailored to the problem of estimating parameters in a non-differentiable statistical model. We prove nonasymptotic bounds for the parameter estimates produced by the different algorithms in the strongly log-concave setting and provide comprehensive numerical experiments on various models to demonstrate the effectiveness of the proposed methods. In particular, we demonstrate the utility of our family of algorithms on a toy hierarchical example where our assumptions can be checked, as well as for sparse Bayesian logistic regression, training of sparse Bayesian neural networks, and sparse matrix completion. Our theory and experiments together show that PIPLA family can be the de facto choice for parameter estimation problems in non-differentiable latent variable models.

## 1 Introduction

Latent variable models (LVMs) are a crucial class of probabilistic models which are widely used in machine learning and computational statistics in multiple applications such as image, audio, and text modelling as well as in the analysis of biological data [Bishop, 2006; Murphy, 2012]. LVMs have demonstrated great success at capturing (often interpretable) latent structure in data and are widely used across different scientific disciplines such as psychology and social sciences [Bollen, 2002; Marsh and Hau, 2007], ecology [Ovaskainen et al., 2016], epidemiology [Chavance et al., 2010; Muthén, 1992] and climate sciences [Christensen and Sain, 2012].

An LVM can be described as compactly as a parametrised joint probability distribution  $p_\theta(x, y)$  (to be specified precisely later), where  $\theta$  is a set of static parameters,  $x$  denotes latent (unobserved, hidden, or missing) variables, and finally  $y$  denotes (fixed) observed data. Given an LVM, there are two fundamental, intertwined statistical estimation tasks: (i) inference, which involves estimating the latent variables given the observed data and the model parameters through the computation of the posterior distribution  $p_\theta(x|y)$ , and (ii) learning, which involves estimating the model parameters  $\theta$  given the observed data  $y$  through the computation and maximisation of the marginal likelihood  $p_\theta(y)$ . These problems often need to be solved simultaneously. In particular, the learning problem is often termed maximum marginal likelihood estimation (MMLE) in the computational statistics literature, and the main challenge of learning in LVMs is that the marginal likelihood is often intractable to compute as we clarify below.

The marginal likelihood  $p_\theta(y)$  (also called the *model evidence* [Bernardo and Smith, 2009]) in an LVM can be expressed as an integral,  $p_\theta(y) = \int p_\theta(x, y)dx$ , over the latent variables. Hence the task of learning in an LVM can be compactly described as solving the following optimisation problem

$$\bar{\theta}_\star \in \arg \max_{\theta \in \Theta} p_\theta(y) = \arg \max_{\theta \in \Theta} \int p_\theta(x, y)dx, \quad (1)$$

where  $\Theta$  is the parameter space (which will be  $\mathbb{R}^{d_\theta}$  in our setting throughout). A classical algorithm for this setting is the celebrated expectation-maximisation (EM) algorithm [Dempster et al., 1977], which was first proposed in the context of missing data. The EM algorithm is an iterative procedure consisting of two main steps. Given a parameter estimate  $\theta_k$ , the expectation step (henceforth E-step) computes the expected value of the log likelihood function  $\log p_\theta(x, y)$  with respect to the current conditional distribution for the latent variables given the observed data  $p_{\theta_k}(x|y)$ , i.e.,  $Q(\theta, \theta_k) = \mathbb{E}_{p_{\theta_k}(x|y)}[\log p_\theta(x, y)]$ . The second step is a maximisation step (henceforth M-step) which consists of maximising the expectation computed in the E-step. The EM algorithm, when it can be implemented exactly, builds a sequence of parameter estimates  $(\theta_k)_{k \in \mathbb{N}}$  where  $\theta_k \in \arg \max_\theta Q(\theta, \theta_{k-1})$ , which monotonically increase the marginal likelihood, i.e.,  $\log p_{\theta_k}(y) \geq \log p_{\theta_{k-1}}(y)$  [Dempster et al., 1977].

The wide use of the EM algorithm is due to the fact that it can be implemented using approximations for both steps [Lange, 1995; Meng and Rubin, 1993; Wei and Tanner, 1990], leveraging significant advances in Monte Carlo methods and numerical optimisation techniques. In some classes of models, it is possible to analytically derive  $p_\theta(x|y)$  for fixed  $\theta$ , which allows an exact (unbiased) Monte Carlo approximation for the E-step [Wei and Tanner, 1990]. The M-step is generally performed by numerical optimisation methods, most notably gradient descent [Meng and Rubin, 1993].

When sampling from the posterior distribution is feasible, then the resulting algorithm is a form of stochastic approximation procedure with unbiased gradients, which is often amenable to analysis [Delyon et al., 1999]. However, in most interesting modern statistical models in machine learning, such posterior distributions are intractable. This issue can be circumvented by designing Markov chain Monte Carlo (MCMC) samplers for the E-step in practice. This has led to significant developments, where Markov kernels based on the unadjusted Langevin algorithm (ULA) [Durmus and Moulines, 2017; Roberts and Tweedie, 1996] have become a widespread choice in high dimensional setting thanks to their favourable theoretical properties [Chewi et al., 2022; Dalalyan, 2017; De Bortoli et al., 2021; Durmus and Moulines, 2019; Vempala and Wibisono, 2019]. Recently, Kuntz et al. [2023] explore an alternative approach based on Neal and Hinton [1998], where they exploit the fact that the EM algorithm is equivalent to performing coordinate descent of a free energy functional, whose minimum is the maximum likelihood estimate of the latent variable model. They propose several interacting particle algorithms to address the optimisation problem. This method has led to many subsequent works including Akyildiz et al. [2023]; Caprio et al. [2024]; Gruffaz et al. [2024]; Johnston et al. [2024]; Lim et al. [2024]; Sharrock et al. [2024] and ours.

**Contribution.** In this work, we deal with models whose joint probability density is non-differentiable, exploiting the use of proximal methods [Combettes and Pesquet, 2011; Parikh and Boyd, 2014]. In the classical sampling case, this setting has been considered in a significant body of works, e.g., Atchadé et al. [2017]; Bernton [2018]; Chen et al. [2022]; Crucinio et al. [2023]; Diao et al. [2023]; Durmus et al. [2018]; Lee et al. [2021]; Pereyra [2016]; Salim and Richtarik [2020]; Salim et al. [2019] due to significant applications in machine learning, most notably in the use of non-differentiable regularisers. For example, this type of models naturally arises when including sparsity-inducing penalties, such as Laplace priors for regression problems or in the context of Bayesian neural networks [Williams, 1995; Yun et al., 2019], and total variation priors in image processing [Durmus et al., 2018].

Specifically, we summarise our contributions below.

- We develop the first proximal interacting particle Langevin algorithm family. Similar algorithms so far are investigated in the usual differentiable setting [Akyildiz et al., 2023; Johnston et al., 2024; Kuntz et al., 2023]. We extend these methods to the non-differentiable setting via the use of proximal techniques. Specifically, we propose two main algorithms, termed Moreau-Yosida interacting particle Langevin algorithm (MYIPLA) and proximal interacting particle gradient Langevin algorithm (PIPLA).
- We provide theoretical analysis of the developed methods. We also provide, for comparisons, proximal extensions of the methods proposed in Kuntz et al. [2023], termed Moreau-Yosida particle gradient descent (MYPGD) and provide a full theoretical analysis under this setting.
- We implement our methods for a variety of examples within toy and realistic settings and demonstrate that the proximal interacting particle Langevin algorithms (PIPLA) family is a viable option for the MMLE problem - similar to the unadjusted Langevin algorithm (ULA) for sampling.

This paper is organised as follows. In Section 2, we present the technical background necessary to develop our methods. In Section 3, we introduce the proposed algorithms—we provide their theoretical analysis in Section 4. Finally, in Section 5, we show comprehensive numerical experiments and we conclude with Section 6. The code is available in the GitHub repository: <https://github.com/paulaoak/proximal-ipla>.

## 1.1 Notation

We endow  $\mathbb{R}^d$  with the Borel  $\sigma$ -field  $\mathcal{B}(\mathbb{R}^d)$  with respect to the Euclidean norm  $\|\cdot\|$  when  $d$  is clear from context.  $\mathcal{N}(x|\mu, \Sigma)$  is the multivariate Gaussian of specified mean and variance,  $I$  is the identity matrix of appropriate dimension when clear from context, and  $\mathcal{U}(x|a, b)$  is a uniform distribution with specified minimum and maximum values.  $\mathcal{C}^1$  denotes the space of continuously differentiable functions. For all differentiable functions  $f$ , we denote the gradient by  $\nabla f$ . We denote by  $\mathcal{P}(\mathbb{R}^d)$  the set of probability measures over  $\mathcal{B}(\mathbb{R}^d)$  and endow this space with the topology of weak convergence. For all  $p \geq 1$ , we denote by  $\mathcal{P}_p(\mathbb{R}^d) = \{\pi \in \mathcal{P}(\mathbb{R}^d) : \int_{\mathbb{R}^d} \|x\|^p d\pi(x) < +\infty\}$  the set of probability measures over  $\mathcal{B}(\mathbb{R}^d)$  with finite  $p$ -th moment. For any  $\mu, \nu \in \mathcal{P}_2(\mathbb{R}^d)$  we define the 2-Wasserstein distance  $W_2(\mu, \nu)$  between  $\mu$  and  $\nu$  by

$$W_2(\mu, \nu) = \left( \inf_{\gamma \in \mathbf{T}(\mu, \nu)} \int_{\mathbb{R}^d \times \mathbb{R}^d} \|x - y\|^2 d\gamma(x, y) \right)^{1/2}$$

where  $\mathbf{T}(\mu, \nu) = \{\gamma \in \mathcal{P}(\mathbb{R}^d \times \mathbb{R}^d) : \gamma(A \times \mathbb{R}^d) = \mu(A), \gamma(\mathbb{R}^d \times A) = \nu(A) \forall A \in \mathcal{B}(\mathbb{R}^d)\}$  denotes the set of all transport plans between  $\mu$  and  $\nu$ . In the following, we metrize  $\mathcal{P}_2(\mathbb{R}^d)$  with  $W_2$ .

## 2 Background

In this section, we introduce background material on Langevin dynamics and proximal methods. We also provide a brief overview of the recent literature on particle-based algorithms for MMLE in latent variable models.

### 2.1 Langevin Dynamics

At the core of our approach is the use of Langevin diffusion processes [Roberts and Tweedie, 1996], which are highly popular for building advanced sampling algorithms. To describe briefly, the Langevin stochastic differential equation (SDE) is given by

$$d\mathbf{X}_t = -\nabla U(\mathbf{X}_t)dt + \sqrt{2}d\mathbf{B}_t, \quad (2)$$

where  $U : \mathbb{R}^d \rightarrow \mathbb{R}$  is a continuously differentiable function and  $(\mathbf{B}_t)_{t \geq 0}$  is a  $d$ -dimensional Brownian motion [Pavliotis, 2014]. Under mild assumptions, (2) has a strong solution and  $\pi(x) \propto e^{-U(x)}$  is the unique invariant distribution of the semigroup associated with the SDE [Pavliotis, 2014]. In most cases it is not possible to solve (2) analytically; however, we can resort to a discrete-time Euler-Maruyama approximation with step size  $\gamma$  which gives the following Markov chain

$$X_{n+1} = X_n - \gamma \nabla U(X_n) + \sqrt{2\gamma} \xi_{n+1}, \quad (3)$$

where  $(\xi_n)_{n \in \mathbb{N}}$  is a sequence of i.i.d.  $d$ -dimensional standard Gaussian random variables. In the sampling literature, the algorithm (3) is known as the unadjusted Langevin algorithm (ULA) [Durmus and Moulines, 2019]. When  $U$  is  $\mu$ -strongly convex and  $L$ -smooth (i.e.  $\nabla U(x)$  is  $L$ -Lipschitz), ULA has very favourable properties. In particular, it can be shown that ULA converges to its own (biased) limit  $\pi^\gamma$  exponentially fast, and that the asymptotic bias is of order  $\gamma^{1/2}$  [Durmus and Moulines, 2019]. This makes ULA a favourable alternative to the Metropolis-adjusted Langevin algorithm (MALA) - which is asymptotically exact - because ULA does not require the computation of acceptance ratios and is cheaper in high dimensions [Durmus and Moulines, 2019].

## 2.2 MMLE with Langevin Dynamics

While Langevin dynamics and ULA, as described above, are a powerful tool for sampling from a given target measure  $\pi$  such as a posterior distribution arising from a statistical model, powerful samplers are not enough in real applications as statistical models often have unknown parameters. In this case, it is necessary to combine the sampling methods with optimisation techniques to learn the parameters.

Given a statistical model  $p_\theta(x, y) : \mathbb{R}^{d_\theta} \times \mathbb{R}^{d_x} \rightarrow \mathbb{R}$  with latent variables  $x$  and parameters  $\theta$  (assuming the observed data  $y$  is fixed), a typical task for finding the optimal parameter is to maximise the marginal likelihood, i.e., solving the following problem

$$\bar{\theta}_* \in \arg \max_{\theta \in \Theta} p_\theta(y) = \arg \max_{\theta \in \Theta} \int_{\mathbb{R}^{d_x}} p_\theta(x, y) dx. \quad (4)$$

As mentioned in the introduction, classical techniques such as the EM algorithm are available for this task, however, they typically require many intermediate approximations which obscure their theoretical properties.

A recent approach is to build an extended stochastic dynamical system which can be run in the space  $\mathbb{R}^{d_\theta} \times \mathbb{R}^{d_x}$ , with the aim of jointly solving the problem of latent variable sampling and parameters optimisation. In this avenue, Kuntz et al. [2023] first proposed a method termed *particle gradient descent* (PGD) which build on the observation made in Neal and Hinton [1998], that the EM algorithm can be expressed as a minimisation problem of the free-energy objective (see Appendix B.1 for details). By constructing the gradient flow w.r.t. this functional, Kuntz et al. [2023] arrive at the following system of SDEs

$$\begin{aligned} d\theta_t^N &= -\frac{1}{N} \sum_{i=1}^N \nabla_\theta U(\theta_t^N, \mathbf{X}_t^{i,N}) dt, \\ d\mathbf{X}_t^{i,N} &= -\nabla_x U(\theta_t^N, \mathbf{X}_t^{i,N}) dt + \sqrt{2} d\mathbf{B}_t^{i,N}, \quad i = 1, \dots, N, \end{aligned}$$

where  $(\mathbf{B}_t^{i,N})_{t \geq 0}$  is a family of independent Brownian motions. The algorithm can be efficiently implemented using an Euler-Maruyama scheme. While the original paper does not contain a nonasymptotic analysis of the resulting discretisation, recently Caprio et al. [2024] have provided a nonasymptotic analysis of the algorithm under strong-convexity and Lipschitz continuity of  $U$ .

Inspired by this approach, Akyildiz et al. [2023] propose an interacting Langevin SDE

$$\begin{aligned} d\theta_t^N &= -\frac{1}{N} \sum_{i=1}^N \nabla_\theta U(\theta_t^N, \mathbf{X}_t^{i,N}) dt + \sqrt{\frac{2}{N}} d\mathbf{B}_t^{0,N}, \\ d\mathbf{X}_t^{i,N} &= -\nabla_x U(\theta_t^N, \mathbf{X}_t^{i,N}) dt + \sqrt{2} d\mathbf{B}_t^{i,N}, \quad i = 1, \dots, N, \end{aligned} \quad (5)$$

where  $(\mathbf{B}_t^{i,N})_{t \geq 0}$  is a family of independent Brownian motions. The main difference with Kuntz et al. [2023] is the noise term in the dynamics of  $\theta$ . This makes the system of SDEs a particular instance of a Langevin SDE, for which well-known tools and techniques can be leveraged for analysis. It is also argued that the added noise may help the method to escape local minima in nonconvex settings [Akyildiz et al., 2023]. Discretising (5), we obtain the interacting particle Langevin algorithm (IPLA)

$$\begin{aligned} \theta_{n+1} &= \theta_n - \frac{\gamma}{N} \sum_{j=1}^N \nabla_\theta U(\theta_n, X_n^{j,N}) + \sqrt{\frac{2\gamma}{N}} \xi_{n+1}^{0,N}, \\ X_{n+1}^{i,N} &= X_n^{i,N} - \gamma \nabla_x U(\theta_n, X_n^{i,N}) + \sqrt{2\gamma} \xi_{n+1}^{i,N}, \end{aligned}$$

where  $(\xi_n^{i,N})_{n \in \mathbb{N}}$  are i.i.d. standard Gaussian random variables of the corresponding dimension for all  $i = 0, 1, \dots, N$ . Under Lipschitz continuity and strong-convexity of  $U$ , IPLA has been shown to enjoy favourable convergence properties [Akyildiz et al., 2023].

Since both methods are proposed for differentiable  $U$ , both of these methods become inapplicable when  $U$  is non-differentiable. In this paper, we propose a new class of algorithms, termed Proximal Interacting Particle Langevin Algorithms (PIPLA), which can be applied when the joint density of the model is non-differentiable.

## 2.3 Proximal Markov chain Monte Carlo

The last component we need to build parameter estimation methods in a non-differentiable setting is the well-known set of algorithms termed Proximal MCMC methods [Durmus et al., 2018, 2019; Ehrhardt et al., 2023; Habring et al., 2023; Klatzer et al., 2023; Pereyra, 2016]. These methods leverage a powerful set of techniques termed proximal methods [Combettes and Pesquet, 2011; Parikh and Boyd, 2014] to handle the non-differentiability present in the target distribution.

The main idea behind proximal methods is to use proximity mappings of convex functions, instead of gradient mappings, to construct fixed point schemes and compute function minima [Combettes and Pesquet, 2011; Parikh and Boyd, 2014]. Constructing these iterative rules is made possible by the proximity operator, which is defined as follows.

**Definition 2.1** (Proximity mappings). *The  $\lambda$ -proximity mapping or proximal operator function of  $U$  is defined for any  $\lambda > 0$  as*

$$\text{prox}_U^\lambda(x) := \arg \min_{z \in \mathbb{R}^d} \{U(z) + \|z - x\|^2/(2\lambda)\}.$$

Intuitively, the proximity operator  $x \mapsto \text{prox}_U^\lambda(x)$  behaves similarly to a gradient mapping and moves points in the direction of the minimisers of  $U$ . In fact, when  $U$  is differentiable, the proximal mapping corresponds to the implicit gradient step, as opposed to the explicit gradient step, which is known to be more stable [Parikh and Boyd, 2014]. In the limit  $\lambda \rightarrow 0$  the quadratic penalty term dominates and the proximity operator coincides with the identity operator, i.e.,  $\text{prox}_U^\lambda(x) = x$ ; in the limit  $\lambda \rightarrow \infty$ , the quadratic penalty term vanishes and the proximity mapping maps all points to the set of minimisers of  $U$ .

Consider a target density of the form  $\pi(x) = \exp(-U(x))/Z$  where  $U : \mathbb{R}^n \rightarrow [0, \infty)$  is a convex lower semi-continuous function satisfying  $\lim_{\|x\| \rightarrow \infty} U(x) = \infty$  and  $Z$  is an unknown normalising constant. The main idea of proximal methods is to approximate the non-differentiable but log-concave target density  $\pi \propto \exp(-U)$  by substituting the potential  $U$  with a smooth approximation  $U^\lambda$  whose level of smoothness is controlled by the proximal parameter  $\lambda > 0$  [Durmus et al., 2018; Pereyra, 2016]. The proximity map (Definition 2.1) allows us to define a family of approximations to  $\pi$ , indexed by  $\lambda$  and referred to as Moreau-Yosida approximation. We provide below the definition of Moreau-Yosida approximations  $U^\lambda$  and the corresponding approximations to the target density  $\pi_\lambda$ .

**Definition 2.2** (Moreau-Yosida approximation [Moreau, 1965]). For any  $\lambda > 0$ , define the  $\lambda$ -Moreau-Yosida approximation of  $U$  as

$$U^\lambda(x) := \min_{z \in \mathbb{R}^d} \{U(z) + \|z - x\|^2/(2\lambda)\} = U(\text{prox}_U^\lambda(x)) + \|\text{prox}_U^\lambda(x) - x\|^2/(2\lambda).$$

Consequently, we define the  $\lambda$ -Moreau-Yosida approximation of  $\pi$  as the following density  $\pi_\lambda(x) \propto \exp(-U^\lambda(x))$ .

The approximation  $\pi_\lambda$  converges to  $\pi$  as  $\lambda \rightarrow 0$  (Rockafellar and Wets [2009, Theorem 1.25] and Durmus et al. [2018, Proposition 1]) and is differentiable even if  $\pi$  is not, with log-gradient

$$\nabla \log \pi_\lambda(x) = -\nabla U^\lambda(x) = (\text{prox}_U^\lambda(x) - x)/\lambda \quad (6)$$

(Rockafellar and Wets [2009, Example 10.32, Theorem 9.18]). Since  $\pi_\lambda$  is now continuously differentiable, it has been suggested in Durmus et al. [2018]; Pereyra [2016] to use the discretisation of the Langevin diffusion associated with  $\pi_\lambda$  given by

$$d\mathbf{X}_{\lambda,t} = \nabla \log \pi_\lambda(\mathbf{X}_{\lambda,t})dt + \sqrt{2}d\mathbf{B}_t, \quad (7)$$

to approximately sample from  $\pi$ . Using (6) we can write the above as

$$d\mathbf{X}_{\lambda,t} = \lambda^{-1}(\text{prox}_U^\lambda(\mathbf{X}_{\lambda,t}) - \mathbf{X}_{\lambda,t})dt + \sqrt{2}d\mathbf{B}_t.$$

In this paper, we consider two classes of proximal Langevin algorithms, obtained by considering different ways to discretise (7): those obtained considering Euler–Maruyama discretisations [Durmus et al., 2018; Pereyra, 2016], and those based on splitting schemes [Durmus et al., 2019; Ehrhardt et al., 2023; Habring et al., 2023; Klatzer et al., 2023; Salim et al., 2019].

### 2.3.1 Proximal Langevin methods

Applying a simple Euler–Maruyama discretisation with time discretisation step  $\gamma > 0$  to (7), we obtain

$$X_{n+1} = \left(1 - \frac{\gamma}{\lambda}\right)X_n + \frac{\gamma}{\lambda} \text{prox}_U^\lambda(X_n) + \sqrt{2\gamma} \xi_{n+1} \quad (8)$$

for  $n \geq 0$ , where  $(\xi_n)$  is a sequence of i.i.d.  $d$ -dimensional standard Gaussians.

Pereyra [2016] proposes the proximal unadjusted Langevin algorithm (PULA) to sample from  $\pi$ , which corresponds to setting  $\lambda = \gamma$  in (8)

$$X_{n+1} = \text{prox}_U^\gamma(X_n) + \sqrt{2\gamma} \xi_{n+1},$$

for  $n \geq 0$ , where  $(\xi_n)$  are i.i.d. standard Gaussians. The computational performance of the algorithm depends strongly on the capacity to evaluate efficiently  $\text{prox}_U^\gamma$ .

In the case where  $U$  can be expressed as  $U(x) = g_1(x) + g_2(x)$ , with  $g_1, g_2$  lower bounded functions,  $g_1 \in \mathcal{C}^1$  convex and gradient Lipschitz, and  $g_2$  proper, convex and lower semi-continuous, Durmus et al. [2018] propose to define  $U^\lambda(x) = g_1(x) + g_2^\lambda(x)$ . In that case, (7) can be rewritten as

$$d\mathbf{X}_{\lambda,t} = -(\nabla g_1(\mathbf{X}_{\lambda,t}) + \nabla g_2^\lambda(\mathbf{X}_{\lambda,t}))dt + \sqrt{2}d\mathbf{B}_t,$$

for  $t \geq 0$ . Using (6) for  $g_2^\lambda$ , we can write the above as

$$d\mathbf{X}_{\lambda,t} = -\nabla g_1(\mathbf{X}_{\lambda,t}) + \lambda^{-1}(\text{prox}_{g_2}^\lambda(\mathbf{X}_{\lambda,t}) - \mathbf{X}_{\lambda,t})dt + \sqrt{2}d\mathbf{B}_t.$$

Using a simply Euler–Maruyama discretisation with time step  $\gamma > 0$ , the above leads to the Moreau–Yosida ULA (MYULA) algorithm

$$X_{n+1} = \left(1 - \frac{\gamma}{\lambda}\right)X_n - \gamma \nabla g_1(X_n) + \frac{\gamma}{\lambda} \text{prox}_{g_2}^\lambda(X_n) + \sqrt{2\gamma} \xi_{n+1},$$

for  $n \geq 0$ . Under some regularity conditions on  $g_1$  and  $g_2$ , Durmus et al. [2018, Theorem 3] establish rigorous bounds on the convergence of the resulting Markov chain.

### 2.3.2 Proximal gradient MCMC methods

Another class of proximal sampling algorithms are based on the idea that in the case  $U(x) = g_1(x) + g_2(x)$  with  $g_1$  smooth and  $g_2$  proper, convex and lower semi-continuous one can employ splitting schemes to modify the gradient in the ULA update (3).

Inspired by the proximal gradient algorithm (see, e.g., Parikh and Boyd [2014, Section 4.2] or Combettes and Pesquet [2011]), which provides a forward-backward splitting optimisation algorithm, Salim et al. [2019] present a sampling algorithm composed of a forward step for  $g_1$  with the addition of a stochastic term (corresponding to one step of ULA with target  $\exp(-g_1)$ ) and a backward step using the proximity map of  $g_2$

$$\begin{aligned} X_{n+1/2} &= X_n - \gamma \nabla g_1(X_n) + \sqrt{2\gamma} \xi_{n+1} \\ X_{n+1} &= \text{prox}_{g_2}^\lambda(X_{n+1/2}), \end{aligned}$$

where  $(\xi_n)_{n \in \mathbb{N}}$  is a sequence of i.i.d.  $d$ -dimensional standard Gaussians and  $\gamma$  is the time discretisation step. Combining all the steps we obtain the proximal gradient Langevin algorithm (PGLA)

$$X_{n+1} = \text{prox}_{g_2}^\lambda \left( X_n - \gamma \nabla g_1(X_n) + \sqrt{2\gamma} \xi_{n+1} \right).$$

These algorithms were originally proposed as an alternative to MYULA to deal with cases in which  $U$  is the sum of a differentiable likelihood  $g_1$  and a compactly supported  $g_2$ , since the application of the proximity map after the addition of the stochastic term guarantees that  $X_{n+1}$  remains in the support of  $g_2$  [Salim and Richtarik, 2020].

The algorithm is further analysed in Salim and Richtarik [2020]. In addition, Ehrhardt et al. [2023] give conditions under which using an approximate proximity map does not affect numerical results and generalise existing nonasymptotic and asymptotic convergence bounds.

### 3 Proximal Interacting Particle Methods for MMLE

Our goal is to extend the interacting particle algorithms proposed for the MMLE problem (1) to cases where the distribution  $p_\theta(x, y)$  is strongly log-concave in  $\theta$  and  $x$  jointly and may be non-differentiable. To achieve this, we build on the previously presented methodology, where we approximate the target distribution  $\pi \propto \exp(-U) = \exp(-g_1 - g_2)$  with a Moreau-Yosida envelope  $\pi_\lambda$  and we derive a numerical scheme based on the Euler-Maruyama discretisation or we employ a splitting scheme. In particular, inspired by interacting particle algorithms for MMLE [Akyildiz et al., 2023; Kuntz et al., 2023] and proximal Langevin methods, we introduce our methodology and three classes of proximal algorithms for the MMLE problem.

Recall that  $U(\theta, x) = -\log p_\theta(x, y)$  as  $y$  is fixed. We start by a remark which clarifies the meaning of the proximal map in the MMLE setting.

**Remark 3.1.** *In our scenario,  $U$  is a function of  $(\theta, x)$ , therefore, the arg min in the proximal map is taken over both variables, that is,*

$$\begin{aligned} \text{prox}_U^\lambda(\theta, x) &= (\text{prox}_U^\lambda(\theta, x)_\theta, \text{prox}_U^\lambda(\theta, x)_x) \\ &= \arg \min_{z_0 \in \mathbb{R}^{d_\theta}, z \in \mathbb{R}^{d_x}} \left\{ U(z_0, z) + \|(z_0, z) - (\theta, x)\|^2 / (2\lambda) \right\}. \end{aligned}$$

◇

#### 3.1 Proximal Interacting Particle Algorithms

Below we provide a set of algorithms each termed differently, that are based on discretisations of the SDE corresponding to the Moreau-Yosida approximations. We start by introducing the continuous-time interacting SDEs that will be discretised to obtain the algorithms:

$$d\theta_t^N = -\frac{1}{N} \sum_{i=1}^N \nabla_\theta U^\lambda(\theta_t^N, \mathbf{X}_t^{i,N}) dt + \sqrt{\frac{2}{N}} d\mathbf{B}_t^{0,N}, \quad (9)$$

$$d\mathbf{X}_t^{i,N} = -\nabla_x U^\lambda(\theta_t^N, \mathbf{X}_t^{i,N}) dt + \sqrt{2} d\mathbf{B}_t^{i,N}, \quad (10)$$

where  $(\mathbf{B}_t^{i,N})_{t \geq 0}$  for  $i = 0, \dots, N$  are a family of independent Brownian motions and  $U^\lambda$  is the Moreau-Yosida approximation of  $U$ . Next, we will employ different discretisation strategies to obtain algorithms from this set of SDEs. We note that similar strategies will also apply to SDEs proposed in Kuntz et al. [2023], which we will come back to later.

As in the case of the interacting SDE in eq. (5), one can show that (9)–(10) converges to an SDE of the McKean–Vlasov type (MKVSDE) as  $N \rightarrow \infty$ . In particular, if the potential  $U$  is regular enough, the MKVSDE that (9)–(10) approximates becomes arbitrarily close to that approximated by (5) if  $\lambda \rightarrow 0$  (see Appendix C for a proof).

##### 3.1.1 Proximal Interacting Particle Unadjusted Langevin algorithm

Using an Euler-Maruyama discretisation of (9)–(10) and using (6) for  $\nabla U^\lambda$  as in Pereyra [2016], we obtain the following algorithm, that we name *PIPULA* (proximal interacting particle ULA)

$$\theta_{n+1}^N = \frac{1}{N} \sum_{i=1}^N \text{prox}_U^\gamma(\theta_n^N, X_n^{i,N})_\theta + \sqrt{\frac{2\gamma}{N}} \xi_{n+1}^{0,N}, \quad (11)$$

$$X_{n+1}^{i,N} = \text{prox}_U^\gamma(\theta_n^N, X_n^{i,N})_x + \sqrt{2\gamma} \xi_{n+1}^{i,N}. \quad (12)$$

where  $(\xi_n^{i,N})_{n \in \mathbb{N}}$  for  $i = 0, \dots, N$  are i.i.d. standard Gaussians of the appropriate dimension. This algorithm is general and does not exploit any special properties of  $U$ .

---

**Algorithm 1** Moreau-Yosida Interacting Particle Langevin Algorithm (MYIPLA)

---

**Require:**  $N, K, \lambda, \gamma, \pi_{\text{init}} \in \mathcal{P}(\mathbb{R}^{d_\theta}) \times \mathcal{P}((\mathbb{R}^{d_x})^N)$

Draw  $(\theta_0, \{X_0^{i,N}\}_{i=1}^N)$  from  $\pi_{\text{init}}$

**for**  $n = 0 : K$  **do**

$$\theta_{n+1}^N = \left(1 - \frac{\gamma}{\lambda}\right) \theta_n^N + \frac{\gamma}{N} \sum_{i=1}^N \left( -\nabla_{\theta} g_1(\theta_n^N, X_n^{i,N}) + \frac{1}{\lambda} \text{prox}_{g_2}^{\lambda}(\theta_n^N, X_n^{i,N})_{\theta} \right) + \sqrt{\frac{2\gamma}{N}} \xi_{n+1}^{0,N}$$

$$X_{n+1}^{i,N} = \left(1 - \frac{\gamma}{\lambda}\right) X_n^{i,N} - \gamma \nabla_x g_1(\theta_n^N, X_n^{i,N}) + \frac{\gamma}{\lambda} \text{prox}_{g_2}^{\lambda}(\theta_n^N, X_n^{i,N})_x + \sqrt{2\gamma} \xi_{n+1}^{i,N}$$

**end for**

**return**  $\theta_{K+1}^N$

---

### 3.1.2 Moreau-Yosida Interacting Particle Langevin Algorithm

On the other hand, if we consider  $U^{\lambda} = g_1 + g_2^{\lambda}$  as in Durmus et al. [2018], and substitute its gradient in the Euler-Maruyama discretisation of (9)–(10) we obtain *MYIPLA* (Moreau-Yosida interacting particle Langevin algorithm):

$$\theta_{n+1}^N = \left(1 - \frac{\gamma}{\lambda}\right) \theta_n^N + \frac{\gamma}{N} \sum_{i=1}^N \left( -\nabla_{\theta} g_1(\theta_n^N, X_n^{i,N}) + \frac{1}{\lambda} \text{prox}_{g_2}^{\lambda}(\theta_n^N, X_n^{i,N})_{\theta} \right) + \sqrt{\frac{2\gamma}{N}} \xi_{n+1}^{0,N}, \quad (13)$$

$$X_{n+1}^{i,N} = \left(1 - \frac{\gamma}{\lambda}\right) X_n^{i,N} - \gamma \nabla_x g_1(\theta_n^N, X_n^{i,N}) + \frac{\gamma}{\lambda} \text{prox}_{g_2}^{\lambda}(\theta_n^N, X_n^{i,N})_x + \sqrt{2\gamma} \xi_{n+1}^{i,N}, \quad (14)$$

where  $(\xi_n^{i,N})_{n \in \mathbb{N}}$  for  $i = 0, \dots, N$  are i.i.d. standard Gaussians and the notation  $\text{prox}_{g_2}^{\lambda}(\theta, X)_{\theta}$ ,  $\text{prox}_{g_2}^{\lambda}(\theta, X)_x$  refers to the  $\theta$  and  $x$  component of the proximal mapping  $\text{prox}_{g_2}^{\lambda}$ , as mentioned in Remark 3.1. The algorithm is given in Algorithm 1.

### 3.1.3 Proximal Interacting Particle Gradient Langevin Algorithm

In the case in which  $U^{\lambda} = g_1 + g_2^{\lambda}$ , inspired by the proximal gradient method [Ehrhardt et al., 2023; Salim et al., 2019], we employ a splitting scheme to discretise (9)–(10) and obtain *PIPGLA* (proximal interacting particle gradient Langevin algorithm). In this case, we perform one ULA step for both the  $\theta$  and  $x$  component using  $\nabla g_1$  followed by a backward step using  $\text{prox}_{g_2}^{\lambda}$ :

$$\theta_{n+1/2}^N = \theta_n^N - \frac{\gamma}{N} \sum_{i=1}^N \nabla_{\theta} g_1(\theta_n^N, X_n^{i,N}) + \sqrt{\frac{2\gamma}{N}} \xi_{n+1}^{0,N}, \quad (15)$$

$$X_{n+1/2}^{i,N} = X_n^{i,N} - \gamma \nabla_x g_1(\theta_n^N, X_n^{i,N}) + \sqrt{2\gamma} \xi_{n+1}^{i,N}, \quad (16)$$

$$\theta_{n+1}^N = \frac{1}{N} \sum_{i=1}^N \text{prox}_{g_2}^{\lambda} \left( \theta_{n+1/2}^N, X_{n+1/2}^{i,N} \right)_{\theta}, \quad (17)$$

$$X_{n+1}^{i,N} = \text{prox}_{g_2}^{\lambda} \left( \theta_{n+1/2}^N, X_{n+1/2}^{i,N} \right)_x, \quad (18)$$

where  $(\xi_n^{i,N})_{n \in \mathbb{N}}$  for  $i = 0, \dots, N$  are i.i.d. standard Gaussians of appropriate dimension.

Similarly to PGLA, this algorithm ensures that  $X_{n+1}^{i,N}$  belongs to the support of  $g_2$  for all  $i = 1, \dots, N$ ; if the parameter space  $\Theta$  is convex, then also  $\theta_{n+1}^N$  belongs to the support of  $g_2$  since  $\theta_{n+1}^N$  is a convex combination of elements of  $\Theta$ .

Using the relationship  $\text{prox}_{g_2}^{\lambda}(v) = v - \lambda \nabla g_2^{\lambda}(v)$  in (6), we can also write (15) in the following form

$$\theta_{n+1}^N = \theta_n^N - \frac{\gamma}{N} \sum_{j=1}^N \nabla_{\theta} g_1(\theta_n^N, X_n^{j,N}) - \frac{\lambda}{N} \sum_{j=1}^N \nabla_{\theta} g_2^{\lambda}(\theta_{n+1/2}^N, X_{n+1/2}^{j,N}) + \sqrt{\frac{2\gamma}{N}} \xi_{n+1}^{0,N},$$

$$X_{n+1}^{i,N} = X_n^{i,N} - \gamma \nabla_x g_1(\theta_n^N, X_n^{i,N}) - \lambda \nabla_x g_2^{\lambda}(\theta_{n+1/2}^N, X_{n+1/2}^{i,N}) + \sqrt{2\gamma} \xi_{n+1}^{i,N},$$



---

**Algorithm 2** Proximal Interacting Particle Gradient Langevin Algorithm (PIPGLA)

---

**Require:**  $N, K, \lambda, \gamma, \pi_{\text{init}} \in \mathcal{P}(\mathbb{R}^{d_\theta}) \times \mathcal{P}((\mathbb{R}^{d_x})^N)$

Draw  $(\theta_0, \{X_0^{i,N}\}_{i=1}^N)$  from  $\pi_{\text{init}}$

**for**  $n = 0 : K$  **do**

$$\theta_{n+1/2}^N = \theta_n^N - \frac{\gamma}{N} \sum_{j=1}^N \nabla_{\theta} g_1(\theta_n^N, X_n^{j,N}) + \sqrt{\frac{2\gamma}{N}} \xi_{n+1}^{0,N},$$

$$X_{n+1/2}^{i,N} = X_n^{i,N} - \gamma \nabla_x g_1(\theta_n^N, X_n^{i,N}) + \sqrt{2\gamma} \xi_{n+1}^{i,N},$$

$$\theta_{n+1}^N = \frac{1}{N} \sum_{i=1}^N \text{prox}_{g_2}^{\lambda} \left( \theta_{n+1/2}^N, X_{n+1/2}^{i,N} \right)_{\theta}, \quad X_{n+1}^{i,N} = \text{prox}_{g_2}^{\lambda} \left( \theta_{n+1/2}^N, X_{n+1/2}^{i,N} \right)_x.$$

**end for**

**return**  $\theta_{K+1}^N$

---

which shows that PIPGLA consists of a Langevin step with respect to  $g_1$  and a gradient descent step with respect to  $g_2^\lambda$  performed on the output of the Langevin step.

Setting  $\lambda = \gamma$ , as is common in proximal gradient algorithms (see, e.g., Salim et al. [2019]), we obtain an algorithm similar to MYIPLA except for the fact that  $\nabla g_2^\lambda$  is evaluated at  $(\theta_{n+1/2}^N, X_{n+1/2}^{i,N})$  instead of  $(\theta_n, X_n^{i,N})$ .

### 3.2 Proximal Particle Gradient Descent Methods

Our methods so far are mainly inspired from Akyildiz et al. [2023] that retain the noise in  $\theta$ -dimension which makes the entire system closer to a Langevin-type system. However, we can also consider removing the noise from the dynamics of  $\theta$  and still provide methods using algorithms developed by Kuntz et al. [2023] and formulate theoretical results based on recent developments by Caprio et al. [2024].

If we remove the noise term in the dynamics of  $\theta$  from (9), we obtain the following system of SDEs:

$$\begin{aligned} d\theta_t^N &= -\frac{1}{N} \sum_{i=1}^N \nabla_{\theta} U^{\lambda}(\theta_t^N, \mathbf{X}_t^{i,N}) dt, \\ d\mathbf{X}_t^{i,N} &= -\nabla_x U^{\lambda}(\theta_t^N, \mathbf{X}_t^{i,N}) dt + \sqrt{2} d\mathbf{B}_t^{i,N}, \end{aligned}$$

where  $i = 1, \dots, N$  and  $(\mathbf{B}_t^{i,N})_{t \geq 0}$  is a family of independent Brownian motions. Discretising this SDE system, we obtain similar algorithms to PIPULA and MYIPLA without the term  $\sqrt{2\gamma/N} \xi_{n+1}^{0,N}$  in (11) and (13), which can be seen as proximal versions of PGD [Kuntz et al., 2023]. Accordingly, we term these methods as proximal PGD (PPGD) and Moreau-Yosida PGD (MYPGD), respectively. We provide a detailed description of these methods and their theoretical analysis in Appendix B.

## 4 Nonasymptotic analysis

In this section, we provide theoretical analysis of the parameter estimates obtained by the proximal interacting particle algorithms. We first introduce the assumptions that will be central for our results. Some further assumptions will be introduced later to refine some of the results.

### 4.1 Assumptions

It is important to note that the assumptions made for the different algorithms are similar and allow a fair comparison between the derived convergence rates. Let  $g_1, g_2 : \mathbb{R}^{d_\theta} \times \mathbb{R}^{d_x} \rightarrow \mathbb{R}$  and recall that  $U(\theta, x) = g_1(\theta, x) + g_2(\theta, x)$ .

**A 1.** We assume that  $g_1 \in \mathcal{C}^1$  is convex, gradient Lipschitz with constant  $L_{g_1}$  and lower bounded, and  $g_2$  is proper, convex, lower semi-continuous and lower bounded.

The requirements on  $g_2$  guarantee that  $\text{prox}_{g_2}^\lambda$  is well defined, and similarly for  $g_1$  and its gradient. **A1** results in  $\nabla U^\lambda$  being Lipschitz in both variables with constant  $L \leq L_{g_1} + \lambda^{-1}$  [Durmus et al., 2018, Proposition 1].

**A2.** There exist a constant  $H > 0$  such that the initial condition  $Z_0^N = (\theta_0, N^{-1/2} X_0^{1,N}, \dots, N^{-1/2} X_0^{N,N})$  satisfies  $\mathbb{E}[\|Z_0^N\|^2] \leq H$ .

**A 3.**  $g_2$  is Lipschitz with constant  $\|g_2\|_{\text{Lip}}$ .

**A 4.**  $g_1$  is  $\mu$ -strongly convex, that is, for all  $v = (\theta, x), v' = (\theta', x')$

$$\langle v - v', \nabla g_1(v) - \nabla g_1(v') \rangle \geq \mu \|v - v'\|^2$$

for some  $\mu > 0$ .

**Remark 4.1.** Observe that  $\nabla g_2^\lambda(v) = (v - \text{prox}_{g_2}^\lambda(v))/\lambda$  and  $\text{prox}_{g_2}^\lambda$  is firmly non expansive [Durmus et al., 2018, Eq. (7)] which implies Lipschitzness  $\|\text{prox}_{g_2}^\lambda(v) - \text{prox}_{g_2}^\lambda(v')\| \leq \|v - v'\|$ , and we have, by the Cauchy-Schwarz inequality,

$$\begin{aligned} \langle v - v', \nabla g_2^\lambda(v) - \nabla g_2^\lambda(v') \rangle &= \frac{1}{\lambda} (\|v - v'\|^2 - \langle v - v', \text{prox}_{g_2}^\lambda(v) - \text{prox}_{g_2}^\lambda(v') \rangle) \\ &\geq \frac{1}{\lambda} (\|v - v'\|^2 - \|v - v'\| \|\text{prox}_{g_2}^\lambda(v) - \text{prox}_{g_2}^\lambda(v')\|) \geq 0. \end{aligned}$$

Therefore, under **A4**,  $\nabla U^\lambda$  is also  $\mu$ -strongly convex

$$\begin{aligned} \langle v - v', \nabla U^\lambda(v) - \nabla U^\lambda(v') \rangle &= \langle v - v', \nabla g_1(v) - \nabla g_1(v') \rangle + \langle v - v', \nabla g_2^\lambda(v) - \nabla g_2^\lambda(v') \rangle \\ &\geq \mu \|v - v'\|^2. \end{aligned}$$

◇

**Remark 4.2.** Let  $\Omega \subset \mathbb{R}^{d_\theta} \times \mathbb{R}^{d_x}$  denote the (nonempty) set where  $g_2$  is twice differentiable. Theorem 25.5 in Rockafellar [1970], guarantees that if  $g_2$  is a proper, convex function, then  $g_2$  is differentiable except in a set of measure zero, i.e.,  $\Omega^c$  has measure zero. Also, by Alexandrov's Theorem [Rockafellar, 1999],  $g_2$  is twice differentiable almost everywhere—in particular, these points form a subset of  $\text{dom}(\nabla g_2)$ . In addition, the matrix  $\nabla^2 g_2$  (or alternatively its distributional counterpart,  $D^2 g_2$ , if  $\nabla^2 g_2$  does not exist) is symmetric and positive definite [Alberti and Ambrosio, 1999, Proposition 7.11]. Thus, we do not need to assume that  $g_2$  is twice differentiable everywhere since the regularity of  $g_2$  in **A1** guarantees that  $g_2$  is differentiable except in a set of measure zero. ◇

Let  $\bar{\theta}_\star$  be the maximiser of  $p_\theta(y)$ . Let  $\mathbf{m}_{\bar{\theta}_\star}$  be the restriction of the Lebesgue measure  $\mathbf{m}$  on  $\mathbb{R}^{d_\theta} \times \mathbb{R}^{d_x}$  to the set  $\{\bar{\theta}_\star\} \times \mathbb{R}^{d_x}$ , which is well defined (see, e.g., Bogachev [2007, Section 10.6]).

**A 5.** We assume that  $\mathbf{m}_{\bar{\theta}_\star}(\Omega^c \cap (\{\bar{\theta}_\star\} \times \mathbb{R}^{d_x})) = 0$ . Moreover,

$$\mathbb{E}_X[\|\nabla_\theta U(\bar{\theta}_\star, X)\|] \leq A \quad \text{and} \quad \mathbb{E}_X[\|\nabla_{(\theta,x)}^2 g_2(\bar{\theta}_\star, X) \nabla_{(\theta,x)} g_2(\bar{\theta}_\star, X)\|] \leq B$$

where  $X \sim \rho_{\bar{\theta}_\star}(x)$  with  $\rho_{\bar{\theta}_\star}(x) \propto \exp(-U^\lambda(\bar{\theta}_\star, x))$ .

## 4.2 The proof strategy

Recall that our aim is to find the MMLE:

$$\bar{\theta}_\star = \arg \max_{\theta} p_\theta(y),$$

where  $p_\theta(y) = \int e^{-U(\theta, x)} dx$ . Therefore, we want to provide an upper bound on the distance between the iterates of our algorithms and  $\bar{\theta}_*$ , that is,  $\mathbb{E}[\|\theta_n - \bar{\theta}_*\|^2]^{1/2}$ .

Let  $(\theta_t^N)_{t \geq 0}$  be the  $\theta$ -marginal of the solution to the SDE (9)–(10) and  $(\theta_n^N)_{n \in \mathbb{N}}$  be the  $\theta$  iterates of any algorithm which is a discretisation of (9)–(10). Denote the  $\theta$ -marginal of the target measure of (9)–(10) by  $\pi_{\lambda, \Theta}^N$ ,

$$\pi_{\lambda, \Theta}^N(\theta) \propto \int_{\mathbb{R}^{d_x}} \dots \int_{\mathbb{R}^{d_x}} e^{-\sum_{i=1}^N U^\lambda(\theta, x_i)} dx_1 dx_2 \dots dx_N = \left( \int_{\mathbb{R}^{d_x}} e^{-U^\lambda(\theta, x)} dx \right)^N.$$

Using  $\mathbb{E}[\|\theta_n^N - \bar{\theta}_*\|^2]^{1/2} = W_2(\delta_{\bar{\theta}_*}, \mathcal{L}(\theta_n^N))$  and the fact that  $W_2$  is a metric, the following triangle inequality holds:

$$W_2(\delta_{\bar{\theta}_*}, \mathcal{L}(\theta_n^N)) \leq \underbrace{W_2(\delta_{\bar{\theta}_*}, \pi_{\lambda, \Theta}^N)}_{\text{concentration}} + \underbrace{W_2(\pi_{\lambda, \Theta}^N, \mathcal{L}(\theta_{n\gamma}^N))}_{\text{convergence}} + \underbrace{W_2(\mathcal{L}(\theta_n^N), \mathcal{L}(\theta_{n\gamma}^N))}_{\text{discretisation}}. \quad (19)$$

The first term is a *concentration* result, characterising the concentration of the  $\theta$ -marginal of the target measure of the SDE (9)–(10) around the maximiser of  $p_\theta(y)$ . Handling this term is not trivial since the maximisers of  $p_\theta(y)$  and of  $p_\theta^\lambda(y) := \int_{\mathbb{R}^{d_x}} p_\theta^\lambda(x, y) dx$  are not necessarily the same as we clarify in the next section. The second term is a *convergence* term, which characterises the convergence of the solution of the SDE to its target measure. The last term is a *discretisation* term, which characterises the error introduced by discretising the SDE. By separately bounding each term, we provide nonasymptotic results for the convergence of the proximal interacting particle algorithms. Proofs of the following results are provided in Appendices A and B.

### 4.3 Nonasymptotic analysis of MYIPLA

We first provide the convergence rate for MYIPLA.

**Theorem 4.1** (MYIPLA). *Let **A1**–**A5** hold. Let  $\theta_n^N$  denote the law of the iterate (13) and  $\bar{\theta}_*$  be the maximiser of  $p_\theta(y)$ . Fix  $\gamma_0 \in (0, \min\{(L_{g_1} + \lambda^{-1})^{-1}, 2\mu^{-1}\})$ . Then for every  $\lambda > 0$  and  $\gamma \in (0, \gamma_0]$ , one has*

$$\begin{aligned} \mathbb{E}[\|\theta_n^N - \bar{\theta}_*\|^2]^{1/2} &\leq \frac{\lambda}{\mu} \left( \frac{\|g_2\|_{\text{Lip}}^2}{2} A + B \right) + \sqrt{\frac{d_\theta}{N\mu}} \\ &\quad + e^{-\mu n \gamma} \left( \mathbb{E}[\|Z_0^N - z_*\|^2]^{1/2} + \left( \frac{d_x N + d_\theta}{N\mu} \right)^{1/2} \right) \\ &\quad + C_1 (1 + \sqrt{d_\theta/N + d_x}) \gamma^{1/2} + \mathcal{O}(\lambda^2), \end{aligned}$$

for all  $n \in \mathbb{N}$ , where  $z_* = (\theta_*, N^{-1/2}x_*, \dots, N^{-1/2}x_*)$  and  $(\theta_*, x_*)$  is the minimiser of  $U^\lambda$  and  $C_1 > 0$  is a constant independent of  $t, n, N, \gamma, \lambda, d_\theta, d_x$ .

*Proof.* See Appendix A.2. □

While the full proof is given in Appendix A.2, let us unpack this result. As stated in the proof strategy, we split the errors into three terms. The first term is the concentration term in (19), which in this case can be bounded as

$$W_2(\delta_{\bar{\theta}_*}, \pi_{\lambda, \Theta}^N) \leq \|\bar{\theta}_* - \bar{\theta}_{*, \lambda}\| + W_2(\delta_{\bar{\theta}_{*, \lambda}}, \pi_{\lambda, \Theta}^N).$$

The first term here can be bounded as

$$\|\bar{\theta}_* - \bar{\theta}_{*, \lambda}\| \leq \frac{\lambda}{\mu} \left( \frac{\|g_2\|_{\text{Lip}}^2}{2} A + B \right) + \mathcal{O}(\lambda^2),$$

with  $A, B$  given in **A5**. This term quantifies the distance between maximisers of  $p_\theta(y)$  and  $p_\theta^\lambda(y)$ . Next, consider the stationary measure of the SDE (9)–(10) denoted by  $\pi_{\lambda, * }^N(\theta, x_1, \dots, x_N)$ . We are interested

in the  $\theta$ -marginal of this measure, denoted by  $\pi_{\lambda, \Theta}^N$ . Using a form of the Prékopa-Leindler inequality for strong convexity [Saumard and Wellner, 2014, Theorem 3.8],  $\pi_{\lambda, \Theta}^N$  is  $N\mu$ -strongly log-concave and by Lemma A.8 of Altschuler and Chewi [2023]

$$W_2(\pi_{\lambda, \Theta}^N, \delta_{\bar{\theta}_*}) \leq \sqrt{\frac{d_\theta}{N\mu}},$$

which concludes the bound of the *concentration* term. The second challenge is the *convergence* term in (19) which is characterised by the exponential decay of the Wasserstein distance between the  $\theta$ -marginal of the solution of the SDE and its stationary measure, i.e., we have

$$W_2(\pi_{\lambda, \Theta}^N, \mathcal{L}(\theta_{n\gamma}^N)) \leq e^{-\mu n \gamma} \left( \mathbb{E}[\|Z_0^N - z_*\|^2]^{1/2} + \left( \frac{d_x N + d_\theta}{N\mu} \right)^{1/2} \right).$$

Finally, we have the *discretisation* term in (19) which is characterised by the error introduced by discretising the SDE. This term is bounded by

$$W_2(\mathcal{L}(\theta_n^N), \mathcal{L}(\theta_{n\gamma}^N)) \leq C_1(1 + \sqrt{d_\theta/N + d_x})\gamma^{1/2}.$$

Merely summing these terms, we obtain the final bound for the convergence of MYIPLA as given in Theorem 4.1.

#### 4.4 Nonasymptotic analysis of PIPGLA

To derive a convergence rate for PIPGLA we make the following additional assumption.

**C1.** We assume that  $\|\nabla^0 g_2(\theta, x)\|^2 \leq C$  for all  $\theta \in \mathbb{R}^{d_\theta}$  and  $x \in \mathbb{R}^{d_x}$ .

This assumption is similar to Salim et al. [2019, Assumption 5] without involving additional random variables.

**Theorem 4.2 (PIPGLA).** Let **A1–A5** and **C1** hold. Let  $\theta_n^N$  denote the law of the iterate (17) and  $\bar{\theta}_*$  be the maximiser of  $p_\theta(y)$ . Then for  $\gamma \leq 1/L_{g_1}$  and  $\gamma \leq \lambda \leq \gamma/(1 - \mu\gamma)$ , the following holds

$$\begin{aligned} \mathbb{E}[\|\theta_n^N - \bar{\theta}_*\|^2]^{1/2} &\leq \sqrt{\frac{d_\theta}{N\mu}} + \frac{\lambda^{n/2}(1 - \gamma\mu)^{n/2}}{\gamma^{n/2}} W_2(\mathcal{L}(Z_0^N), \pi^N) \\ &\quad + \left( \frac{\lambda(2\gamma L_{g_1}(d_\theta + Nd_x) + \lambda NC)}{N(1 - \lambda(1 - \mu\gamma)/\gamma)} \right)^{1/2}, \end{aligned} \quad (20)$$

for all  $n \in \mathbb{N}$ , with  $Z_0^N$  given in **A2** and  $C > 0$  given in **C1** and independent of  $t, n, N, \gamma, d_\theta, d_x$ .

*Proof.* See Appendix A.4. □

Similarly to the previous result, we can split the errors as follows:

$$W_2(\mathcal{L}(\theta_n^N), \delta_{\bar{\theta}_*}) \leq W_2(\delta_{\bar{\theta}_*}, \pi_\Theta^N) + W_2(\pi_\Theta^N, \mathcal{L}(\theta_n^N)).$$

Using a similar result to Altschuler and Chewi [2023, Lemma 8], the concentration term  $W_2(\delta_{\bar{\theta}_*}, \pi_\Theta^N)$  is bounded by

$$W_2(\delta_{\bar{\theta}_*}, \pi_\Theta^N) \leq \sqrt{\frac{d_\theta}{N\mu}}.$$

We derive novel nonasymptotic bounds for the other error term (see Corollary A.6 in Appendix A.4). Intuitively,  $W_2(\pi_\Theta^N, \mathcal{L}(\theta_n^N))$  controls the convergence to  $\pi_\Theta^N$  and the error due to time discretisation.

## 4.5 Algorithm comparison

Theorem 4.1 and 4.2 and Theorem B.1 in Appendix B permit the following bounds for  $\mathbb{E} [\|\theta_n^N - \bar{\theta}^*\|^2]^{1/2} = \mathcal{O}(\varepsilon)$  in terms of the key parameters  $d_\theta, d_x$

|        | $\lambda$                    | $N$                                      | $\gamma$                              | $n$  |
|--------|------------------------------|--|---------------------------------------|--|
| MYIPLA | $\mathcal{O}(\varepsilon)$   | $\mathcal{O}(d_\theta \varepsilon^{-2})$ | $\mathcal{O}(d_x^{-1} \varepsilon^2)$ | $\mathcal{O}(d_x \varepsilon^{-2-\delta})$   |
| PIPGLA | $\mathcal{O}(\varepsilon^2)$ | $\mathcal{O}(d_\theta \varepsilon^{-2})$ | $\mathcal{O}(d_x^{-1} \varepsilon^2)$ | $\mathcal{O}(\log \varepsilon^2 / \log d_x)$ |
| MYPGD  | $\mathcal{O}(\varepsilon)$   | $\mathcal{O}(d_x \varepsilon^{-2})$      | $\mathcal{O}(d_x^{-1} \varepsilon^2)$ | $\mathcal{O}(d_x \varepsilon^{-2-\delta})$   |

where  $\delta > 0$  is any small positive constant.

The bound for MYIPLA follows from first choosing  $\lambda$  so that the first term in Theorem 4.1 is  $\mathcal{O}(\varepsilon)$ , then choosing  $N$  so that the second term is  $\mathcal{O}(\varepsilon)$  and  $\gamma$  sufficiently small to counteract the dependence on  $d_x$  in the fourth term. Finally, since for every  $p \in \mathbb{N}$  one has  $e^x \geq x^p/p!$  for  $x > 0$ , for every  $\delta > 0$  (by choosing  $p \in \mathbb{N}$  large enough) one has  $e^{-\varepsilon^\delta} \leq C\varepsilon$ . Therefore, as long as  $n$  is chosen sufficiently large that  $\mu n \gamma = \mathcal{O}(\varepsilon^{-\delta})$ , the exponential decay is strong enough so that the middle term is of order  $\mathcal{O}(\varepsilon)$ . A similar approach based on the bound in Theorem B.1 provides the bounds for MYPGD.

On the other hand, the bound for PIPGLA follows from first choosing  $N$  so that the first term in Theorem 4.2 is  $\mathcal{O}(\varepsilon)$ , then  $\lambda$  and  $\gamma$  to counteract the dependence of  $d_x$  on the third term. Finally, considering the values of  $\lambda$  and  $\gamma$ , we select  $n$  to ensure that the second term is  $\mathcal{O}(\varepsilon)$ .

We point out that even if all algorithms allow for the same bound w.r.t.  $\gamma$ , the bound for MYPGD in Theorem B.1 requires more stringent assumptions on  $\gamma$ : while Theorem 4.1 requires  $\gamma_0 < \min\{(L_{g_1} + \lambda^{-1})^{-1}, 2\mu^{-1}\}$ , Theorem B.1 requires  $\gamma_0 < (L_{g_1} + \lambda^{-1} + \mu)^{-1}$  which is smaller than  $\min\{(L_{g_1} + \lambda^{-1})^{-1}, 2\mu^{-1}\}$ . PIPGLA allows for a less restrictive choice of  $\gamma < L_{g_1}$ , but requires more stringent assumptions on  $\lambda$ .

We can compare the algorithms in terms of their computational requirements too. We account for the computational cost of running each algorithm for  $n$  iterations with  $N$  particles and time discretisation step  $\gamma$ , while guaranteeing an  $\mathcal{O}(\varepsilon)$  error, in terms of component-wise evaluations of  $\nabla g_1$  and  $\text{prox}_{g_2}^\lambda$ , and sampling of independent standard 1-dimensional Gaussians.

For every step of MYIPLA, PIPGLA and MYPGD one requires  $N(d_\theta + d_x)$  evaluations of  $\nabla g_1$  component-wise and  $N(d_\theta + d_x)$  evaluations of  $\text{prox}_{g_2}^\lambda$  component-wise. In the case of MYIPLA and PIPGLA, we need  $d_\theta + Nd_x$  independent standard 1-dimensional Gaussians for each iteration; since MYPGD does not have a noise in the  $\theta$ -component this reduces to  $Nd_x$ .

|        | Evaluations of $\nabla g_1$   | Evaluations of $\text{prox}_{g_2}^\lambda$  | Indep. 1d Gaussians  |
|--------|---|---|--|
| MYIPLA | $\mathcal{O}(d_\theta d_x (d_\theta + d_x) \varepsilon^{-4-\delta})$                          | $\mathcal{O}(d_\theta d_x (d_\theta + d_x) \varepsilon^{-4-\delta})$                          | $\mathcal{O}(d_\theta d_x^2 \varepsilon^{-4-\delta})$                            |
| PIPGLA | $\mathcal{O}(d_\theta (d_\theta + d_x) \varepsilon^{-2} \frac{\log \varepsilon^2}{\log d_x})$ | $\mathcal{O}(d_\theta (d_\theta + d_x) \varepsilon^{-2} \frac{\log \varepsilon^2}{\log d_x})$ | $\mathcal{O}(d_\theta d_x \varepsilon^{-2} \frac{\log \varepsilon^2}{\log d_x})$ |
| MYPGD  | $\mathcal{O}(d_x^2 (d_\theta + d_x) \varepsilon^{-4-\delta})$                                 | $\mathcal{O}(d_x^2 (d_\theta + d_x) \varepsilon^{-4-\delta})$                                 | $\mathcal{O}(d_x^3 \varepsilon^{-4-\delta})$                                     |

## 5 Numerical Experiments

We evaluate the numerical performance of the proximal interacting particle algorithms proposed in Section 3 by applying them to train a Bayesian logistic regression model, a Bayesian neural network for MNIST classification and a sparse matrix completion model.

### 5.1 A hierarchical model

As a first example, we consider a hierarchical model involving a single scalar unknown parameter  $\theta$ ,  $d_x$  i.i.d. latent random variables following a distribution inspired by the elastic net. The prior  $p_\theta(x)$  is

defined as a product of the Gaussian and the Laplace distribution, with mean parameter  $\theta$  [Li and Lin, 2010], that is,

$$p_\theta(x_i) \propto e^{-\beta_1|x_i-\theta|-\beta_2(x_i-\theta)^2}, \beta_1, \beta_2 \geq 0.$$

We consider a Gaussian likelihood  $p(y_i|x_i) = \mathcal{N}(y_i; x_i, 1)$  which results in the joint log-likelihood:

$$-\log p_\theta(x, y) = \underbrace{\beta_1 \sum_{i=1}^{d_x} |x_i - \theta|}_{g_2(\theta, x)} + C + \underbrace{\beta_2 \sum_{i=1}^{d_x} (x_i - \theta)^2 + \sum_{i=1}^{d_x} \frac{(y_i - x_i)^2}{2}}_{g_1(\theta, x)},$$

where we identify the functions  $g_1$  and  $g_2$  as above. In the standard posterior sampling setting, potentials similar to the one considered here appear in Bayesian inverse problems [Crucinio et al., 2023; Durmus et al., 2018; Pereyra, 2016].

Note that the function  $g_1$  is gradient Lipschitz and lower bounded by  $C$ , and  $g_2$  is proper, convex, lower semi-continuous, lower bounded and Lipschitz. If we take  $\beta_2$  bounded away from zero, i.e.,  $\beta_2 \geq \varepsilon > 0$ , then  $g_1$  is  $\mu$ -strongly convex, where  $\mu$  is given by the lowest eigenvalue of the Hessian matrix of  $g_1$  and depends on  $\beta_2$ . Besides, in the set where  $g_2$  is differentiable it satisfies  $\|\nabla_\theta g_2\| = \|\nabla_x g_2\| = 1$  and  $\|\nabla_{(\theta, x)}^2 g_2\| = 0$ . Therefore, assumption **A5** is also satisfied.

We derive the proximal mapping for  $g_2$  in Appendix D.1.1. Table 2 shows the normalised MSEs (NMSE) for  $\theta$ ,  $\|\theta_{K+1}^N - \theta\|^2 / \|\theta\|^2$ . Each algorithm is run 100 times using different starting points for 50 and 500 particles and 2500 steps. The NMSEs and computation times provided are averaged over the 100 replicates. The values of  $\lambda$  and  $\gamma$  are the optimal values found by performing a grid search. The execution times for the three algorithms MYIPLA, PIPGLA and MYPGD are very similar. The performance of MYIPLA and MYPGD is better than that of PIPGLA for  $N = 50$  particles while PIPGLA clearly outperforms the others for  $N = 500$  particles. Note also how the NMSE decreases when increasing the number of particles for PIPGLA and MYPGD.

Table 1: Toy hierarchical example. Normalised MSE (NMSE) for  $\theta$  for different algorithm when run 100 times using 50 and 500 particles, 2500 steps and different starting points. Computation times and NMSEs are averaged over the 100 replicates.

| Algorithm | NMSE ( $\times 10^{-4}$ )         |                                   | Times (s)                     |                                | $\lambda$ | $\gamma$ |
|-----------|-----------------------------------|-----------------------------------|-------------------------------|--------------------------------|-----------|----------|
|           | $N = 50$                          | $N = 500$                         | $N = 50$                      | $N = 500$                      |           |          |
| MYIPLA    | <b>1.98 <math>\pm</math> 3.27</b> | 3.06 $\pm$ 0.74                   | 31 $\pm$ 12                   | <b>170 <math>\pm</math> 23</b> | 0.25      | 0.03     |
| PIPGLA    | 10.74 $\pm$ 13.35                 | <b>0.25 <math>\pm</math> 0.12</b> | 36 $\pm$ 15                   | 185 $\pm$ 31                   | 0.005     | 0.05     |
| MYPGD     | 3.62 $\pm$ 4.81                   | 3.59 $\pm$ 1.60                   | <b>27 <math>\pm</math> 10</b> | 175 $\pm$ 22                   | 0.25      | 0.05     |

## 5.2 Bayesian logistic regression

Here we analyse a Bayesian logistic regression latent variable model. We consider a similar set-up to the one described in De Bortoli et al. [2021] and employ a synthetic dataset consisting of  $d_y = 900$  datapoints (see Appendix D.2 for details). The latent variables are the  $d_x = 50$  regression weights, to which we assign an isotropic Laplace prior  $p_\theta(x) = \prod_{i=1}^{d_x} \text{Laplace}(x_i|\theta, 1)$  or a uniform prior  $p_\theta(x) = \prod_{i=1}^{d_x} \mathcal{U}(x_i|-\theta, \theta)$ . The likelihood is given by  $p_\theta(y|x) = \prod_{j=1}^{d_y} s(v_j^T x)^{y_j} s(-v_j^T x)^{1-y_j}$ , where  $v_j \sim \mathcal{U}(-1, 1)^{\otimes d_x}$  are a set of synthetic  $d_x$ -dimensional covariates sampled from a uniform distribution and  $s(u) := e^u / (1 + e^u)$  is the logistic function. The true value of  $\theta$  is set to  $\theta = -4$  for the Laplace prior and  $\theta = 1.5$  for the uniform one.

In the case of the Laplace prior, the negative log joint likelihood is given by

$$-\log p_\theta(x, y) = \underbrace{\sum_{i=1}^{d_x} |x_i - \theta|}_{g_2(\theta, x)} + \underbrace{d_x \log 2 - \log p(y|x)}_{g_1(\theta, x)};$$

and for the uniform prior, we obtain

$$-\log p_\theta(x, y) = \underbrace{d_x \log(2\theta) + \sum_{i=1}^{d_x} \iota_{[-\theta, \theta]}(x_i)}_{g_2(\theta, x)} - \underbrace{\log p(y|x)}_{g_1(\theta, x)},$$

where we introduce  $g_1$  and  $g_2$  as above and  $\iota_{\mathcal{K}}$  is the convex indicator of  $\mathcal{K}$  defined by  $\iota_{\mathcal{K}}(x) = 0$  if  $x \in \mathcal{K}$  and  $\iota_{\mathcal{K}}(x) = \infty$  otherwise.

In both cases we have that

$$g_1(\theta, x) = \sum_{j=1}^{d_y} (y_j \log(s(v_j^T x)) + (1 - y_j) \log(s(-v_j^T x))) + C$$

where  $C$  is a constant. As shown in Akyildiz et al. [2023, Section 6.1.1], the function  $g_1$  is gradient Lipschitz and strictly convex but not strongly convex. The function  $g_2$  satisfies **A1** for both the Laplace and the uniform prior, as observed in Pereyra [2016], in the case of the Laplace prior  $g_2$  also satisfies **A3** while the uniform prior does not lead to a Lipschitz  $g_2$ . Since  $g_1$  does not depend on  $\theta$ , **A5** holds for the Laplace prior as shown in the previous example.

### 5.2.1 Comparing approximations of $\text{prox}_{g_2}^\lambda$

We derive approximations of the proximal mapping for  $g_2$  for both the Laplace prior and the uniform prior in Appendices D.1.1 and D.1.3, respectively. The exact solution for the proximal operator for these two priors is not available in closed form, however Ehrhardt et al. [2023]; Schmidt et al. [2011] provide convergence guarantees when the minimisation in Definition 2.1 can only be solved up to a certain accuracy. In particular, they show that the error in the proximity operator calculation is controlled in an appropriate way and, in some cases, inexact proximal-gradient strategies can attain the same convergence rates as exact methods. The proximity map for PIPULA and PPGD (i.e. when  $\lambda = \gamma$ ) is derived in D.1.4

We consider both an iterative approach [Parikh and Boyd, 2014, Section 2.3] and an approximation of  $\text{prox}_{g_2}^\lambda$ . Since the true value of  $\theta$  is known, we use this experiment to validate the proposed algorithms (and their variations) and to investigate the effect of an approximate proximity map against one obtained by an iterative fixed-point procedure for the Laplace prior. In the case of the uniform prior, we only consider an approximation to the proximity map.

Figure 1 shows the variance of the  $\theta$  estimates produced by MYIPLA and PIPGLA computed over 100 Monte Carlo runs with different initialisations  $\theta_0$ . We observe that the second moment,  $\mathbb{E}[\|\theta_n^N - \bar{\theta}^*\|^2]$ , decreases with rate  $\mathcal{O}(1/N)$  as suggested by Theorems 4.1 and 4.2, and that the iterative algorithms have a slightly lower variance compared to their approximate versions, with PIPGLA having better performance than MYIPLA. It is also important to highlight that for all algorithms considered, approximate solvers are on average 25% faster than iterative solvers (see Table 2).

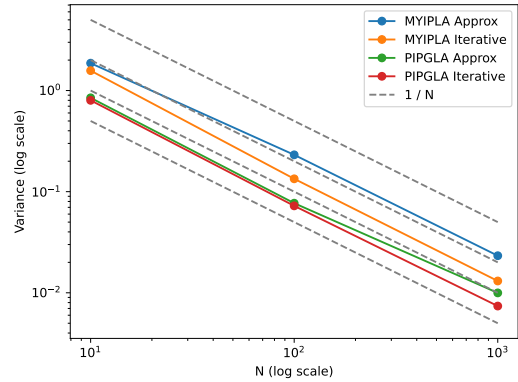


Figure 1: Convergence rate of the variance of the parameter estimates produced by MYIPLA and PIPGLA over 100 Monte Carlo runs for different initialisations each  $N \in 10, 100, 1000$ . We can see that the  $\mathcal{O}(1/N)$  convergence rate holds for the second moments as suggested by our results in Section 4.

Table 2: Bayesian logistic regression for Laplace and uniform priors. Normalised MSE (NMSE) for  $\theta$  for different algorithm when run 500 times using 50 particles, 5000 steps and different starting points. Computation times and NMSEs are averaged over the 500 replicates. The second column indicates whether the proximal map is calculated approximately or iteratively, using 40 steps in each iteration. For the uniform prior case we have not implemented the iterative method.

| Algorithm | Approx./Iterative | NMSE (%)                          |                                   | Times (s)                        |                                  |
|-----------|-------------------|-----------------------------------|-----------------------------------|----------------------------------|----------------------------------|
|           |                   | Laplace                           | Unif                              | Laplace                          | Unif                             |
| PPGD      | Approx            | $14.70 \pm 4.42$                  | $3.63 \pm 4.93$                   | $102.6 \pm 5.1$                  | $107.9 \pm 5.5$                  |
|           | Iterative         | $19.04 \pm 1.34$                  | —                                 | $122.3 \pm 5.1$                  | —                                |
| PIPULA    | Approx            | $12.18 \pm 1.62$                  | $4.71 \pm 6.02$                   | $98.8 \pm 5.7$                   | $101.0 \pm 4.0$                  |
|           | Iterative         | $19.22 \pm 1.28$                  | —                                 | $126.2 \pm 3.8$                  | —                                |
| MYPGD     | Approx            | $6.09 \pm 0.34$                   | <b><math>0.60 \pm 0.23</math></b> | $91.9 \pm 4.8$                   | $109.3 \pm 4.6$                  |
|           | Iterative         | $4.44 \pm 1.40$                   | —                                 | $129.7 \pm 15.8$                 | —                                |
| MYIPLA    | Approx            | $4.42 \pm 1.32$                   | $15.26 \pm 4.44$                  | <b><math>89.9 \pm 4.2</math></b> | <b><math>97.0 \pm 4.2</math></b> |
|           | Iterative         | $4.67 \pm 1.60$                   | —                                 | $120.5 \pm 10.1$                 | —                                |
| PIPGLA    | Approx            | $2.30 \pm 0.58$                   | $6.83 \pm 3.97$                   | $116.5 \pm 5.5$                  | $103.1 \pm 8.0$                  |
|           | Iterative         | <b><math>2.02 \pm 0.54</math></b> | —                                 | $122.9 \pm 6.9$                  | —                                |

### 5.2.2 Overall performances

We compare the performances of MYIPLA, PIPGLA, MYPGD, PIPULA and PPGD through the normalised MSEs (NMSE) for  $\theta$ ,  $\|\theta_{K+1}^N - \theta\|^2 / \|\theta\|^2$ . Each algorithm is run 500 times using different starting points for 50 particles and 5000 steps. When using an iterative solver for the proximity map we use 40 iterations at each step. Table 2 provides the NMSEs and computation times which are averaged over the 500 replicates. The values for  $\lambda, \gamma$  in the different algorithms are chosen optimally after performing a grid search. The specific values are provided in Appendix D.2, Table 7. In the case of PIPGLA the optimal values for  $\lambda, \gamma$  are obtained when  $\lambda = \gamma$  as suggested by Salim et al. [2019].

For the Laplace prior, PIPGLA attains the best performance followed by MYIPLA, with the iterative solver being slightly better but considerably slower and therefore computationally more expensive. Therefore, considering a trade-off between accuracy and computational cost, PIPGLA and MYIPLA implemented with the iterative solver outperform the other algorithms.

For the uniform prior, MYPGD demonstrates significantly better performance than all the other algorithms; this is likely due to the lack of diffusive term in the corresponding SDE which is beneficial when dealing with a compactly supported prior. Figure 4 in Appendix D.2 shows that the  $\theta$ -iterates of MYPGD, MYIPLA, and PIPGLA converge to similar stationary points for the different initial values  $\theta_0$  although for the last two algorithms the stationary distribution does not coincide with the true parameter value.

## 5.3 Bayesian neural network with sparse prior

To test our algorithms on an example with more complex posteriors, we turn to Bayesian neural networks whose posteriors are notoriously multimodal, where we consider a sparsity-inducing prior on the weights, which is non-smooth and therefore it cannot be handled using the framework of Akyildiz et al. [2023]; Kuntz et al. [2023].

We consider an analogous setting to Yao et al. [2022] and Kuntz et al. [2023], and apply a Bayesian two-layer neural network to classify MNIST images. Similarly to Yao et al. [2022], we avoid the cost of computing the gradients on a big dataset by subsampling 1000 data points with labels 4 and 9. The input layer of the network has 40 nodes and 784 inputs (since we are considering  $28 \times 28$  images), and the output layer has 2 nodes. The latent variables are the weights,  $w \in \mathbb{R}^{d_w := 40 \times 784}$ , of the input layer and



those,  $v \in \mathbb{R}^{d_v := 2 \times 40}$ , of the output layer. We use tanh activation functions, a softmax output layer, and also simplify the problem by setting all network biases to zero. This scenario is equivalent to assuming that the datapoints' labels  $l$  are conditionally independent given the features  $f$  and network weights  $x = (w, v)$ , and therefore have the following probability density

$$p(l|f, x) \propto \exp \left( \sum_{j=1}^{40} v_{lj} \tanh \left( \sum_{i=1}^{784} w_{ji} f_i \right) \right).$$

We assign priors  $p_\alpha(w) = \prod_i \text{Laplace}(w_i|0, e^{2\alpha})$  and  $p_\beta(v) = \prod_i \text{Laplace}(v_i|0, e^{2\beta})$  to the input and output layer's weights, respectively, and learn  $\theta = (\alpha, \beta)$  from the data. The model's density is given by

$$p_\theta(x, \mathcal{Y}_{\text{train}}) = \prod_i \text{Laplace}(w_i|0, e^{2\alpha}) \prod_j \text{Laplace}(v_j|0, e^{2\beta}) \prod_{(f,l) \in \mathcal{Y}_{\text{train}}} p(l|f, x).$$

We note that the log density can be decomposed as

$$-\log p_\theta(x, \mathcal{Y}_{\text{train}}) = \underbrace{2d_w\alpha + \sum_i |w_i|e^{-2\alpha} + 2d_v\beta + \sum_j |v_j|e^{-2\beta}}_{g_2(\theta, x)} - \underbrace{\sum_{(f,l) \in \mathcal{Y}_{\text{train}}} \log p(l|f, x)}_{g_1(\theta, x)},$$

where  $d_w$  and  $d_v$  denote the dimensions of the weights  $w$  and  $v$ , respectively,  $g_1$  is differentiable and does not depend on  $\theta$  and  $g_2$  is proper, convex and lower semi-continuous. We derive an approximation to the proximity map of  $g_2$  in Appendix D.1.2.

To allow a fair comparison with other algorithms, we use the same performance metrics as in Kuntz et al. [2023]; see Appendix D.3 for their precise definition. We consider the average classification error over the test set  $\mathcal{Y}_{\text{test}}$ , i.e.

$$\text{Error} := \frac{1}{|\mathcal{Y}_{\text{test}}|} \sum_{(f,l) \in \mathcal{Y}_{\text{test}}} \mathbb{1}\{l = \hat{l}(f)\},$$

where  $\hat{l}(f)$  denotes the most likely label for feature  $f$  (i.e. the arg max of the approximation of the posterior predictive distribution at  $\bar{\theta}_*$ ), and the log pointwise predictive density (LPD, Vehtari et al. [2017])

$$\text{LPD} := \frac{1}{|\mathcal{Y}_{\text{test}}|} \sum_{(f,l) \in \mathcal{Y}_{\text{test}}} \log \left( \frac{1}{N} \sum_{i=1}^N p(l|f, X_{K+1}^i) \right),$$

where  $X_{K+1}^i$  are the samples of the final particle cloud.

### 5.3.1 Laplace vs Normal prior

One may ask whether the Laplace prior is more appropriate in this setting than the Normal one. Jaynes [1968] provides two reasons why the Laplace prior is particularly suitable for Bayesian neural network models. Firstly, for any feedforward network there is a functionally equivalent network in which the weight of a non-direct connection has the same size but opposite sign, therefore consistency demands that the prior for a given weight  $w$  is a function of  $|w|$  alone. Secondly, if it is assumed that all that is known about  $|w|$  is its scale, and that the scale of a positive quantity is determined by its mean rather than some higher order moment, then the maximum entropy distribution for a positive quantity constrained to a given mean is the exponential distribution. It would follow that the each signed weight  $w$  has a Laplace density [Williams, 1995].

We analyse if the sparsity-inducing nature of the Laplace prior has in practice this effect on the value of the final weights in the case of MYIPLA. For this, we set  $N = 100$  and observe the distribution of the weights for a randomly chosen particle from the final particle cloud  $X_{500}^1, \dots, X_{500}^N$  and compare it to that obtained with a Normal prior (Figure 2). We note that our experiment (Fig. 2a) leads to final weights with values highly concentrated around zero in comparison to the normal prior (Fig. 2b) where the values of the weights are more spread out, leading to a posterior distribution with heavier tails (see also the standard deviation column in Table 4).

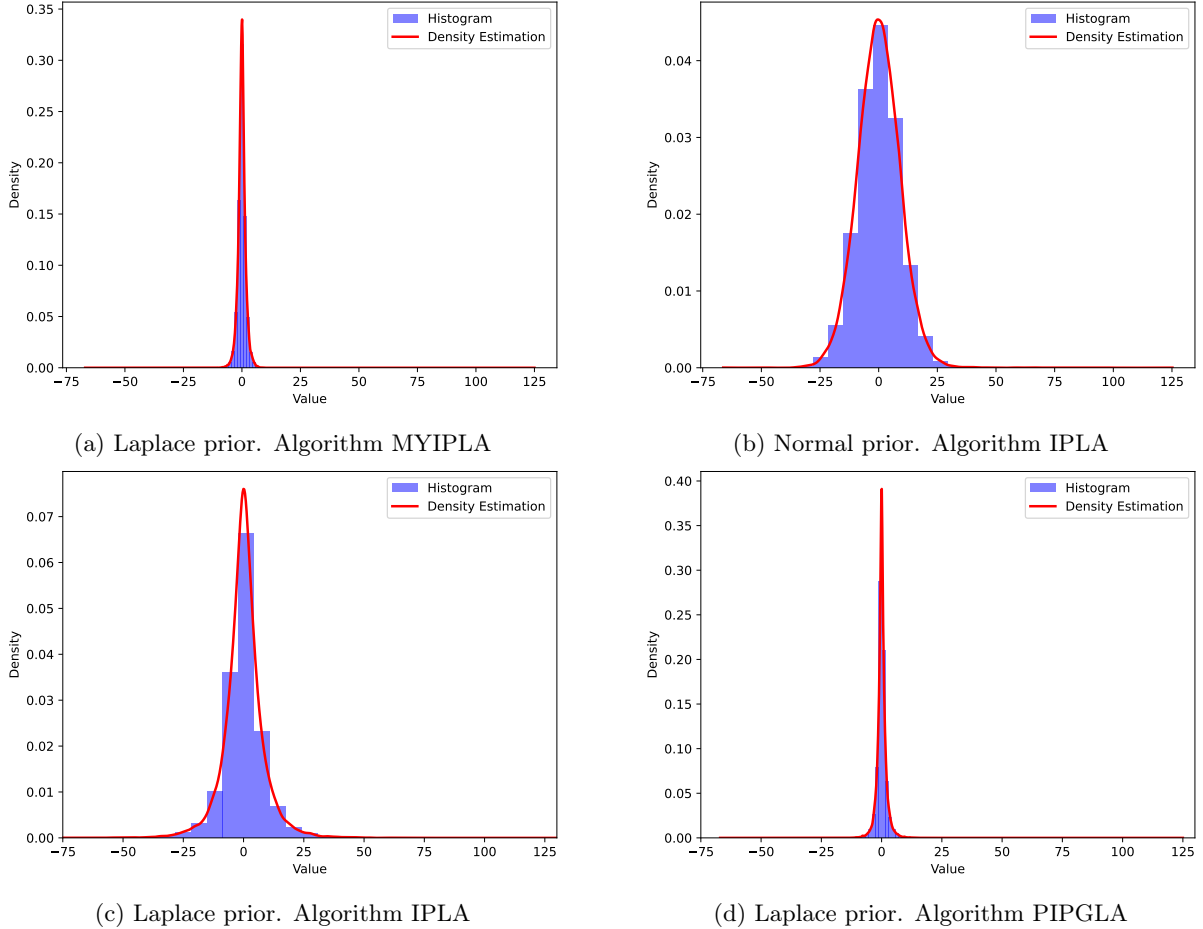


Figure 2: Histogram and density estimation of the weights of a BNN for a randomly chosen particle from the final (500 steps) cloud of 100 particles.

The sparse representation of our experiment also has the advantage of producing models that are smaller in terms of memory usage when small weights are zeroed out. To investigate this, we set to zero all weights below a certain threshold and analyse the performance of the compressed weight matrices. We consider two cases, averaging the particles of the final cloud  $X_{500}^1, \dots, X_{500}^{100}$ , applying the threshold and then calculating the performance, and secondly, setting to zero small values of each particle of the cloud and averaging the performance of each particle. We compare the results for the Bayesian neural networks with Laplace and Normal priors (Table 3). It is important to note that when applying the same threshold to both cases, the Laplace prior leads to a very compressed weight matrix compared to the Normal prior, i.e. there is a significant difference in the percentage of weights set to zero. We observe that when setting the same proportion of weights to zero in both layers, the performance of the BNN with Laplace priors is better in terms of the log pointwise predictive density than that of the BNN with Normal priors, especially when averaging the final cloud of particles before computing the performance. Further results for other proposed algorithms are presented in Appendix D.3.

### 5.3.2 Comparing proximal algorithms with IPLA

We compare the performance of MYIPLA, MYPGD and PIPGLA with IPLA [Akyildiz et al., 2023] obtained by ignoring the non-differentiability of the model density. Adapting the results of Johnston and Sabanis [2023], one can show that IPLA can be analysed within this setting and would have a similar convergence guarantee to that given in Akyildiz et al. [2023]. In this section, we show that, even with a Laplace prior, the IPLA implementation does not produce sufficient sparsity, compared to the methods

Table 3: Bayesian neural network. Performance of BNN with Laplace (implemented using MYIPLA) and Normal priors (implementation with PGD) when setting weights from the final particle cloud below a certain threshold to zero. The second column refers to whether the particles are averaged before ( $\checkmark$ ) or after ( $\times$ ) calculating the performance.

| Prior   | Average over particles? | % of zero weights |         | Thresholds |         | Error (%)  | LPD          |
|---------|-------------------------|-------------------|---------|------------|---------|------------|--------------|
|         |                         | Layer 1           | Layer 2 | Layer 1    | Layer 2 |            |              |
| Laplace | $\checkmark$            | 74                | 48      | 0.2        | 0.2     | <b>7.0</b> | <b>-0.23</b> |
|         | $\times$                | 56                | 35      | 1          | 1       | <b>1.5</b> | <b>-0.07</b> |
| Normal  | $\checkmark$            | 74                | 48      | 0.5        | 1.1     | 15         | -0.74        |
|         | $\checkmark$            | 16                | 15      | 0.2        | 0.2     | 16         | -0.78        |
|         | $\times$                | 56                | 35      | 7          | 4       | 2.0        | -0.11        |
|         | $\times$                | 8.6               | 7.1     | 1          | 1       | 1.5        | -0.10        |

Table 4: Bayesian neural network. Test errors and log pointwise predictive density (LPD) achieved using the final particle cloud  $X_{250}^1, \dots, X_{250}^N$  for different algorithm when using 50 particles. Computation times and standard deviation of the empirical distribution of the weight matrix  $w$  for a randomly chosen particle are also provided.

| Algorithm | Error (%)   | LPD           | Times (s) | Std. $w$    |
|-----------|-------------|---------------|-----------|-------------|
| MYIPLA    | 2.00        | -0.107        | 22        | 2.27        |
| MYPGD     | <b>1.50</b> | -0.102        | 20        | 2.02        |
| PIPGLA    | 2.00        | <b>-0.096</b> | 33        | <b>1.73</b> |
| PGD       | 2.00        | -0.098        | <b>19</b> | 8.80        |
| IPLA      | 1.99        | -0.101        | <b>19</b> | 11.70       |

we propose in this paper.

These results are summarised in Table 4 when using 50 particles, 250 steps and choosing  $\lambda$  and  $\gamma$  optimally after performing a grid search. The table also includes computation times and the standard deviation of the weight matrix  $w$  for a randomly chosen particle in the final cloud. This latter value is included to assess whether the model is able to induce sparsity in the computed weights. We observe that while the performance of all the algorithms is similar, the standard deviation of the weights for the non-proximal method, IPLA, is significantly higher compared to the proximal algorithms. This results in posterior distributions for the weights which are less concentrated (see, e.g., Figure 2c) and thus the sparsity-inducing effect of the Laplace prior is reduced by the use of algorithms which do not take into account the non-differentiability of the target. We can visually verify that proximal algorithms lead to concentrated posterior distributions, see, e.g., Figures 2a and 2d. In particular when using PIPGLA, 70% and 12% of the weights of  $w$  and  $v$  of the final particle cloud are exactly zero up to machine precision.

### 5.3.3 Overall performances

We analyse the test errors and log pointwise predictive density (LPD) achieved using the final particle cloud  $X_{500}^1, \dots, X_{500}^N$  for MYIPLA, MYPGD and PIPGLA, with  $N = 1, 10, 100$ , and corresponding computation times averaged over 10 replicates.

The test errors (Table 5) have similar values to that of PGD under the setting of Kuntz et al. [2023, Table 2], which is similar to ours but with Normal instead of Laplace priors on the weights. We observe in Table 5 that performance improves as the number of particles  $N$  increases, especially for PIPGLA. When the number of particles is 100, the three algorithms MYIPLA, PIPGLA and MYPGD have similar performance and runtimes, with MYIPLA having a slightly better performance and PIPGLA being slightly faster.

Table 5: Bayesian neural network. Test errors achieved using the final particle cloud  $X_{500}^1, \dots, X_{500}^N$  for MYIPLA, MYPGD and PIPGLA, with  $N = 1, 10, 100$ , and corresponding computation times averaged over 10 replicates. The highlighted value show the best error and runtime in the case  $N = 100$ .

| Algorithm | $N$ | Error (%)                         | Times (s)                          |
|-----------|-----|-----------------------------------|------------------------------------|
| MYIPLA    | 1   | $7.90 \pm 5.17$                   | $1.84 \pm 0.03$                    |
|           | 10  | $3.35 \pm 1.05$                   | $10.43 \pm 0.48$                   |
|           | 100 | <b><math>2.45 \pm 0.91</math></b> | $89.72 \pm 3.37$                   |
| PIPGLA    | 1   | $21.65 \pm 9.88$                  | $1.83 \pm 0.04$                    |
|           | 10  | $7.45 \pm 2.13$                   | $9.59 \pm 0.15$                    |
|           | 100 | $2.65 \pm 1.32$                   | <b><math>81.98 \pm 1.64</math></b> |
| MYPGD     | 1   | $5.15 \pm 1.48$                   | $1.90 \pm 0.06$                    |
|           | 10  | $3.15 \pm 1.14$                   | $10.40 \pm 0.46$                   |
|           | 100 | $2.55 \pm 0.90$                   | $83.20 \pm 6.01$                   |

## 5.4 Sparse matrix completion

In this section, we demonstrate another application of our methods: the problem of matrix completion. Matrix completion [Candès and Plan, 2010; Liu et al., 2018] focuses on recovering an intact matrix with low-rank property from incomplete data. Its application varies from wireless communications [Kortas et al., 2017], traffic sensing [Mardani and Giannakis, 2014] to integrated radar and recommender systems [Gogna and Majumdar, 2015]. We consider two different settings for this problem and analyse the performance of MYIPLA.

### 5.4.1 Example 1

Given matrices  $Y^l = \Phi X^l + \varepsilon^l \in \mathbb{R}^{m \times n}$ , where  $X^l \in \mathbb{R}^{r \times n}$  is sparse,  $\Phi \in \mathbb{R}^{m \times r}$ ,  $r \ll m < n$  and  $\varepsilon^l$  has normally distributed entries  $\varepsilon_{i,j}^l \sim \mathcal{N}(0, \sigma^2)$  with known variance  $\sigma^2$ . Let  $\Omega^l$  denote the set of observed entries for matrix  $Y^l$ , that is, suppose we only observe  $Y_{ij}^l$ ,  $(i, j) \in \Omega^l, l = 1, \dots, L$ . Our goal is to estimate the missing entries. This problem can be restated using the following probability density

$$p_\beta(Y, X) = p_\beta(X) p_\beta(Y|X) = C(\theta) e^{-e^{-\theta} \sum_l \|X^l\|_{\text{tr}}} \prod_l \prod_{(i,j) \in \Omega^l} \mathcal{N}(Y_{ij} | \Phi X_{ij}^l, \sigma^2),$$

where  $\beta = (\theta, \Phi)$ ,  $p_\beta(X)$  is a sparsity-inducing prior and  $\|\cdot\|_{\text{tr}}$  is the trace (or nuclear) norm, which is a convex envelope of the rank function [Bach, 2008], and is defined as

$$\|X\|_{\text{tr}} = \sum_{i=1}^r \sigma_i(X),$$

$r = \text{rank}(X)$  and  $\sigma_1(X) \geq \dots \geq \sigma_r(X) \geq 0$  are the singular values. The resulting prior can be seen as a regularisation term [Boursier et al., 2022; Grave et al., 2011]. The negative log density or potential is decomposed as

$$U(\theta, \Phi, X) = \underbrace{-\log(C(\theta)) + e^{-\theta} \sum_l \|X^l\|_{\text{tr}}}_{g_2(\beta, X)} + \underbrace{\sum_l \sum_{(i,j) \in \Omega^l} \frac{(Y_{ij} - \Phi X_{ij}^l)^2}{2}}_{g_1(\beta, X)}.$$

To implement MYIPLA we need to compute the proximal operator of  $g_2$  which can be found in Appendix D.4.1. The data used for this example is described in the same appendix.

To analyse the performance of the algorithm, we compute the normalised MSE for the missing entries, that is,

$$\frac{\|P_{\Omega^c} Y_{\text{true}} - P_{\Omega^c} Y_K^N\|^2}{\|P_{\Omega^c} Y_{\text{true}}\|^2},$$

where  $P_{\Omega^c}$  denotes the projection operator over the unobserved entries. The normalised error of the missing entries for the final particle cloud is  $3.11 \times 10^{-2}$ , where we have considered  $N = 30$  particles and  $K = 500$  steps. The last value of the  $\theta$  iterates is  $\theta = 0.1$ , which provides a data-driven estimation of the regularisation parameter.

### 5.4.2 Example 2

Let  $Y$  be the following matrix  $Y = \Phi X + \varepsilon$ , where  $Y \in \mathbb{R}^{m \times n}$ ,  $X \in \mathbb{R}^{r \times n}$  is sparse,  $\Phi \in \mathbb{R}^{m \times r}$  with  $r \ll m < n$  and  $\varepsilon$  has normally distributed entries  $\varepsilon_{i,j} \sim \mathcal{N}(0, \sigma^2)$  with known variance  $\sigma^2$ . Suppose we only observe entries  $Y_{ij}$ ,  $(i, j) \in \Omega$ , where  $\Omega$  denote the set of indices for the observed entries. We want to recover the matrix  $\Phi X$  and also estimate the distribution of the entries of  $\Phi$ , which we assume follow a Normal distribution with mean  $\theta$  and variance  $\sigma^2$ , that is,  $\Phi_{i,j} \sim \mathcal{N}(\theta, \tilde{\sigma}^2)$ , where  $\tilde{\sigma}$  is known. This problem can be formulated using the following probability density

$$\begin{aligned} p_\beta(Y, X, \Phi) &= p_\beta(X) p_\beta(\Phi) p_\beta(Y|X, \Phi) \\ &= C(\xi) e^{-e^{-\xi} \|X\|_{\text{tr}}} \prod_{i,j} \mathcal{N}(\Phi_{ij}|\theta, \tilde{\sigma}^2) \prod_{(i,j) \in \Omega} \mathcal{N}(Y_{ij} | (\Phi X)_{ij}, \sigma^2), \end{aligned}$$

where  $\beta = (\xi, \theta)$  and  $p_\beta(X)$  is a sparsity-inducing prior. The negative log density or potential can be expressed as

$$U(\beta, X, \Phi) = \underbrace{-\log(C(\xi)) + e^{-\xi} \|X\|_{\text{tr}}}_{g_2(\beta, X, \Phi)} + \underbrace{\sum_{i,j} \frac{(\Phi_{ij} - \theta)^2}{2\tilde{\sigma}^2} + \sum_{(i,j) \in \Omega} \frac{(Y_{ij} - (\Phi X)_{ij})^2}{2\sigma^2}}_{g_1(\beta, X, \Phi)}.$$

To estimate  $\beta$  from the data, we compute the proximal operator of  $g_2$  in Appendix D.4.2. The data generation process is also described in this appendix. It is important to highlight that in this example we consider a cloud of particles for both  $X$  and  $\Phi$ .

To evaluate the performance, we compute the normalised MSE for the missing entries of  $Y$ , the average normalised MSE of the final particle cloud  $\Phi_K^1, \dots, \Phi_K^N$ , as well as the normalised MSE of an estimator of  $\theta$  given by the last value of the iterates of the  $\theta$  chain (Table 6). The evolution of the performance metrics across steps is shown in Figure 9, Appendix D.4.2.

Table 6: Performance metrics for the sparse matrix completion Example 2, when the true value of  $\theta = 1.4$  for the final particle cloud for  $N = 30$  particles and  $K = 500$  steps.

| NMSE missing entries $Y$ (%) | NMSE $\Phi$ (%) | NMSE $\theta$ (%) |
|------------------------------|-----------------|-------------------|
| 4.70                         | 8.94            | 9.69              |

## 6 Conclusions

This work focuses on the maximum marginal likelihood problem for non-differentiable latent variable models arising in many machine learning and signal processing applications. Our main contribution is to propose an interacting particle Langevin algorithm, extending the methods proposed for differentiable latent variable models [Akyildiz et al., 2023; Kuntz et al., 2023]. To do so, we have leveraged proximal methods [Combettes and Pesquet, 2011; Parikh and Boyd, 2014], akin to proximal MCMC methods [Pereyra, 2016]. We have analysed the resulting family of algorithms and provided nonasymptotic analysis bounding the optimisation error  $\mathbb{E}[\|\theta_n^N - \theta^*\|^2]^{1/2}$ . These results are direct analogues of sampling methods within the non-differentiable setting, extended to the case of estimation in latent variable models where the problem is a mixture of sampling and optimisation.

We have demonstrated the applicability and efficiency of our methods on different numerical examples. Specifically, we have conducted four experiments, the first involving a hierarchical toy model in which

all assumptions are satisfied to verify the performance of our methods. Secondly, a Bayesian logistic regression model, in which we have studied the differences between using an iterative approach or an approximation of  $\text{prox}_{g_2}^\lambda$ , concluding that although their accuracy is very similar, the approximate methods are considerably faster, specifically by around 25%. Next, we have considered a classification problem using a Bayesian neural network, whose posteriors are highly multimodal, with sparsity-inducing priors on the weights. We have analysed the advantages and performance of using Laplace priors versus Normal priors, and investigated how pruning affects performance in both cases. We have also compared how proximal algorithms lead to more concentrated posteriors compared to algorithms which ignore the set of non-differentiable points. Finally, we have dealt with sparse matrix completion problems, which has wide ranging applications in machine learning.

We note that, for the cases where the set of non-differentiable points is measure zero, our methods outperform the standard methods which ignores this and uses standard gradient based methods. In particular, these methods, adapted to our setting, would have similar theoretical guarantees [Johnston and Sabanis, 2023], however, the use of proximal operators and proximal methods significantly outperform subgradient based variants. In particular, using sparsity-inducing priors (like Laplace priors) the posterior distribution is more concentrated when employing proximal interacting particle Langevin algorithms compared to Langevin algorithms such as those in Akyildiz et al. [2023]; Kuntz et al. [2023], as we showed in the Bayesian neural network experiment (Section 5.3).

Our algorithms present a novel approach to work with latent variable models with sparsity-inducing priors, priors with compact support such as uniform priors, among others. This allows working with Bayesian models arising from different types of non-differentiable regularisations, such as the Lasso regularisation, the elastic net or the total-variation norm, to name a few.

Future work holds many promising avenues. First, we envisage our methods to be expanded beyond the convex setting (as they already perform well in the non-convex empirical examples as we have shown in Section 5.3). Our theoretical framework can be extended to the non-convex case, using recent non-convex optimisation bounds [Akyildiz and Sabanis, 2024; Zhang et al., 2023] and their non-differentiable adaptations. We can further adapt stochastic gradients straightforwardly as in Akyildiz et al. [2023]. This is especially important in a machine learning context, as gradients are calculated using a mini-batch of data to improve efficiency. Our novel bounds on the difference between the true minimiser and the minimiser of the Moreau-Yosida approximation can also be used within the recent multiscale approaches to extend them to non-differentiable settings, see, e.g., Akyildiz et al. [2024].

## Acknowledgments and Disclosure of Funding

PCE is supported by EPSRC through the Modern Statistics and Statistical Machine Learning (StatML) CDT programme, grant no. EP/S023151/1.

## References

- Ö. Deniz Akyildiz and Sotirios Sabanis. Nonasymptotic analysis of Stochastic Gradient Hamiltonian Monte Carlo under local conditions for nonconvex optimization. *Journal of Machine Learning Research*, 25(113):1–34, 2024.
- Ö. Deniz Akyildiz, Francesca Romana Crucinio, Mark Girolami, Tim Johnston, and Sotirios Sabanis. Interacting Particle Langevin Algorithm for Maximum Marginal Likelihood Estimation. *arXiv preprint arXiv:2303.13429*, 2023.
- Ö Deniz Akyildiz, Michela Ottobre, and Iain Souttar. A multiscale perspective on maximum marginal likelihood estimation. *arXiv preprint arXiv:2406.04187*, 2024.
- Giovanni Alberti and Luigi Ambrosio. A geometrical approach to monotone functions in  $\mathbb{R}^n$ . *Mathematische Zeitschrift*, 230(2):259–316, 1999.
- Jason M. Altschuler and Sinho Chewi. Faster high-accuracy log-concave sampling via algorithmic warm starts. In *2023 IEEE 64th Annual Symposium on Foundations of Computer Science (FOCS)*, pages 2169–2176, 2023.
- Yves F. Atchadé, Gersende Fort, and Éric Moulines. On perturbed proximal gradient algorithms. *Journal of Machine Learning Research*, 18(10):1–33, 2017.
- Francis R. Bach. Consistency of trace norm minimization. *Journal of Machine Learning Research*, 9(35):1019–1048, 2008.
- Heinz H. Bauschke and Patrick L. Combettes. *Convex Analysis and Monotone Operator Theory in Hilbert Spaces*. Springer Cham, 2017.
- José M Bernardo and Adrian FM Smith. *Bayesian theory*, volume 405. John Wiley & Sons, 2009.
- Espen Bernton. Langevin Monte Carlo and JKO splitting. In Sébastien Bubeck, Vianney Perchet, and Philippe Rigollet, editors, *Proceedings of the 31st Conference On Learning Theory*, volume 75 of *Proceedings of Machine Learning Research*, pages 1777–1798. PMLR, 06–09 Jul 2018.
- Christopher M Bishop. *Pattern recognition and machine learning*, volume 4. Springer, 2006.
- Vladimir I. Bogachev. *Measure Theory*, volume 2. Springer Berlin Heidelberg, Berlin, Heidelberg, 2007.
- Kenneth A. Bollen. Latent variables in psychology and the social sciences. *Annual Review of Psychology*, 53(Volume 53, 2002):605–634, 2002.
- Etienne Boursier, Mikhail Konobeev, and Nicolas Flammarion. Trace norm regularization for multi-task learning with scarce data. In Po-Ling Loh and Maxim Raginsky, editors, *Proceedings of Thirty Fifth Conference on Learning Theory*, volume 178 of *Proceedings of Machine Learning Research*, pages 1303–1327. PMLR, 02–05 Jul 2022.
- Jian-Feng Cai, Emmanuel J. Candès, and Zuowei Shen. A singular value thresholding algorithm for matrix completion. *SIAM Journal on Optimization*, 20(4):1956–1982, 2010.
- Emmanuel J. Candès and Yaniv Plan. Matrix completion with noise. *Proceedings of the IEEE*, 98(6):925–936, 2010.
- Rocco Caprio, Juan Kuntz, Samuel Power, and Adam M. Johansen. Error bounds for particle gradient descent, and extensions of the log-Sobolev and Talagrand inequalities. *arXiv preprint arXiv:2403.02004*, 2024.
- Michel Chavance, Sylvie Escolano, Monique Romon, Arnaud Basdevant, Blandine de Lauzon-Guillain, and Marie Aline Charles. Latent variables and structural equation models for longitudinal relationships: an illustration in nutritional epidemiology. *BMC Medical Research Methodology*, 10(1):37, 2010.

- Yongxin Chen, Sinho Chewi, Adil Salim, and Andre Wibisono. Improved analysis for a proximal algorithm for sampling. In Po-Ling Loh and Maxim Raginsky, editors, *Proceedings of Thirty Fifth Conference on Learning Theory*, volume 178 of *Proceedings of Machine Learning Research*, pages 2984–3014. PMLR, 02–05 Jul 2022.
- Sinho Chewi, Murat A Erdogdu, Mufan Li, Ruoyi Shen, and Shunshi Zhang. Analysis of Langevin Monte Carlo from Poincaré to log-Sobolev. In Po-Ling Loh and Maxim Raginsky, editors, *Proceedings of Thirty Fifth Conference on Learning Theory*, volume 178 of *Proceedings of Machine Learning Research*, pages 1–2. PMLR, 02–05 Jul 2022.
- William F. Christensen and Stephan R. Sain. Latent variable modeling for integrating output from multiple climate models. *Mathematical Geosciences*, 44(4):395–410, 2012.
- Patrick L Combettes and Jean-Christophe Pesquet. Proximal splitting methods in signal processing. *Fixed-point algorithms for inverse problems in science and engineering*, pages 185–212, 2011.
- Francesca R. Crucinio, Alain Durmus, Pablo Jiménez, and Gareth O. Roberts. Optimal Scaling Results for Moreau-Yosida Metropolis-adjusted Langevin Algorithms. *arXiv preprint arXiv:2301.02446*, 2023.
- Arnak S. Dalalyan. Theoretical guarantees for approximate sampling from smooth and log-concave densities. *Journal of the Royal Statistical Society. Series B (Statistical Methodology)*, 79(3):651–676, 2017.
- Valentin De Bortoli, Alain Durmus, Marcelo Pereyra, and Ana F. Vidal. Efficient stochastic optimisation by unadjusted Langevin Monte Carlo. *Statistics and Computing*, 31(3):29, 2021.
- Bernard Delyon, Marc Lavielle, and Éric Moulines. Convergence of a stochastic approximation version of the em algorithm. *The Annals of Statistics*, 27(1):94–128, 1999.
- Arthur P. Dempster, Nan M. Laird, and Donald B. Rubin. Maximum likelihood from incomplete data via the EM algorithm. *Journal of the Royal Statistical Society. Series B (Methodological)*, 39(1):1–38, 1977.
- Michael Diao, Krishnakumar Balasubramanian, Sinho Chewi, and Adil Salim. Forward-backward Gaussian variational inference via JKO in the Bures–Wasserstein space. In *Proceedings of the 40th International Conference on Machine Learning, ICML’23*. JMLR, 2023.
- Alain Durmus and Éric Moulines. Nonasymptotic convergence analysis for the unadjusted Langevin Algorithm. *The Annals of Applied Probability*, 27(3):1551–1587, 2017.
- Alain Durmus and Éric Moulines. High-dimensional Bayesian inference via the unadjusted Langevin algorithm. *Bernoulli*, 25(4A):2854–2882, 2019.
- Alain Durmus, Éric Moulines, and Marcelo Pereyra. Efficient Bayesian Computation by Proximal Markov Chain Monte Carlo: When Langevin Meets Moreau. *SIAM Journal on Imaging Sciences*, 11(1):473–506, 2018.
- Alain Durmus, Szymon Majewski, and Błażej Miasojedow. Analysis of Langevin Monte Carlo via convex optimization. *Journal of Machine Learning Research*, 20(73):1–46, 2019.
- Matthias J Ehrhardt, Lorenz Kuger, and Carola-Bibiane Schönlieb. Proximal Langevin sampling with inexact proximal mapping. *arXiv preprint arXiv:2306.17737*, 2023.
- Bolin Gao and Lacra Pavel. On the properties of the softmax function with application in game theory and reinforcement learning. *arXiv preprint arXiv:1704.00805*, 2017.
- Anupriya Gogna and Angshul Majumdar. Matrix completion incorporating auxiliary information for recommender system design. *Expert Systems with Applications*, 42(14):5789–5799, 2015.
- Edouard Grave, Guillaume R Obozinski, and Francis Bach. Trace lasso: a trace norm regularization for correlated designs. In J. Shawe-Taylor, R. Zemel, P. Bartlett, F. Pereira, and K.Q. Weinberger, editors, *Advances in Neural Information Processing Systems*, volume 24. Curran Associates, Inc., 2011.



- Samuel Gruffaz, Kyurae Kim, Alain Oliviero Durmus, and Jacob R. Gardner. Stochastic Approximation with Biased MCMC for Expectation Maximization. *arXiv preprint arXiv:2402.17870*, 2024.
- Andreas Habring, Martin Holler, and Thomas Pock. Subgradient Langevin methods for sampling from non-smooth potentials. *arXiv preprint arXiv:2308.01417*, 2023.
- Edwin T. Jaynes. Prior probabilities. *IEEE Transactions on Systems Science and Cybernetics*, 4(3): 227–241, 1968.
- Tim Johnston and Sotirios Sabanis. Convergence of the unadjusted Langevin algorithm for discontinuous gradients. *arXiv preprint arXiv:2312.01950*, 2023.
- Tim Johnston, Nikolaos Makras, and Sotirios Sabanis. Taming the Interacting Particle Langevin Algorithm – the superlinear case. *arXiv preprint arXiv:2403.19587*, 2024.
- Ioannis Karatzas and Steven E. Shreve. *Brownian Motion and Stochastic Calculus*. Springer New York, NY, 1991.
- Teresa Klatzer, Paul Dobson, Yoann Altmann, Marcelo Pereyra, Jesús María Sanz-Serna, and Konstantinos C Zygalakis. Accelerated Bayesian imaging by relaxed proximal-point Langevin sampling. *arXiv preprint arXiv:2308.09460*, 2023.
- Manel Kortas, Ammar Bouallegue, Tahar Ezzeddine, Vahid Meghdadi, Oussama Habachi, and Jean-Pierre Cances. Compressive sensing and matrix completion in wireless sensor networks. In *2017 International Conference on Internet of Things, Embedded Systems and Communications (IINTEC)*, pages 9–14, 2017.
- Juan Kuntz, Jen Ning Lim, and Adam M. Johansen. Particle algorithms for maximum likelihood training of latent variable models. In Francisco Ruiz, Jennifer Dy, and Jan-Willem van de Meent, editors, *Proceedings of The 26th International Conference on Artificial Intelligence and Statistics*, volume 206 of *Proceedings of Machine Learning Research*, pages 5134–5180. PMLR, 2023.
- Kenneth Lange. A gradient algorithm locally equivalent to the EM algorithm. *Journal of the Royal Statistical Society. Series B (Methodological)*, 57(2):425–437, 1995.
- Yin Tat Lee, Ruoqi Shen, and Kevin Tian. Structured logconcave sampling with a restricted Gaussian oracle. In Mikhail Belkin and Samory Kpotufe, editors, *Proceedings of Thirty Fourth Conference on Learning Theory*, volume 134 of *Proceedings of Machine Learning Research*, pages 2993–3050. PMLR, 15–19 Aug 2021.
- Qing Li and Nan Lin. The Bayesian elastic net. *Bayesian Analysis*, 5(1):151 – 170, 2010.
- Jen Ning Lim, Juan Kuntz, Samuel Power, and Adam M. Johansen. Momentum Particle Maximum Likelihood. *arXiv preprint arXiv:2312.07335*, 2024.
- Chun Sheng Liu, Bin Wang, Hong Shan, and Shan-shan Li. Survey of matrix completion models. In *2018 Eighth International Conference on Instrumentation & Measurement, Computer, Communication and Control (IMCCC)*, pages 782–787, 2018.
- Morteza Mardani and Georgios B. Giannakis. Estimating traffic and anomaly maps via network tomography. *IEEE/ACM Transactions on Networking*, 24:1533–1547, 2014.
- Giosué Cataldo Marinó, Alessandro Petrini, Dario Malchiodi, and Marco Frasca. Deep neural networks compression: A comparative survey and choice recommendations. *Neurocomputing*, 520:152–170, 2023.
- Herbert W. Marsh and Kit-Tai Hau. Applications of latent-variable models in educational psychology: The need for methodological-substantive synergies. *Contemporary Educational Psychology*, 32(1):151–170, 2007.
- Xiao-Li Meng and Donald B. Rubin. Maximum likelihood estimation via the ECM algorithm: A general framework. *Biometrika*, 80(2):267–278, 1993.

- J.J. Moreau. Proximité et dualité dans un espace Hilbertien. *Bulletin de la Société Mathématique de France*, 93:273–299, 1965.
- Kevin P Murphy. *Machine learning: a probabilistic perspective*. MIT press, 2012.
- Bengt O. Muthén. Latent variable modeling in epidemiology. *Alcohol Health & Research World*, 16(4): 286–292, 1992.
- Radford M. Neal and Geoffrey E. Hinton. *A View of the EM Algorithm that Justifies Incremental, Sparse, and other Variants*, pages 355–368. Springer Netherlands, Dordrecht, 1998.
- Otso Ovaskainen, Nerea Abrego, Panu Halme, and David Dunson. Using latent variable models to identify large networks of species-to-species associations at different spatial scales. *Methods in Ecology and Evolution*, 7(5):549–555, 2016.
- Neal Parikh and Stephen Boyd. Proximal algorithms. *Foundations and Trends in Optimization*, 1(3): 127–239, 2014.
- Grigorios A Pavliotis. *Stochastic Processes and Applications. Diffusion Processes, the Fokker-Planck and Langevin Equations*, volume 60. Springer. Texts in Applied Mathematics., 2014.
- Marcelo Pereyra. Proximal Markov chain Monte Carlo algorithms. *Statistics and Computing*, 26(4): 745–760, 2016.
- Gareth O. Roberts and Richard L. Tweedie. Exponential convergence of Langevin distributions and their discrete approximations. *Bernoulli*, 2(4):341 – 363, 1996.
- Ralph Tyrell Rockafellar. *Convex Analysis*. Princeton University Press, Princeton, 1970.
- Ralph Tyrell Rockafellar. Proximal algorithms. *Journal of Nonlinear and Convex Analysis*, 1:1–16, 1999.
- Ralph Tyrell Rockafellar and Roger J-B Wets. *Variational analysis*, volume 317. Springer Science & Business Media, 2009.
- Adil Salim and Peter Richtarik. Primal dual interpretation of the proximal stochastic gradient Langevin algorithm. In H. Larochelle, M. Ranzato, R. Hadsell, M.F. Balcan, and H. Lin, editors, *Advances in Neural Information Processing Systems*, volume 33, pages 3786–3796. Curran Associates, Inc., 2020.
- Adil Salim, Dmitry Kovalev, and Peter Richtarik. Stochastic proximal Langevin algorithm: Potential splitting and nonasymptotic rates. In H. Wallach, H. Larochelle, A. Beygelzimer, F. d'Alché-Buc, E. Fox, and R. Garnett, editors, *Advances in Neural Information Processing Systems*, volume 32. Curran Associates, Inc., 2019.
- Adrien Saumard and Jon A Wellner. Log-concavity and strong log-concavity: a review. *Statistics Surveys*, 8:45, 2014.
- Mark Schmidt, Nicolas Roux, and Francis Bach. Convergence rates of inexact proximal-gradient methods for convex optimization. In J. Shawe-Taylor, R. Zemel, P. Bartlett, F. Pereira, and K.Q. Weinberger, editors, *Advances in Neural Information Processing Systems*, volume 24. Curran Associates, Inc., 2011.
- Louis Sharrock, Daniel Dodd, and Christopher Nemeth. Tuning-free maximum likelihood training of latent variable models via coin betting. *arXiv preprint arXiv:2305.14916*, 2024.
- Alain-Sol Sznitman. Topics in propagation of chaos. In *Ecole d’été de probabilités de Saint-Flour XIX—1989*, volume 1464 of *Lecture Notes in Mathematics*, pages 165–251. Springer, Berlin, 1991.
- Aki Vehtari, Andrew Gelman, and Jonah Gabry. Practical Bayesian model evaluation using leave-one-out cross-validation and WAIC. *Statistics and Computing*, 27(5):1413–1432, 2017.
- Santosh Vempala and Andre Wibisono. Rapid convergence of the unadjusted Langevin algorithm: Isoperimetry suffices. In H. Wallach, H. Larochelle, A. Beygelzimer, F. d'Alché-Buc, E. Fox, and R. Garnett, editors, *Advances in Neural Information Processing Systems*, volume 32. Curran Associates, Inc., 2019.

- Greg CG Wei and Martin A Tanner. A Monte Carlo implementation of the EM algorithm and the poor man’s data augmentation algorithms. *Journal of the American statistical Association*, 85(411): 699–704, 1990.
- Peter M. Williams. Bayesian Regularization and Pruning Using a Laplace Prior. *Neural Computation*, 7(1):117–143, 1995.
- Yuling Yao, Aki Vehtari, and Andrew Gelman. Stacking for Non-mixing Bayesian Computations: The Curse and Blessing of Multimodal Posteriors. *Journal of Machine Learning Research*, 23(79):1–45, 2022.
- Jihun Yun, Peng Zheng, Eunho Yang, Aurelie Lozano, and Aleksandr Aravkin. Trimming the  $\ell_1$  regularizer: Statistical analysis, optimization, and applications to deep learning. In Kamalika Chaudhuri and Ruslan Salakhutdinov, editors, *Proceedings of the 36th International Conference on Machine Learning*, volume 97 of *Proceedings of Machine Learning Research*, pages 7242–7251. PMLR, 09–15 Jun 2019.
- Ying Zhang, Ö Deniz Akyildiz, Theodoros Damoulas, and Sotirios Sabanis. Nonasymptotic estimates for stochastic gradient Langevin dynamics under local conditions in nonconvex optimization. *Applied Mathematics & Optimization*, 87(2):25, 2023.

# A Theoretical Analysis of Proximal Interacting Langevin Algorithms

## A.1 Approximation of minimisers

Before proceeding with the proof of Theorem 4.1 and 4.2, we derive a result controlling the distance between the maximiser of  $p_\theta(y) = \int_{\mathbb{R}^{d_x}} e^{-U(\theta, x)} dx$ , denoted by  $\bar{\theta}_*$ , and the maximiser of  $p_\theta^\lambda(y) = \int_{\mathbb{R}^{d_x}} e^{-U^\lambda(\theta, x)} dx$ , denoted by  $\bar{\theta}_{\lambda,*}$ .

For simplicity let us denote

$$k_\lambda(\theta) := \int_{\mathbb{R}^{d_x}} e^{-U^\lambda(\theta, x)} dx, \quad k(\theta) := \int_{\mathbb{R}^{d_x}} e^{-U(\theta, x)} dx$$

and  $K_\lambda(\theta) := -\log k_\lambda(\theta)$ .

Let  $\Omega \subset \mathbb{R}^{d_\theta} \times \mathbb{R}^{d_x}$  denote the set on which  $g_2$  is twice differentiable. Let  $\bar{\theta}_*$  be the maximiser of  $k$  and let  $\tilde{\Omega} = \Omega \cap (\{\bar{\theta}_*\} \times \mathbb{R}^{d_x})$ . By **A5**

$$k(\bar{\theta}_*) = \int_{\tilde{\Omega}} e^{-U(\bar{\theta}_*, x)} dx = \int_{\tilde{\Omega}} e^{-U^\lambda(\bar{\theta}_*, x)} dx.$$

Since,  $k$  achieves a maximum at  $\bar{\theta}_*$  and  $g_1, g_2$  are differentiable in  $\tilde{\Omega}$ , then

$$0 = \nabla_\theta k(\bar{\theta}_*) = \nabla_\theta \int_{\tilde{\Omega}} e^{-U(\bar{\theta}_*, x)} dx = - \int_{\tilde{\Omega}} \left( \nabla_\theta g_1(\bar{\theta}_*, x) + \nabla_\theta g_2(\bar{\theta}_*, x) \right) e^{-U(\bar{\theta}_*, x)} dx. \quad (21)$$

**Proposition A.1** (Convergence of minimisers). *Under assumption **A1**, the Lipschitzness of  $g_2$  given by **A3**, the strong convexity assumption **A4** and **A5**, it follows that*

$$\|\bar{\theta}_{\lambda,*} - \bar{\theta}_*\| \leq \frac{\lambda}{\mu} \left( \frac{\|g_2\|_{\text{Lip}}^2}{2} A + B \right) + \mathcal{O}(\lambda^2),$$

where  $\|g_2\|_{\text{Lip}}$  is the Lipschitz constant of  $g_2$  and  $A, B$  are given in **A5**.

*Proof.* To obtain a bound of  $\|\bar{\theta}_{\lambda,*} - \bar{\theta}_*\|$  in terms of  $\lambda$ , we first define the measure  $\pi_\lambda^1 \propto e^{-U^\lambda(\theta, x)}$  and observe that  $\pi_\lambda^1$  is  $\mu$ -strongly log-concave, since  $\pi_\lambda^1 \propto e^{-U^\lambda(\theta, x)}$  and  $U^\lambda$  is strongly convex by **A4**. Therefore, by a form of the Prékopa-Leindler inequality for strong convexity [Saumard and Wellner, 2014, Theorem 3.8],  $\pi_{\lambda,\theta}^1 \propto e^{-K_\lambda(\theta)} = k_\lambda(\theta)$  is  $\mu$ -strongly log-concave, which results in

$$\langle \bar{\theta}_{\lambda,*} - \bar{\theta}_*, \nabla K_\lambda(\bar{\theta}_{\lambda,*}) - \nabla K_\lambda(\bar{\theta}_*) \rangle \geq \mu \|\bar{\theta}_{\lambda,*} - \bar{\theta}_*\|^2. \quad (22)$$

Since,  $\bar{\theta}_{\lambda,*}$  is the maximiser of  $k_\lambda(\theta)$  and  $k_\lambda(\theta)$  is differentiable, it follows that  $\nabla k_\lambda(\bar{\theta}_{\lambda,*}) = 0$  and therefore  $\nabla K_\lambda(\bar{\theta}_{\lambda,*}) = 0$ . Using the Cauchy-Schwarz inequality, we can rearrange (22) to obtain

$$\|\bar{\theta}_{\lambda,*} - \bar{\theta}_*\| \leq \frac{1}{\mu} \|\nabla K_\lambda(\bar{\theta}_{\lambda,*}) - \nabla K_\lambda(\bar{\theta}_*)\| = \frac{1}{\mu} \|\nabla K_\lambda(\bar{\theta}_*)\| = \frac{1}{\mu k_\lambda(\bar{\theta}_*)} \|\nabla k_\lambda(\bar{\theta}_*)\|. \quad (23)$$

We now focus on the term  $\|\nabla k_\lambda(\bar{\theta}_*)\|$

$$\|\nabla k_\lambda(\bar{\theta}_*)\| = \left\| \nabla_\theta \int_{\tilde{\Omega}} e^{-U^\lambda(\bar{\theta}_*, x)} dx \right\| = \left\| \int_{\tilde{\Omega}} \nabla_\theta U^\lambda(\bar{\theta}_*, x) e^{-U^\lambda(\bar{\theta}_*, x)} dx \right\|.$$

Recall that  $U^\lambda(\theta, x) = g_1(\theta, x) + g_2^\lambda(\theta, x)$ . For simplicity, let us assume that  $\nabla_\theta g_1(\theta, x) = 0$ , later we will show that this condition is not necessary. Then, we have that

$$\|\nabla k_\lambda(\bar{\theta}_*)\| = \left\| \int_{\tilde{\Omega}} \nabla_\theta g_2^\lambda(\bar{\theta}_*, x) e^{-U^\lambda(\bar{\theta}_*, x)} dx \right\| = \left\| \int_{\tilde{\Omega}} \frac{\bar{\theta}_* - \text{prox}_{g_2}^\lambda(\bar{\theta}_*, x)_\theta}{\lambda} e^{-U^\lambda(\bar{\theta}_*, x)} dx \right\|. \quad (24)$$

Since  $g_2$  is convex, the problem  $\min_u \{g_2(u) + \|v - u\|^2/(2\lambda)\}$  with  $v = (\theta, x)$  has a unique minimum  $w$  that satisfies  $\lambda \nabla g_2(w) - (v - w) = 0$ . We consider the implicit system  $\phi(\lambda, w) = \lambda \nabla g_2(w) - (v - w)$ , and note that  $\phi(0, v) = 0$  and

$$\frac{\partial \phi(\lambda, w)}{\partial w} = \lambda \nabla^2 g_2(w) + I \succ 0,$$

i.e. positive definite due to Remark 4.2 and assumption **A5**. Thus the Jacobian of  $\phi$  w.r.t.  $w$  is invertible. Hence, the implicit function theorem shows that there is some locally defined  $\zeta$ , such that  $\zeta(0) = v$  and  $\phi(\lambda, \zeta(\lambda)) = 0$ . Furthermore,

$$\begin{aligned} \left. \frac{\partial \phi(\lambda, \zeta(\lambda))}{\partial \lambda} \right|_{\lambda=0} &= \left( \nabla g_2(\zeta(\lambda)) + \lambda \nabla^2 g_2(\zeta(\lambda)) \frac{\partial \zeta(\lambda)}{\partial \lambda} + \frac{\partial \zeta(\lambda)}{\partial \lambda} \right) \Big|_{\lambda=0} = 0, \\ \left. \frac{\partial^2 \phi(\lambda, \zeta(\lambda))}{\partial \lambda^2} \right|_{\lambda=0} &= \left( 2 \nabla^2 g_2(\zeta(\lambda)) \frac{\partial \zeta(\lambda)}{\partial \lambda} + \lambda \frac{\partial}{\partial \lambda} \left( \nabla^2 g_2(\zeta(\lambda)) \frac{\partial \zeta(\lambda)}{\partial \lambda} \right) + \frac{\partial^2 \zeta(\lambda)}{\partial^2 \lambda} \right) \Big|_{\lambda=0} = 0, \end{aligned}$$

which provides

$$\begin{aligned} \frac{\partial \zeta(0)}{\partial \lambda} &= -\nabla g_2(v), \\ \frac{\partial^2 \zeta(0)}{\partial \lambda^2} &= -2 \nabla^2 g_2(v) \nabla g_2(v). \end{aligned}$$

Using Taylor's expansion at  $\lambda = 0$  we have

$$\text{prox}_{g_2}^\lambda(v) = \zeta(\lambda) = v - \lambda \nabla g_2(v) - \lambda^2 \nabla^2 g_2(v) \nabla g_2(v) + \mathcal{O}(\lambda^3). \quad (25)$$

Therefore

$$\frac{\bar{\theta}_* - \text{prox}_{g_2}^\lambda(\bar{\theta}_*, x)_\theta}{\lambda} = \nabla_\theta g_2(\bar{\theta}_*, x) + \lambda [\nabla_{(\theta, x)}^2 g_2(\bar{\theta}_*, x)]_{1:d_\theta} \nabla_{(\theta, x)} g_2(\bar{\theta}_*, x) + \mathcal{O}(\lambda^2), \quad (26)$$

where the notation  $[\nabla_{(\theta, x)}^2 g_2(\bar{\theta}_*, x)]_{1:d_\theta}$  means that we only take the first  $d_\theta$  rows of the Hessian. For simplicity, we denote  $h(\bar{\theta}_*, x) = [\nabla_{(\theta, x)}^2 g_2(\bar{\theta}_*, x)]_{1:d_\theta} \nabla_{(\theta, x)} g_2(\bar{\theta}_*, x)$ .

Substituting (26) in (24), we have

$$\begin{aligned} \|\nabla k_\lambda(\bar{\theta}_*)\| &= \left\| \int_{\bar{\Omega}} (\nabla_\theta g_2(\bar{\theta}_*, x) + \lambda h(\bar{\theta}_*, x) + \mathcal{O}(\lambda^2)) e^{-U^\lambda(\bar{\theta}_*, x)} dx \right\| \\ &\leq \left\| \int_{\bar{\Omega}} \nabla_\theta g_2(\bar{\theta}_*, x) e^{-U^\lambda(\bar{\theta}_*, x)} dx \right\| + \lambda \left( \int_{\bar{\Omega}} \|h(\bar{\theta}_*, X)\| \frac{e^{-U^\lambda(\bar{\theta}_*, x)}}{k_\lambda(\bar{\theta}_*)} dx \right) k_\lambda(\bar{\theta}_*) + \mathcal{O}(\lambda^2) k_\lambda(\bar{\theta}_*) \\ &= \left\| \int_{\bar{\Omega}} \nabla_\theta g_2(\bar{\theta}_*, x) e^{-U^\lambda(\bar{\theta}_*, x)} dx \right\| + \lambda \mathbb{E}_X[\|h(\bar{\theta}_*, X)\|] k_\lambda(\bar{\theta}_*) + \mathcal{O}(\lambda^2) k_\lambda(\bar{\theta}_*). \end{aligned}$$

Subtracting (21) in the first term, we have

$$\begin{aligned} \|\nabla k_\lambda(\bar{\theta}_*)\| &\leq \left\| \int_{\bar{\Omega}} \nabla_\theta g_2(\bar{\theta}_*, x) (e^{-U^\lambda(\bar{\theta}_*, x)} - e^{-U(\bar{\theta}_*, x)}) dx \right\| + (\lambda \mathbb{E}_X[\|h(\bar{\theta}_*, X)\|] + \mathcal{O}(\lambda^2)) k_\lambda(\bar{\theta}_*) \\ &\leq \int_{\bar{\Omega}} \|\nabla_\theta g_2(\bar{\theta}_*, x)\| e^{-U^\lambda(\bar{\theta}_*, x)} (1 - e^{-U(\bar{\theta}_*, x) + U^\lambda(\bar{\theta}_*, x)}) dx + (\lambda \mathbb{E}_X[\|h(\bar{\theta}_*, X)\|] + \mathcal{O}(\lambda^2)) k_\lambda(\bar{\theta}_*) \\ &\leq (1 - e^{-\lambda \|g_2\|_{\text{Lip}}^2/2}) \int_{\bar{\Omega}} \|\nabla_\theta g_2(\bar{\theta}_*, x)\| e^{-U^\lambda(\bar{\theta}_*, x)} dx + (\lambda \mathbb{E}_X[\|h(\bar{\theta}_*, X)\|] + \mathcal{O}(\lambda^2)) k_\lambda(\bar{\theta}_*) \\ &= (1 - e^{-\lambda \|g_2\|_{\text{Lip}}^2/2}) \left( \int_{\bar{\Omega}} \|\nabla_\theta g_2(\bar{\theta}_*, x)\| \frac{e^{-U^\lambda(\bar{\theta}_*, x)}}{k_\lambda(\bar{\theta}_*)} dx \right) k_\lambda(\bar{\theta}_*) \\ &\quad + (\lambda \mathbb{E}_X[\|h(\bar{\theta}_*, X)\|] + \mathcal{O}(\lambda^2)) k_\lambda(\bar{\theta}_*) \end{aligned}$$

where we used the fact that, since  $g_2$  is Lipschitz by **A1**,  $0 \leq U(v) - U^\lambda(v) \leq \frac{\lambda \|g_2\|_{\text{Lip}}^2}{2}$  for  $v = (\theta, x)$ , as shown in the proof of Durmus et al. [2018, Proposition 1].

By **A5**, we further have  $\mathbb{E}_X[\|\nabla_\theta g_2(\bar{\theta}_*, X)\|] \leq A$ ,  $\mathbb{E}_X[\|h(\bar{\theta}_*, X)\|] \leq B$  and thus

$$\begin{aligned} \|\nabla k_\lambda(\bar{\theta}_*)\| &\leq (1 - e^{-\lambda \|g_2\|_{\text{Lip}}^2/2}) \mathbb{E}_X[\|\nabla_\theta g_2(\bar{\theta}_*, X)\|] k_\lambda(\bar{\theta}_*) + (\lambda \mathbb{E}_X[\|h(\bar{\theta}_*, X)\|] + \mathcal{O}(\lambda^2)) k_\lambda(\bar{\theta}_*) \\ &= \left( \lambda \frac{\|g_2\|_{\text{Lip}}^2}{2} \mathbb{E}_X[\|\nabla_\theta g_2(\bar{\theta}_*, X)\|] + \lambda \mathbb{E}_X[\|h(\bar{\theta}_*, X)\|] + \mathcal{O}(\lambda^2) \right) k_\lambda(\bar{\theta}_*) \\ &\leq \lambda \left( \frac{\|g_2\|_{\text{Lip}}^2}{2} A + B \right) k_\lambda(\bar{\theta}_*) + \mathcal{O}(\lambda^2) k_\lambda(\bar{\theta}_*). \end{aligned} \quad (27)$$

Putting together (23) and (27), we get that

$$\|\bar{\theta}_{\lambda,*} - \bar{\theta}_*\| \leq \frac{1}{\mu k_\lambda(\bar{\theta}_*)} \|\nabla k_\lambda(\bar{\theta}_*)\| \leq \frac{\lambda}{\mu} \left( \frac{\|g_2\|_{\text{Lip}}^2}{2} A + B \right) + \frac{1}{\mu} \mathcal{O}(\lambda^2) = \frac{\lambda}{\mu} \left( \frac{\|g_2\|_{\text{Lip}}^2}{2} A + B \right) + \mathcal{O}(\lambda^2).$$

For the case  $\nabla_\theta g_1(\theta, x) \neq 0$ , the same results follows since

$$\begin{aligned}
\|\nabla k_\lambda(\bar{\theta}_*)\| &= \left\| \int_{\bar{\Omega}} \left( \nabla_\theta g_1(\bar{\theta}_*, x) + \frac{\bar{\theta}_* - \text{prox}_{g_2}^\lambda(\bar{\theta}_*, x)}{\lambda} \right) e^{-U^\lambda(\bar{\theta}_*, x)} dx \right\| \\
&\leq \left\| \int_{\bar{\Omega}} (\nabla_\theta g_1(\bar{\theta}_*, x) + \nabla_\theta g_2(\bar{\theta}_*, x)) e^{-U^\lambda(\bar{\theta}_*, x)} dx \right\| + (\lambda \mathbb{E}_X[\|h(\bar{\theta}_*, X)\|] + \mathcal{O}(\lambda^2)) k_\lambda(\bar{\theta}_*) \\
&= \left\| \int_{\bar{\Omega}} \nabla_\theta U(\bar{\theta}_*, x) (e^{-U^\lambda(\bar{\theta}_*, x)} - e^{-U(\bar{\theta}_*, x)}) dx \right\| + (\lambda \mathbb{E}_X[\|h(\bar{\theta}_*, X)\|] + \mathcal{O}(\lambda^2)) k_\lambda(\bar{\theta}_*) \\
&\leq \int_{\bar{\Omega}} \|\nabla_\theta U(\bar{\theta}_*, x)\| e^{-U^\lambda(\bar{\theta}_*, x)} (1 - e^{-U(\bar{\theta}_*, x) + U^\lambda(\bar{\theta}_*, x)}) dx \\
&\quad + (\lambda \mathbb{E}_X[\|h(\bar{\theta}_*, X)\|] + \mathcal{O}(\lambda^2)) k_\lambda(\bar{\theta}_*) \\
&\leq (1 - e^{-\lambda \|g_2\|_{\text{Lip}}^2/2}) \int_{\bar{\Omega}} \|\nabla_\theta U(\bar{\theta}_*, x)\| e^{-U^\lambda(\bar{\theta}_*, x)} dx + (\lambda \mathbb{E}_X[\|h(\bar{\theta}_*, X)\|] + \mathcal{O}(\lambda^2)) k_\lambda(\bar{\theta}_*) \\
&= (1 - e^{-\lambda \|g_2\|_{\text{Lip}}^2/2}) \mathbb{E}_X[\|\nabla_\theta U(\bar{\theta}_*, x)\|] k_\lambda(\bar{\theta}_*) + (\lambda \mathbb{E}_X[\|h(\bar{\theta}_*, X)\|] + \mathcal{O}(\lambda^2)) k_\lambda(\bar{\theta}_*) \\
&= \left( \lambda \frac{\|g_2\|_{\text{Lip}}^2}{2} \mathbb{E}_X[\|\nabla_\theta g_2(\bar{\theta}_*, X)\|] + \lambda \mathbb{E}_X[\|h(\bar{\theta}_*, X)\|] + \mathcal{O}(\lambda^2) \right) k_\lambda(\bar{\theta}_*) \\
&\leq \lambda \left( \frac{\|g_2\|_{\text{Lip}}^2}{2} A + B \right) k_\lambda(\bar{\theta}_*) + \mathcal{O}(\lambda^2) k_\lambda(\bar{\theta}_*).
\end{aligned}$$

□

## A.2 MYIPLA

Following Akyildiz et al. [2023], we have the following results.

**Proposition A.2.** *Assuming conditions **A1** and **A2** hold, there exist a unique strong solution to (9)–(10).*

*Proof.* The proof follows from Karatzas and Shreve [1991] and Akyildiz et al. [2023, Proposition 1]. □

**Proposition A.3** (Invariant measure). *For any  $N \in \mathbb{N}$ , the measure  $\pi_{\lambda, \star}^N(\theta, x_1, \dots, x_N) \propto \exp(-\sum_{i=1}^N U^\lambda(\theta, x_i))$  is an invariant measure for the interacting particle system (9)–(10).*

*Proof.* The proof follows from Proposition 2 of Akyildiz et al. [2023]. □

Therefore, the system (9)–(10) has an invariant measure which admits

$$\pi_{\lambda, \Theta}^N(\theta) \propto \int_{\mathbb{R}^{d_x}} \dots \int_{\mathbb{R}^{d_x}} e^{-\sum_{i=1}^N U^\lambda(\theta, x_i)} dx_1 \dots dx_N = \left( \int_{\mathbb{R}^{d_x}} e^{-U^\lambda(\theta, x)} dx \right)^N = k_\lambda(\theta)^N,$$

as  $\theta$ -marginal and can therefore act as a global optimiser of  $k_\lambda(\theta)$ , or more precisely of  $\log k_\lambda(\theta)$ . That is, let  $K_\lambda(\theta) = -\log k_\lambda(\theta)$ , then  $\pi_{\lambda, \Theta}^N(\theta) \propto \exp(-NK_\lambda(\theta))$ , concentrates around the minimiser of  $K_\lambda(\theta)$ , hence the maximiser of  $k_\lambda(\theta)$  as  $N \rightarrow \infty$ . This is a classical setting in global optimisation, where  $N$  acts as the inverse temperature parameter. We now analyse the rate at which  $\pi_{\lambda, \Theta}$  concentrates around the maximiser of  $k(\theta)$ .

**Proposition A.4** (Concentration bound). *Let  $\pi_{\lambda, \Theta}^N$  be as defined above and  $\bar{\theta}_*$ ,  $\bar{\theta}_{\lambda, \star}$  be the maximisers of  $k(\theta)$ ,  $k_\lambda(\theta)$ , respectively. Then, under assumption **A1**, the Lipschitzness of  $g_2$  (**A3**), the strong convexity assumption **A4** and assumption **A5**, it follows*

$$W_2(\pi_{\lambda, \Theta}^N, \delta_{\bar{\theta}_*}) \leq W_2(\pi_{\lambda, \Theta}^N, \delta_{\bar{\theta}_{\lambda, \star}}) + \|\bar{\theta}_{\lambda, \star} - \bar{\theta}_*\| \leq \sqrt{\frac{d_\theta}{\mu N}} + \frac{\lambda}{\mu} \left( \frac{\|g_2\|_{\text{Lip}}^2}{2} A + B \right) + \mathcal{O}(\lambda^2),$$

where  $d_\theta$  is the dimension of the parameter space  $\Theta$  and  $\|g_2\|_{\text{Lip}}$  is the Lipschitz constant for  $g_2$ .

*Proof.* Using a form of the Prékopa-Leindler inequality for strong convexity [Saumard and Wellner, 2014, Theorem 3.8],  $\pi_{\lambda, \Theta}^N$  is  $N\mu$ -strongly log-concave. Since it is also smooth, we can apply Lemma A.8 of Altschuler and Chewi [2023] to obtain a convergence bound for  $W_2(\pi_{\lambda, \Theta}^N, \delta_{\bar{\theta}_{\lambda, \star}})$ ,

$$W_2(\pi_{\lambda, \Theta}^N, \delta_{\bar{\theta}_{\lambda, \star}}) \leq \sqrt{\frac{d_\theta}{\mu N}}. \quad (28)$$

On the other hand, the 2-Wasserstein distance between two degenerate distributions satisfies

$$W_2(\delta_{\bar{\theta}_{\lambda,*}}, \delta_{\bar{\theta}_*}) = \|\bar{\theta}_{\lambda,*} - \bar{\theta}_*\|. \quad (29)$$

By the triangular inequality the Wasserstein distance  $W_2(\pi_{\lambda,\Theta}^N, \delta_{\bar{\theta}_*})$  is upper bounded by the sum of (28)-(29). We then conclude using Proposition A.1.  $\square$

The main difference with earlier works in the previous concentration bound are the second and third terms, which result from the Moreau-Yosida approximation of the non-differentiable target density  $\pi$ . Following on the assumptions made above and the smoothness of  $\pi_{\lambda,\Theta}^N$ , we have similar results to Propositions 4 and 5 of Akyildiz et al. [2023], establishing exponential ergodicity of (9)-(10) and analysing the time-discretised scheme (13)-(14).

Combining all these results, we can provide specific bounds on the accuracy of MYIPLA in terms of  $N, \gamma, n, \lambda$  and the convexity properties of  $U$ .

**Theorem A.1** (Theorem 4.1 restated). *Let **A1–A5** hold. Then for every  $\lambda$  and  $\gamma_0 \in (0, \min\{(L_{g_1} + \lambda^{-1})^{-1}, 2\mu^{-1}\})$  there exist constants  $C_1 > 0$  independent of  $t, n, N, \gamma, \lambda, d_\theta, d_x$  such that for every  $\gamma \in (0, \gamma_0]$ , one has*

$$\begin{aligned} \mathbb{E}[\|\theta_n^N - \bar{\theta}_*\|^2]^{1/2} &\leq \sqrt{\frac{d_\theta}{N\mu}} + \frac{\lambda}{\mu} \left( \frac{\|g_2\|_{\text{Lip}}^2}{2} A + B \right) + e^{-\mu n \gamma} \left( \mathbb{E}[\|Z_0^N - z_*\|^2]^{1/2} + \left( \frac{d_x N + d_\theta}{N\mu} \right)^{1/2} \right) \\ &\quad + C_1(1 + \sqrt{d_\theta/N + d_x})\gamma^{1/2} + \mathcal{O}(\lambda^2) \end{aligned}$$

for all  $n \in \mathbb{N}$ , where  $z_* = (\theta_*, N^{-1/2}x_*, \dots, N^{-1/2}x_*)$  and  $(\theta_*, x_*)$  is the minimiser of  $U^\lambda$ .

*Proof.* Let us denote by  $\mathcal{L}(\theta_n^N)$  the  $\theta$ -marginal of the measure associated to the law of MYIPLA and  $\mathcal{L}(\theta_t^N)$  the  $\theta$ -marginal of the measure associated to the law of interacting particle system (9)-(10) at time  $t$ . The expectation of the norm can be decomposed into a term involving the difference between the maximisers of the marginal maximum likelihood of the Moreau-Yosida approximation of the joint density and the original density, a term concerning the concentration of  $\pi_{\lambda,\Theta}^N$  around the marginal maximum likelihood estimator  $\bar{\theta}_*$ , a term describing the convergence of (9)-(10) to its invariant measure, and a term involving the error induced by the time discretisation.

The first two terms are upper bounded by Proposition A.4, the third and fourth inequalities result from Proposition 4 and Proposition 5 of Akyildiz et al. [2023].  $\square$

### A.3 PIPULA

To study the theoretical guarantees of PIPULA, we observe that PIPULA is equivalent to MYIPLA when  $\gamma = \lambda$  and  $g_1 = 0$ . We recall that in the case  $g_1 = 0$ ,  $\nabla U^\gamma$  is Lipschitz in both variables with constant  $L \leq \gamma^{-1}$  [Durmus et al., 2018]. To obtain a similar result to Theorem 4.1 we introduce the following additional assumption.

**B 1.** *We assume that there exists  $\mu > 0$  such that  $\langle v - v', \text{prox}_U^\gamma(v) - \text{prox}_U^\gamma(v') \rangle \leq (1 - \mu)\|v - v'\|^2$ , for all  $v, v' \in \mathbb{R}^{d_\theta} \times \mathbb{R}^{d_x}$ .*

**B1** implies that  $\nabla U^\gamma$  is  $\mu$ -strongly convex, i.e.  $\langle v - v', \nabla U^\gamma(v) - \nabla U^\gamma(v') \rangle \geq \mu\|v - v'\|^2$  for all  $v, v' \in \mathbb{R}^{d_x} \times \mathbb{R}^{d_\theta}$ . In addition, since  $U$  is a proper convex function we have that  $U$  is twice differentiable almost everywhere (see the discussion below **A5**). Let  $\Omega \subset \mathbb{R}^{d_\theta} \times \mathbb{R}^{d_x}$  denote the points where  $U$  is twice differentiable,  $\bar{\theta}_*$  be the maximiser of  $k$  and  $\tilde{\Omega} = \Omega \cap (\{\bar{\theta}_*\} \times \mathbb{R}^{d_x})$ .

Using a similar strategy to that used to obtain the error bound in Theorem 4.1, we obtain the following result for PIPULA.

**Corollary A.2.** *Let **A1–A3**, **A5** and **B1** hold. Then for every  $\gamma_0 \in (0, 2\mu^{-1})$  there exist constants  $C_1 > 0$  independent of  $t, n, N, \gamma, \lambda, d_\theta, d_x$  such that for every  $\gamma \in (0, \gamma_0]$ , one has*

$$\begin{aligned} \mathbb{E}[\|\theta_n^N - \bar{\theta}_*\|^2]^{1/2} &\leq \sqrt{\frac{d_\theta}{N\mu}} + \frac{\gamma}{\mu} \left( \frac{\|g_2\|_{\text{Lip}}^2}{2} A + B \right) \\ &\quad + e^{-\mu n \gamma} \left( \mathbb{E}[\|Z_0^N - z_*\|^2]^{1/2} + \left( \frac{d_x N + d_\theta}{N\mu} \right)^{1/2} \right) \\ &\quad + C_1(1 + \sqrt{d_\theta/N + d_x})\gamma^{1/2} + \mathcal{O}(\gamma^2) \end{aligned}$$

for all  $n \in \mathbb{N}$ , where  $z_* = (\theta_*, N^{-1/2}x_*, \dots, N^{-1/2}x_*)$  and  $(\theta_*, x_*)$  is the minimiser of  $U^\gamma$ .

*Proof.* Under **A1–A3**, **A5** and **B1** Propositions A.1, A.2, A.3, A.4 and Proposition 4 of Akyildiz et al. [2023] hold with  $\lambda = \gamma$ . To obtain a bound on the discretisation error observe that under **B1**  $U^\gamma$  is strongly convex, since  $\nabla U^\gamma$  is also Lipschitz continuous with constant  $L \leq \gamma^{-1}$  [Durmus et al., 2018, Proposition 1], we have that  $\nabla U^\gamma$  is co-coercive (see Theorem 1 in Gao and Pavel [2017])

$$\begin{aligned} \langle \nabla U^\gamma(x) - \nabla U^\gamma(y), x - y \rangle &\geq \frac{1}{L} \|\nabla U^\gamma(x) - \nabla U^\gamma(y)\|^2 \\ &\geq \gamma \|\nabla U^\gamma(x) - \nabla U^\gamma(y)\|^2, \end{aligned} \quad (30)$$

for every  $x, y \in \mathbb{R}^d$ . By plugging this result into the proof of Akyildiz et al. [2023, Lemma B.1] we obtain an equivalent result to that of Akyildiz et al. [2023, Proposition 5]:

$$W_2(\mathcal{L}(\theta_n^N), \mathcal{L}(\theta_{n\gamma}^N)) \leq C_1(1 + \sqrt{d_\theta/N + d_x})\gamma^{1/2},$$

where  $C_1 > 0$  is independent of  $t, n, N, \gamma, d_\theta, d_x$  and  $\gamma \in (0, \gamma_0)$  with  $\gamma_0 \in (0, 2\mu^{-1})$ .  $\square$

## A.4 PIPGLA

Recall that PIPGLA is given by the following scheme

$$\begin{aligned} \theta_{n+1/2}^N &= \theta_n^N - \frac{\gamma}{N} \sum_{j=1}^N \nabla_{\theta} g_1(\theta_n^N, X_n^{j,N}) + \sqrt{\frac{2\gamma}{N}} \xi_{n+1}^{0,N}, \\ X_{n+1/2}^{i,N} &= X_n^{i,N} - \gamma \nabla_x g_1(\theta_n^N, X_n^{i,N}) + \sqrt{2\gamma} \xi_{n+1}^{i,N}, \\ \theta_{n+1}^N &= \frac{1}{N} \sum_{i=1}^N \text{prox}_{g_2}^\lambda \left( \theta_{n+1/2}^N, X_{n+1/2}^{i,N} \right)_\theta, \quad X_{n+1}^{i,N} = \text{prox}_{g_2}^\lambda \left( \theta_{n+1/2}^N, X_{n+1/2}^{i,N} \right)_x. \end{aligned}$$

We want to prove a bound for  $W_2(\mathcal{L}(\theta_n^N), \delta_{\bar{\theta}_*})$ , where  $\mathcal{L}(\theta_n^N)$  denotes the distribution of the random variable  $\theta_n^N$ . Applying the triangular inequality for Wasserstein distances

$$W_2(\mathcal{L}(\theta_n^N), \delta_{\bar{\theta}_*}) \leq W_2(\delta_{\bar{\theta}_*}, \pi_\Theta^N) + W_2(\pi_\Theta^N, \mathcal{L}(\theta_n^N)). \quad (31)$$

We begin by presenting some results that will be useful for proving a bound for  $W_2(\pi_\Theta^N, \mathcal{L}(\theta_n^N))$ .

### A.4.1 Error bound for proximal gradient Langevin algorithm

We collect here a number of results adapted from Salim et al. [2019] which show convergence of the proximal gradient Langevin algorithm (PGLA) introduced in Salim et al. [2019] and recalled in Section 2.3.2. In particular, we derive convergence of the splitting scheme for general  $\lambda$  (which includes as a special case  $\lambda = \gamma$ ) when both  $\nabla g_1$  and  $\text{prox}_{g_2}^\lambda$  can be computed exactly (which is a special case of the result in Salim et al. [2019] in the case  $\lambda = \gamma$ ).

For convenience we consider the following decomposition of the PGLA update targeting a distribution  $\pi_\lambda \propto \exp(-(g_1 + g_2^\lambda))$  over  $\mathbb{R}^d$

$$\begin{aligned} Z_n &= X_n - \gamma \nabla g_1(X_n), \\ Y_n &= Z_n + \sqrt{2\gamma} \xi_n, \\ X_{n+1} &= \text{prox}_{g_2}^\lambda(Y_n). \end{aligned}$$

We are going to derive a bound for  $W_2(\mathcal{L}(X_{n+1}), \pi_\lambda)$ , where  $\mathcal{L}(X_{n+1})$  denotes the distribution of the random variable  $X_{n+1}$ . For every  $\pi$ -integrable function  $g : \mathbb{R}^d \rightarrow \mathbb{R}$ , we define  $\mathcal{E}_g(\pi) = \int g d\pi$  and we denote  $\mathcal{F} = \mathcal{E}_{g_1+g_2} + \mathcal{H}$ , where  $\mathcal{H}$  is the negative entropy  $\mathcal{H}(\pi) = \int \log \pi d\pi$ . We also introduce the subdifferential of a convex function and its minimal section, since we will use them for our proofs.

**Definition A.1** (Subdifferential and minimal section). For any convex function  $g : \mathbb{R}^d \rightarrow \mathbb{R}$ , its subdifferential evaluated at  $x$  is the set

$$\partial g(x) := \{d \in \mathbb{R}^d \mid g(x) + \langle d, y - x \rangle \leq g(y) \forall y \in \mathbb{R}^d\}.$$

Thanks to Bauschke and Combettes [2017, Proposition 16.4], we have that  $\partial g(x)$  is a nonempty closed convex set. So the projection of 0 onto  $\partial g(x)$ , that is, the least norm element in the set  $\partial g(x)$ , is well defined, and we refer to this element as  $\nabla^0 g(x)$ . Following Salim et al. [2019, Section 3.1], we name the function  $\nabla^0 g : \mathbb{R}^d \rightarrow \mathbb{R}$  the minimal section of  $\partial g$ .



Following Salim et al. [2019], we derive our results under the following assumptions on  $g_1, g_2$ .

**D1.** We assume that  $g_1 \in \mathcal{C}^1$  is convex, gradient Lipschitz with constant  $L_{g_1}$  and lower bounded, and  $g_2$  is proper, convex, lower semi-continuous and lower bounded.

**D2.**  $g_1$  is  $\mu$ -strongly convex.

**D3.** Assume that  $\|\nabla^0 g_2(x)\|^2 \leq C$  for every  $x \in \mathbb{R}^d$ .

In particular, **D1** and **D2** are equivalent to **A1** and **A4** for the target  $\pi_\lambda(\theta, x) \propto \exp(-U^\lambda(\theta, x))$ . Similarly, **D3** is equivalent to **C1**.

**Lemma A.5.** Let **D1** and **D2** hold and assume  $\gamma \leq 1/L_{g_1}$ . Then, for all  $n \in \mathbb{N}$

$$2\gamma[\mathcal{E}_{g_1}(\mathcal{L}(Z_n)) - \mathcal{E}_{g_1}(\pi)] \leq (1 - \gamma\mu)W_2^2(\mathcal{L}(X_n), \pi) - W_2^2(\mathcal{L}(Z_n), \pi).$$

*Proof.* Let  $a \in \mathbb{R}^d$ , using that  $g_1$  is  $\mu$ -strongly convex

$$\begin{aligned} \|Z_n - a\|^2 &= \|X_n - a\|^2 - 2\gamma\langle \nabla g_1(X_n), X_n - a \rangle + \gamma^2 \|\nabla g_1(X_n)\|^2 \\ &\leq \|X_n - a\|^2 + 2\gamma(g_1(a) - g_1(X_n) - \frac{\mu}{2}\|X_n - a\|^2) + \gamma^2 \|\nabla g_1(X_n)\|^2 \\ &= (1 - \gamma\mu)\|X_n - a\|^2 + 2\gamma(g_1(a) - g_1(X_n)) + \gamma^2 \|\nabla g_1(X_n)\|^2. \end{aligned} \quad (32)$$

Since  $g_1$  is gradient Lipschitz with constant  $L_{g_1}$  and  $Z_n - X_n = -\gamma\nabla g_1(X_n)$

$$\begin{aligned} g_1(Z_n) &\leq g_1(X_n) + \langle \nabla g_1(X_n), Z_n - X_n \rangle + \frac{L_{g_1}}{2}\|Z_n - X_n\|^2 \\ &= g_1(X_n) - \gamma\left(1 - \frac{\gamma L_{g_1}}{2}\right)\|\nabla g_1(X_n)\|^2 \\ &\leq g_1(X_n) - \frac{\gamma}{2}\|\nabla g_1(X_n)\|^2, \end{aligned}$$

where in the last inequality we have used that  $\gamma \leq 1/L_{g_1}$ . Reordering terms gives the following upper bound

$$\gamma^2 \|\nabla g_1(X_n)\|^2 \leq 2\gamma(g_1(X_n) - g_1(Z_n)).$$

Plugging this into (32) we have

$$\|Z_n - a\|^2 \leq (1 - \gamma\mu)\|X_n - a\|^2 + 2\gamma(g_1(a) - g_1(Z_n)).$$

It is important to note, the above inequality is true for any  $a$ ,  $X_n$ , and  $Z_n$  where  $Z_n = X_n - \gamma\nabla g_1(X_n)$  (as deterministic vectors with appropriate dimension). Now, let  $(a, X_n) \sim \nu(\mathrm{d}a, \mathrm{d}x_n)$  with marginal  $\nu^a(\mathrm{d}a) = \pi(\mathrm{d}a)$ . Taking conditional expectation w.r.t.  $Z_n$  given  $\sigma(a, X_n)$ , we obtain

$$\mathbb{E}[\|Z_n - a\|^2 | \sigma(a, X_n)] \leq (1 - \gamma\mu)\|X_n - a\|^2 + 2\gamma(g_1(a) - \mathbb{E}[g_1(Z_n) | \sigma(a, X_n)]).$$

By taking the unconditional expectation (i.e. w.r.t.  $\nu$ ), we get

$$\mathbb{E}[\|Z_n - a\|^2] \leq (1 - \gamma\mu)\mathbb{E}_\nu[\|X_n - a\|^2] + 2\gamma(\mathcal{E}_{g_1}(\pi) - \mathcal{E}_{g_1}(\mathcal{L}(Z_n))).$$

By the definition of the Wasserstein distance we get

$$W_2^2(\mathcal{L}(Z_n), \pi) \leq (1 - \gamma\mu)\mathbb{E}_\nu[\|X_n - a\|^2] + 2\gamma(\mathcal{E}_{g_1}(\pi) - \mathcal{E}_{g_1}(\mathcal{L}(Z_n))).$$

Note that the last inequality is true for all  $\nu$  with prescribed marginal above. In particular, we can take the infimum over all such couplings and inequality would still hold for the infimum. This leads to

$$W_2^2(\mathcal{L}(Z_n), \pi) \leq (1 - \gamma\mu)W_2^2(\mathcal{L}(X_n), \pi) + 2\gamma(\mathcal{E}_{g_1}(\pi) - \mathcal{E}_{g_1}(\mathcal{L}(Z_n))),$$

which is the desired result.  $\square$

**Lemma A.6.** Let  $g : \mathbb{R}^d \rightarrow \mathbb{R}$  be a convex function and  $g^\lambda$  its  $\lambda$ -Moreau-Yosida approximation. Consider  $a, y_0, y_1 \in \mathbb{R}^d$  such that  $y_1 = \text{prox}_g^\lambda(y_0)$ . Then,

$$\|y_1 - a\|^2 \leq \|y_0 - a\|^2 - 2\lambda(g(y_0) - g(a)) + \lambda^2 \|\nabla g^0(y_0)\|^2.$$

*Proof.* Recalling that  $\text{prox}_g^\lambda(y_0) = y_0 - \lambda \nabla g^\lambda(y_0)$  we have

$$\|y_1 - a\|^2 = \|y_0 - a\|^2 - 2\lambda \langle \nabla g^\lambda(y_0), y_0 - a \rangle + \lambda^2 \|\nabla g^\lambda(y_0)\|^2. \quad (33)$$

Using that  $y_1 = y_0 - \lambda \nabla g^\lambda(y_0)$  we can write

$$\langle \nabla g^\lambda(y_0), y_0 - a \rangle = \langle \nabla g^\lambda(y_0), y_1 - a \rangle + \lambda \|\nabla g^\lambda(y_0)\|^2.$$

Since  $\nabla g^\lambda(y_0)$  belongs to the subdifferential of  $g(y_1)$ , i.e.  $\nabla g^\lambda(x) \in \partial g(\text{prox}_g^\lambda(x))$  [Bauschke and Combettes, 2017, Proposition 16.44], we further have that

$$\langle \nabla g^\lambda(y_0), y_1 - a \rangle \geq g(y_1) - g(a),$$

from which we obtain

$$-2\lambda \langle \nabla g^\lambda(y_0), y_0 - a \rangle \leq -2\lambda (g(y_1) - g(a) + \lambda \|\nabla g^\lambda(y_0)\|^2).$$

Recalling the definition of Moreau-Yosida approximation in Definition 2.2 we have that  $g^\lambda(y_0) = g(y_1) + \|y_0 - y_1\|^2/(2\lambda)$ ; plugging this into the equation above gives

$$\begin{aligned} -2\lambda \langle \nabla g^\lambda(y_0), y_0 - a \rangle &\leq -2\lambda (g^\lambda(y_0) - g(a)) - 2\lambda^2 \|\nabla g^\lambda(y_0)\|^2 + \|y_1 - y_0\|^2 \\ &= -2\lambda (g^\lambda(y_0) - g(a)) - \lambda^2 \|\nabla g^\lambda(y_0)\|^2. \end{aligned} \quad (34)$$

Finally, using Salim et al. [2019, Lemma 9] which states that  $g^\lambda(x) \geq g(x) - \lambda \|\nabla^0 g(x)\|/2$ , where  $\nabla^0 g$  is the minimal section introduced in Definition A.1, and combining (33) and (34) we have

$$\|y_1 - a\|^2 \leq \|y_0 - a\|^2 - 2\lambda (g^\lambda(y_0) - g(a)) \leq \|y_0 - a\|^2 - 2\lambda (g(y_0) - g(a)) + \lambda^2 \|\nabla^0 g(x)\|^2.$$

□

**Lemma A.7.** *Let D1–D3 hold. Then,*

$$2\lambda [\mathcal{E}_{g_2}(\mathcal{L}(Y_n)) - \mathcal{E}_{g_2}(\pi)] \leq W_2^2(\mathcal{L}(Y_n), \pi) - W_2^2(\mathcal{L}(X_{n+1}), \pi) + \lambda^2 C$$

*Proof.* Applying Lemma A.6 with  $y_0 = Y_n$ ,  $y_1 = X_{n+1}$  and  $g = g_2$ , we have

$$\|X_{n+1} - a\|^2 \leq \|Y_n - a\|^2 - 2\lambda (g_2(Y_n) - g_2(a)) + \lambda^2 \|\nabla^0 g_2(Y_n)\|^2.$$

Now, let  $a$  be a random vector sampled from the distribution with density  $\pi$ . Taking expectations in the previous expression and using the definition of the Wasserstein distance we obtain

$$\begin{aligned} W_2^2(\mathcal{L}(X_{n+1}), \pi) &\leq \mathbb{E}[\|Y_n - a\|^2] - 2\lambda (\mathcal{E}_{g_2}(\mathcal{L}(Y_n)) - \mathcal{E}_{g_2}(\pi)) + \lambda^2 \mathbb{E}[\|\nabla^0 g_2(Y_n)\|^2] \\ &\leq \mathbb{E}[\|Y_n - a\|^2] - 2\lambda (\mathcal{E}_{g_2}(\mathcal{L}(Y_n)) - \mathcal{E}_{g_2}(\pi)) + \lambda^2 C. \end{aligned}$$

Finally, taking the infimum over all couplings  $Y_n, a$  of  $\mathcal{L}(Y_n), \pi$ , it follows that

$$W_2^2(\mathcal{L}(X_{n+1}), \pi) \leq W_2^2(\mathcal{L}(Y_n), \pi) - 2\lambda (\mathcal{E}_{g_2}(\mathcal{L}(Y_n)) - \mathcal{E}_{g_2}(\pi)) + \lambda^2 C.$$

□

**Theorem A.3.** *Let D1–D3 hold and assume that  $\gamma \leq 1/L_{g_1}$ . Then, for all  $n \in \mathbb{N}$*

$$\begin{aligned} 2\gamma \text{KL}(\mathcal{L}(Y_n) \mid \pi) &\leq (1 - \gamma\mu) W_2^2(\mathcal{L}(X_n), \pi) - \frac{\gamma}{\lambda} W_2^2(\mathcal{L}(X_{n+1}), \pi) \\ &\quad - \left(1 - \frac{\gamma}{\lambda}\right) W_2^2(\mathcal{L}(Y_n), \pi) + \gamma(2\gamma L_{g_1} d + \lambda C). \end{aligned}$$

*Proof.* Since  $g_1 + g_2$  is convex by assumption the following holds  $\pi \in \mathcal{P}_2(\mathbb{R}^d)$ ,  $\mathcal{H}(\pi) < \infty$ ,  $\mathcal{E}_{g_1+g_2}(\pi) < \infty$  and for all  $\mu \in \mathcal{P}_2(\mathbb{R}^d)$  satisfying  $\mathcal{E}_{g_1+g_2}(\mu) < \infty$ ,

$$\text{KL}(\mu \mid \pi) = \mathcal{E}_{g_1+g_2}(\mu) + \mathcal{H}(\mu) - (\mathcal{E}_{g_1+g_2}(\pi) + \mathcal{H}(\pi)) = \mathcal{F}(\mu) - \mathcal{F}(\pi).$$

We can further decompose  $\mathcal{E}_{g_1+g_2}(\mu) = \mathcal{E}_{g_1}(\mu) + \mathcal{E}_{g_2}(\mu)$ . Using Durmus et al. [2019, Lemma 5] we have that the negative entropy satisfies the following inequality

$$2\gamma [\mathcal{H}(\mathcal{L}(Y_n)) - \mathcal{H}(\pi)] \leq W_2^2(\mathcal{L}(Z_n), \pi) - W_2^2(\mathcal{L}(Y_n), \pi). \quad (35)$$

Since  $g_1$  is  $L_{g_1}$ -gradient Lipschitz and strongly convex, it follows that

$$0 \leq g_1(Y_n) - g_1(Z_n) + \langle \nabla g_1(Z_n), Z_n - Y_n \rangle \leq \frac{L_{g_1}}{2} \|Y_n - Z_n\|^2.$$

Note that  $Y_n - Z_n = \sqrt{2\gamma}\xi_n$  is independent of  $Z_n$ ,  $\mathbb{E}[Y_n - Z_n] = 0$  and  $\mathbb{E}[\|Y_n - Z_n\|^2] = 2\gamma d$ , where  $d$  is the dimension of the standard Gaussian random variable  $\xi_n$ . Therefore, taking expectations in the previous inequality we get

$$2\gamma[\mathcal{E}_{g_1}(\mathcal{L}(Y_n)) - \mathcal{E}_{g_1}(\mathcal{L}(Z_n))] \leq 2\gamma^2 L_{g_1} d. \quad (36)$$

On the other hand, by Lemmas A.5 and A.7 we have

$$2\gamma[\mathcal{E}_{g_1}(\mathcal{L}(Z_n)) - \mathcal{E}_{g_1}(\pi)] \leq (1 - \gamma\mu)W_2^2(\mathcal{L}(X_n), \pi) - W_2^2(\mathcal{L}(Z_n), \pi), \quad (37)$$

$$2\gamma[\mathcal{E}_{g_2}(\mathcal{L}(Y_n)) - \mathcal{E}_{g_2}(\pi)] \leq \frac{\gamma}{\lambda}W_2^2(\mathcal{L}(Y_n), \pi) - \frac{\gamma}{\lambda}W_2^2(\mathcal{L}(X_{n+1}), \pi) + \gamma\lambda C. \quad (38)$$

Summing up (35)-(38) and using that  $\text{KL}(\mathcal{L}(Y_n) \mid \pi) = \mathcal{F}(\mathcal{L}(Y_n)) - \mathcal{F}(\pi)$  we have the desired result.  $\square$

**Corollary A.4.** *Let **D1-D3** hold and assume that  $\gamma \leq 1/L_{g_1}$  and  $\gamma \leq \lambda \leq \gamma/(1 - \mu\gamma)$ . Then*

$$W_2^2(\mathcal{L}(X_n), \pi) \leq \frac{\lambda^n(1 - \gamma\mu)^n}{\gamma^n} W_2^2(\mathcal{L}(X_0), \pi) + \frac{\lambda(2\gamma L_{g_1} d + \lambda C)}{1 - \lambda(1 - \mu\gamma)/\gamma}.$$

*Proof.* Since the KL divergence and the Wasserstein distance are always non-negative and we assume that  $\gamma \leq \lambda$ , we have by Theorem A.3 that for all  $n \in \mathbb{N}$

$$W_2^2(\mathcal{L}(X_{n+1}), \pi) \leq \frac{\lambda(1 - \gamma\mu)}{\gamma} W_2^2(\mathcal{L}(X_n), \pi) + \lambda(2\gamma L_{g_1} d + \lambda C).$$

Unrolling this recurrence we get

$$\begin{aligned} W_2^2(\mathcal{L}(X_n), \pi) &\leq \frac{\lambda^n(1 - \gamma\mu)^n}{\gamma^n} W_2^2(\mathcal{L}(X_0), \pi) + \lambda(2\gamma L_{g_1} d + \lambda C) \sum_{i=0}^{n-1} \frac{\lambda^i(1 - \gamma\mu)^i}{\gamma^i} \\ &\leq \frac{\lambda^n(1 - \gamma\mu)^n}{\gamma^n} W_2^2(\mathcal{L}(X_0), \pi) + \frac{\lambda(2\gamma L_{g_1} d + \lambda C)}{1 - \lambda(1 - \gamma\mu)/\gamma}, \end{aligned}$$

where we have used the assumption  $\lambda \leq \gamma/(1 - \mu\gamma)$ .  $\square$

#### A.4.2 Convergence and discretisation bounds

We start by showing that the results established above can be applied to a proximal gradient scheme in which the noise is scaled by  $\sqrt{N}$

$$\begin{aligned} V_{n+1/2} &= V_n - \gamma \nabla g_1(V_n) + \sqrt{\frac{2\gamma}{N}} \xi_n, \\ V_{n+1} &= V_{n+1/2} - \lambda \nabla g_2^\lambda(V_{n+1/2}). \end{aligned} \quad (39)$$

**Corollary A.5** (Rescaled noise). *Let **D1-D3** hold and assume that  $\gamma \leq 1/L_{g_1}$  and  $\gamma \leq \lambda \leq \gamma/(1 - \mu\gamma)$ . Then,*

$$W_2^2(\mathcal{L}(V_n), \pi^N) \leq \frac{\lambda^n(1 - \gamma\mu)^n}{\gamma^n} W_2^2(\mathcal{L}(V_0), \pi^N) + \frac{\lambda(2\gamma L_{g_1} d + \lambda N C)}{N(1 - \lambda(1 - \mu\gamma)/\gamma)}.$$

*Proof.* Let  $\tilde{g}_1 = Ng_1$  and  $\tilde{g}_2 = Ng_2$ . It is easy to check that  $\tilde{g}_1$  is  $(NL_{g_1})$ -gradient Lipschitz and  $(N\mu)$ -strongly convex. In addition, we have that

$$\text{prox}_{g_2}^\lambda(x) = \arg \min_{z \in \mathbb{R}^d} \frac{\tilde{g}_2(x)}{N} + \frac{\|x - z\|^2}{2\lambda} = \arg \min_{z \in \mathbb{R}^d} \frac{1}{N} \left( \tilde{g}_2(x) + \frac{\|x - z\|^2}{2\lambda/N} \right) = \text{prox}_{\tilde{g}_2}^{\lambda/N}(x),$$

since the arg min does not change if the function is multiplied by a constant, which results in  $\nabla g_2^\lambda = \nabla \tilde{g}_2^{\lambda/N}/N$ . Thus, (39) can be rewritten as

$$\begin{aligned} V_{n+1/2} &= V_n - \tilde{\gamma} \nabla \tilde{g}_1(V_n) + \sqrt{2\tilde{\gamma}} \xi_n, \\ V_{n+1} &= V_{n+1/2} - \tilde{\lambda} \nabla \tilde{g}_2^{\tilde{\lambda}}(V_{n+1/2}), \end{aligned}$$

where  $\tilde{\gamma} = \gamma/N$  and  $\tilde{\lambda} = \lambda/N$ . Note that the subdifferential set satisfies  $\partial\tilde{g}_2 = N\partial g_2$ . Therefore, since  $\|\nabla^0 g_2(x)\|^2 \leq C$  for all  $x \in \mathbb{R}^d$  by **D3**, it follows that  $\|\nabla^0 \tilde{g}_2(x)\|^2 \leq N^2 C$ . Therefore, taking  $\tilde{\gamma} \leq 1/(NL_{g_1})$  which is equivalent to  $\gamma \leq 1/L_{g_1}$ , and applying Corollary A.4 the result follows.  $\square$

In order to be able to use the bound obtained in Corollary A.5, we rewrite PIPGLA as the algorithm given in (39). To do so, define

$$G_1(z_\theta, z_1, \dots, z_N) = \frac{1}{N} \sum_{i=1}^N g_1(z_\theta, \sqrt{N}z_i),$$

$$G_2^\lambda(z_\theta, z_1, \dots, z_N) = \frac{1}{N} \sum_{i=1}^N g_2^\lambda(z_\theta, \sqrt{N}z_i).$$

Note that the gradients of these functions are given by

$$\nabla G_1(z_\theta, z_1, \dots, z_N) = \left( N^{-1} \sum_{i=1}^N \nabla_{\theta} g_1(z_\theta, \sqrt{N}z_i), N^{-1/2} \nabla_{z_1} g_1(z_\theta, \sqrt{N}z_1), \dots, N^{-1/2} \nabla_{z_N} g_1(z_\theta, \sqrt{N}z_N) \right)^\top$$

and similarly for  $G_2^\lambda$ .

Taking  $Z_n = (\theta_n^N, N^{-1/2} X_n^{1,N}, \dots, N^{-1/2} X_n^{N,N})$ , PIPGLA can be expressed as

$$Z_{n+1/2} = Z_n - \gamma \nabla G_1(Z_n) + \sqrt{\frac{2\gamma}{N}} \xi_{n+1}, \quad (40)$$

$$Z_{n+1} = Z_{n+1/2} - \lambda \nabla G_2^\lambda(Z_{n+1/2}).$$

**Corollary A.6.** *Let  $Z_n = (\theta_n^N, N^{-1/2} X_n^{1,N}, \dots, N^{-1/2} X_n^{N,N})$  and  $\pi^N \propto \exp(-N(G_1 + G_2))$ . Suppose that **A1**, **A4** and **C1** hold true and assume  $\gamma \leq 1/L_{g_1}$  and  $\gamma \leq \lambda \leq \gamma/(1 - \mu\gamma)$ . Then,*

$$W_2^2(\mathcal{L}(Z_n), \pi^N) \leq \frac{\lambda^n (1 - \gamma\mu)^n}{\gamma^n} W_2^2(\mathcal{L}(Z_0), \pi^N) + \frac{\lambda(2\gamma L_{g_1}(d_\theta + Nd_x) + \lambda NC)}{N(1 - \lambda(1 - \mu\gamma)/\gamma)}.$$

*Proof.* Note that if **C1** holds then  $\|\nabla^0 G_2(z)\|^2 \leq C$  for every  $z$ . To see this note that

$$\partial G_2(z) = \partial G_2(z_\theta, z_1, \dots, z_N) = \frac{1}{N} \sum_{i=1}^N \partial g_2(z_\theta, \sqrt{N}z_i).$$

Therefore, using the fact that  $(N^{-1} \sum_i a_i)^2 \leq N^{-1} \sum_i a_i^2$ , we get that the minimal section satisfies

$$\|\nabla^0 G_2(z)\|^2 \leq \frac{1}{N} \sum_{i=1}^N \|\nabla^0 g_2(z_\theta, \sqrt{N}z_i)\|^2 \leq C.$$

In addition, observe that **A1**, **A4** imply that  $G_1, G_2$  and  $G_2^\lambda$  are convex since  $g_1, g_2$  and  $g_2^\lambda$  are convex, and  $G_1$  is also  $\mu$ -strongly convex and  $L_{g_1}$ -gradient Lipschitz. The proof then follows from Corollary A.5.  $\square$

Before proving our final result for  $W_2(\mathcal{L}(\theta_n^N), \delta_{\bar{\theta}_*})$ , we provide a result adapted from Altschuler and Chewi [2023, Lemma A.8] to our non-differentiable setting that will be useful to bound the first term of (31).

**Lemma A.8.** *Suppose that the distribution  $\pi \propto \exp(-f)$  on  $\mathbb{R}^d$  is  $\alpha$ -strongly log-concave, almost everywhere differentiable and that  $x^*$  is the minimiser of  $f$ . Then,*

$$\mathbb{E}_{X \sim \pi}[\|X - x^*\|^2] \leq d/\alpha.$$

*Proof.* Let  $\Omega \subset \mathbb{R}^d$  denote the set of differentiable points of  $f$ , note that when  $f$  is convex and differentiable at  $x \in \Omega$ , then  $\partial f(x) = \{\nabla f(x)\}$ , that is, its gradient is its only subgradient. Recall also that  $f$  is strongly convex, so for every  $x, y \in \mathbb{R}^d$  we have that

$$\langle \partial f(x), x - y \rangle \geq \alpha \|x - y\|^2.$$

Integration by parts shows that for any smooth function  $\phi : \mathbb{R}^d \rightarrow \mathbb{R}$  of controlled growth, it holds that

$$0 = \int_{\Omega} (\Delta \phi - \langle \nabla f, \nabla \phi \rangle) d\pi = \mathbb{E}_{X \sim \pi}[\Delta \phi - \langle \nabla f, \nabla \phi \rangle]. \quad (41)$$

Applying (41) to the function  $\phi(x) := \|x - x^*\|^2/2$ , for which  $\nabla \phi(x) = x - x^*$  and  $\Delta \phi = d$ , together with the strong convexity of  $f$ , the result follows.  $\square$

To conclude we present the following theorem that provides a convergence bound for PIPGLA in terms of  $N, \gamma, n, \lambda$  and the convexity properties of  $U$ .

**Theorem A.7** (Theorem 4.2 restated). *Let **A1–A5** and **C1** hold. Then for  $\gamma \leq 1/L_{g_1}$  and  $\gamma \leq \lambda \leq \gamma/(1 - \mu\gamma)$ , PIPGLA satisfies*

$$W_2(\mathcal{L}(\theta_n^N), \delta_{\theta_*}) \leq \sqrt{\frac{d_\theta}{N\mu}} + \frac{\lambda^{n/2}(1 - \gamma\mu)^{n/2}}{\gamma^{n/2}} W_2(\mathcal{L}(Z_0^N), \pi^N) + \left( \frac{\lambda(2\gamma L_{g_1}(d_\theta + Nd_x) + \lambda NC)}{N(1 - \lambda(1 - \mu\gamma)/\gamma)} \right)^{1/2}$$

for all  $n \in \mathbb{N}$ .

*Proof.* Using a form of the Prékopa-Leindler inequality for strong convexity [Saumard and Wellner, 2014, Theorem 3.8],  $\pi_\Theta$  is  $\mu$ -strongly log-concave. Therefore,  $\pi_\Theta^N$  is  $N\mu$ -strongly log-concave and satisfies all the assumptions of Lemma A.8. So, we have that

$$W_2(\delta_{\theta_*}, \pi_\Theta^N)^2 \leq \frac{d_\theta}{N\mu}.$$

On the other hand, note that  $\pi^N(z) \propto \exp(-N(G_1(z) + G_2(z))) = \exp(-\sum_i U(z_\theta, \sqrt{N}z_i))$ . By Corollary A.6 it follows that

$$W_2(\mathcal{L}(\theta_n^N), \pi_\Theta^N) \leq W_2(\mathcal{L}(Z_n), \pi^N) \leq \sqrt{\frac{\lambda^n(1 - \gamma\mu)^n}{\gamma^n} W_2^2(\mathcal{L}(Z_0^N), \pi^N) + \frac{\lambda(2\gamma L_{g_1}(d_\theta + Nd_x) + \lambda NC)}{N(1 - \lambda(1 - \mu\gamma)/\gamma)}}.$$

Using that  $\sqrt{x+y} \leq \sqrt{x} + \sqrt{y}$ , we have

$$W_2(\mathcal{L}(\theta_n^N), \pi_\Theta^N) \leq \frac{\lambda^{n/2}(1 - \gamma\mu)^{n/2}}{\gamma^{n/2}} W_2(\mathcal{L}(Z_0^N), \pi^N) + \left( \frac{\lambda(2\gamma L_{g_1}(d_\theta + Nd_x) + \lambda NC)}{N(1 - \lambda(1 - \mu\gamma)/\gamma)} \right)^{1/2}.$$

The proof then follows from (31) and the above.  $\square$

## B Theoretical Analysis of Proximal Particle Gradient Descent

### B.1 Background on Particle Gradient Descent of Kuntz et al. [2023]

The PGD algorithm relies on the perspective that the MMLE problem can be solved by minimising the free energy

$$F(\theta, q) = \int \log(q(x))q(x)dx + \int U(\theta, x)q(x)dx \quad (42)$$

for all  $(\theta, q) \in \Theta \times \mathcal{P}(\mathbb{R}^{d_x})$ , where  $\Theta$  denotes the parameter space and  $U(\theta, x) := -\log p_\theta(x, y)$ . Kuntz et al. [2023] propose a discretisation of a gradient flow associated with (42), where they endow  $\Theta$  with the Euclidean geometry and  $\mathcal{P}(\mathbb{R}^{d_x})$  with the 2-Wasserstein one to take gradients. This leads to the Euclidean-Wasserstein gradient flow of  $F$

$$\begin{aligned} \dot{\theta}_t &= -\nabla_\theta F(\theta_t, q_t) = -\int \nabla_\theta U(\theta_t, x)q_t(x)dx, \\ \dot{q}_t &= -\nabla_q F(\theta_t, q_t) = \nabla_x \cdot \left[ q_t \nabla_x \log \left( \frac{q_t}{p_{\theta_t}(\cdot, y)} \right) \right]. \end{aligned} \quad (43)$$

Kuntz et al. [2023] prove that the gradient  $\nabla F(\theta, q)$  vanishes if and only if  $\theta$  is a stationary point of  $p_\theta(y)$  and  $q$  is its corresponding posterior. Based on the observation that (43) is a Fokker-Planck equation satisfied by the law of a McKean-Vlasov SDE, and using a finite number of particles  $(X_t^{i,N})_{i=1}^N$  to estimate  $q_t$ , they obtain the following approximation, for  $t \geq 0$ ,

$$\begin{aligned} d\theta_t^N &= -\frac{1}{N} \sum_{i=1}^N \nabla_\theta U(\theta_t^N, \mathbf{X}_t^{i,N})dt, \\ d\mathbf{X}_t^{i,N} &= -\nabla_x U(\theta_t^N, \mathbf{X}_t^{i,N})dt + \sqrt{2}d\mathbf{B}_t^{i,N}, \quad i = 1, \dots, N, \end{aligned} \quad (44)$$

---

**Algorithm 3** Moreau-Yosida Particle Gradient Descent (MYPGD)

---

**Require:**  $N, K, \lambda, \gamma, \pi_{\text{init}} \in \mathcal{P}(\mathbb{R}^{d_\theta}) \times \mathcal{P}((\mathbb{R}^{d_x})^N)$

Draw  $(\theta_0, \{X_0^{i,N}\}_{i=1}^N)$  from  $\pi_{\text{init}}$

**for**  $n = 0 : K$  **do**

$$\theta_{n+1}^N = \left(1 - \frac{\gamma}{\lambda}\right) \theta_n^N + \frac{\gamma}{N} \sum_{i=1}^N \left( -\nabla_{\theta} g_1(\theta_n^N, X_n^{i,N}) + \frac{1}{\lambda} \text{prox}_{g_2}^{\lambda}(\theta_n^N, X_n^{i,N})_{\theta} \right)$$

$$X_{n+1}^{i,N} = \left(1 - \frac{\gamma}{\lambda}\right) X_n^{i,N} - \gamma \nabla_x g_1(\theta_n^N, X_n^{i,N}) + \frac{\gamma}{\lambda} \text{prox}_{g_2}^{\lambda}(\theta_n^N, X_n^{i,N})_x + \sqrt{2\gamma} \xi_{n+1}^{i,N}$$

**end for**

**return**  $\theta_{K+1}^N$

---

where  $(\mathbf{B}_t^{i,N})_{t \geq 0}$  for  $i = 0, \dots, N$  are  $d_x$ -dimensional Brownian motions. Using a simple Euler–Maruyama discretisation with step size  $\gamma > 0$  of (44) one obtains the particle gradient descent (PGD) algorithm [Kuntz et al., 2023]

$$\begin{aligned} \theta_{n+1} &= \theta_n - \frac{\gamma}{N} \sum_{j=1}^N \nabla_{\theta} U(\theta_n, X_n^{j,N}), \\ X_{n+1}^{i,N} &= X_n^{i,N} - \gamma \nabla_x U(\theta_n, X_n^{i,N}) + \sqrt{2\gamma} \xi_{n+1}^{i,N}, \quad i = 1, \dots, N, \end{aligned}$$

where  $(\xi_n)$  for  $n \geq 0$  are  $d_x$ -dimensional i.i.d. standard Gaussians.

## B.2 Proximal Particle Gradient Descent

Similar to the approach we have taken in the main text, we can also provide a proximal version of the PGD algorithm. As mentioned in the main text, if we remove the noise term in the dynamics of  $\theta$ , we obtain

$$d\theta_t^N = -\frac{1}{N} \sum_{i=1}^N \nabla_{\theta} U^{\lambda}(\theta_t^N, \mathbf{X}_t^{i,N}) dt, \quad (45)$$

$$d\mathbf{X}_t^{i,N} = -\nabla_x U^{\lambda}(\theta_t^N, \mathbf{X}_t^{i,N}) dt + \sqrt{2} d\mathbf{B}_t^{i,N}. \quad (46)$$

We can then provide an algorithm which is a discretisation of (45)-(46), termed Moreau-Yosida Particle Gradient Descent (MYPGD), analogous to MYIPLA. The algorithm is given in Algorithm 3.

We extend the results of Caprio et al. [2024] to provide a nonasymptotic bound for MYPGD. To do so, we consider the following metric on  $\mathbb{R}^{d_\theta} \times \mathcal{P}_2(\mathbb{R}^{d_x})$

$$\mathbf{d}((\theta, q), (\theta', q')) = \sqrt{\|\theta - \theta'\|^2 + W_2^2(q, q')}.$$

Under similar assumptions to those used in Theorem 4.1 we obtain the following result.

**Theorem B.1** (MYPGD). *Let **A1–A5** hold. If  $X_0^1, \dots, X_0^N$  are drawn independently from a distribution  $q_0$  in  $\mathcal{P}_2(\mathbb{R}^{d_x})$  and  $\lambda > 0$ ,  $\gamma \leq 1/(L_{g_1} + \lambda^{-1} + \mu)$ , then*

$$\begin{aligned} \mathbb{E}[\|\theta_n^N - \bar{\theta}_*\|^2]^{1/2} &\leq \frac{\lambda}{\mu} \left( \frac{\|g_2\|_{\text{Lip}}^2}{2} A + B \right) + \frac{(L_{g_1} + \lambda^{-1})\sqrt{2}}{\mu\sqrt{N}} \sqrt{B_0 + \frac{2d_x}{\mu}} \\ &\quad + \mathbf{d}((\theta_0, q_0), (\bar{\theta}_{*,\lambda}, \pi_{*,\lambda})) e^{-\mu n \gamma} + A_{0,\gamma,\lambda} \gamma^{1/2} + \mathcal{O}(\lambda^2) \end{aligned}$$

for all  $n \in \mathbb{N}$ ; where  $B_0 = \|\theta_0\|^2 + \sup_{i \in 1, \dots, N} \mathbb{E}[\|X_0^{i,N}\|^2] < \infty$  and

$$A_{0,\gamma,\lambda} = \sqrt{\frac{4\gamma + 4/a}{a} 220(L_{g_1} + \lambda^{-1})^2 \left( \gamma(L_{g_1} + \lambda^{-1})^2 \left[ B_0 + \frac{2d_x}{\mu} \right] + d_x \right)}, \quad a = \frac{2(L_{g_1} + \lambda^{-1})\mu}{L_{g_1} + \lambda^{-1} + \mu}.$$

*Proof.* Let us denote by  $(\theta_n^N, Q_n^{N,\gamma})$  the MYPGD output after  $n$  iterations using a discretisation step  $\gamma$  and by  $Q_{*,\lambda}^N$  the empirical distribution of  $N$  i.i.d. particles drawn from  $\pi_{\bar{\theta}_{*,\lambda}}$ . Using the triangular inequality, we have

$$\mathbb{E}[\|\theta_n^N - \bar{\theta}_*\|^2]^{1/2} \leq \|\bar{\theta}_* - \bar{\theta}_{*,\lambda}\| + \mathbb{E}[\|\theta_n^N - \bar{\theta}_{*,\lambda}\|^2]^{1/2} \leq \|\bar{\theta}_* - \bar{\theta}_{*,\lambda}\| + \mathbf{d}((\theta_n^N, Q_n^{N,\gamma}), (\bar{\theta}_{*,\lambda}, Q_{*,\lambda}^N)).$$

The term  $\|\bar{\theta}_* - \bar{\theta}_{*,\lambda}\|$  can be upper bounded by  $\frac{\lambda}{\mu} \left( \frac{\|g_2\|_{\text{Lip}}^2}{2} A + B \right) + \mathcal{O}(\lambda^2)$  using Proposition A.1, while a bound for the second term  $\mathbf{d}((\theta_n^N, Q_n^{N,\gamma}), (\bar{\theta}_{*,\lambda}, Q_{*,\lambda}^N))$  is derived in Caprio et al. [2024, Theorem 7], which gives the desired result.  $\square$

Selecting  $\gamma = \lambda$  and  $g_1 = 0$  in MYPGD we obtain an extension of PGD corresponding to the PIPULA algorithm introduced in Section 3.1.1, that we termed Proximal PGD (PPGD). Obtaining a rigorous bound like that in Theorem B.1 for this algorithm is more challenging due to the presence of  $\gamma$  both as time discretisation parameter and in the Lipschitz constant of  $\nabla U^\gamma$ . In particular, while under **A1–A3**, **A5** and **B1** Caprio et al. [2024, Lemma 10 and 11] hold with  $\lambda = \gamma$ , establishing a result controlling the time discretisation error like that in Caprio et al. [2024, Lemma 12] is not straightforward.

## C Convergence to Wasserstein gradient flow

We now show that the continuous time interacting particle system introduced in (9)–(10) converges in the large  $N$  limit (i.e.  $N \rightarrow \infty$ ) to a McKean–Vlasov SDE with a solution whose law satisfies the Euclidean–Wasserstein gradient flow

$$\begin{aligned}\dot{\theta}_{\lambda,t} &= -\nabla_\theta F(\theta_{\lambda,t}, q_{\lambda,t}) = -\int \nabla_\theta U^\lambda(\theta_{\lambda,t}, x) q_{\lambda,t}(x) dx, \\ \dot{q}_{\lambda,t} &= -\nabla_q F(\theta_{\lambda,t}, q_{\lambda,t}) = \nabla_x \cdot \left[ q_{\lambda,t} \nabla_x \log \left( \frac{q_{\lambda,t}}{p_{\theta_{\lambda,t}}^\lambda(\cdot, y)} \right) \right],\end{aligned}$$

where  $p_{\theta_{\lambda,t}}^\lambda$  denotes the Moreau–Yosida envelope of  $p_{\theta_{\lambda,t}}$ . This result is classical in the study of McKean–Vlasov SDEs, where is referred to as *propagation of chaos* (e.g. Sznitman [1991, Theorem 1.4]).

We start by proving the following auxiliary result. Let us denote, for any  $\theta \in \mathbb{R}^{d_\theta}$  and  $\nu \in \mathcal{P}(\mathbb{R}^{d_x})$ ,  $g(\theta, \nu) := \int_{\mathbb{R}^{d_x}} \nabla_\theta U^\lambda(\theta, x') \nu(x') dx'$ .

**Lemma C.1.** *The function  $g : \mathbb{R}^{d_\theta} \times \mathcal{P}(\mathbb{R}^{d_x}) \rightarrow \mathbb{R}^{d_\theta}$  is Lipschitz continuous in both arguments, i.e.,*

$$\|g(\theta_1, \nu_1) - g(\theta_2, \nu_2)\| \leq \lambda^{-1} (\|\theta_1 - \theta_2\| + W_1(\nu_1, \nu_2)).$$

*Proof.* Rockafellar and Wets [2009, Proposition 12.19] shows that  $\nabla U^\lambda$  is Lipschitz continuous with Lipschitz constant  $\lambda^{-1}$ . Then the result follows from Akyildiz et al. [2023, Lemma 5].  $\square$

We can now show convergence of (9)–(10) to the following McKean–Vlasov SDE

$$\begin{aligned}d\theta_{\lambda,t} &= - \left[ \int \nabla_\theta U^\lambda(\theta_{\lambda,t}, x) q_{\lambda,t}(x) dx \right] dt \\ d\mathbf{X}_{\lambda,t} &= -\nabla_x U^\lambda(\theta_{\lambda,t}, \mathbf{X}_{\lambda,t}) dt + \sqrt{2} d\mathbf{B}_t.\end{aligned}\tag{47}$$

**Proposition C.2** (Propagation of chaos). *For any (exchangeable) initial condition  $(\theta_0^N, X_0^{1:N})$  such that  $(\theta_0^N, X_0^{j,N}) = (\theta_0, X_0)$  for  $j = 1, \dots, N$  with  $\mathbb{E} [|\theta_0|^2 + |X_0|^2] < \infty$ , we have for any  $T \geq 0$*

$$\mathbb{E} \left[ \sup_{t \in [0, T]} \left( \|\theta_{\lambda,t} - \theta_t^N\| + \|\mathbf{X}_{\lambda,t} - \mathbf{X}_t^{j,N}\| \right) \right] \leq \frac{\sqrt{2}(\sqrt{C_T} \lambda^{-1} + \sqrt{T}) e^{2T\lambda^{-1}}}{N^{1/2}}\tag{48}$$

where  $C_T := \sup_{t \leq T} \mathbb{E} [|\theta_t^N|^2 + |\mathbf{X}_t^{j,N}|^2] < \infty$ , for any  $j = 1, \dots, N$ .

*Proof.* The proof exploits the Lipschitz continuity of  $\nabla U^\lambda$  and of  $g$  established in Lemma C.1. The argument is classical and omitted, see Akyildiz et al. [2023, Proposition 8] for the proof in a similar context.  $\square$

We can further show that (47) converges to the following MKVSDE

$$\begin{aligned}d\theta_t &= - \left[ \int \nabla_\theta U(\theta_t, x) q_t(x) dx \right] dt \\ d\mathbf{X}_t &= -\nabla_x U(\theta_t, \mathbf{X}_t) dt + \sqrt{2} d\mathbf{B}_t,\end{aligned}\tag{49}$$

associated with the gradient flow (43), when  $\lambda \rightarrow 0$ .

**Proposition C.3.** Assume that  $U$  is gradient Lipschitz with constant  $\|\nabla U\|_{\text{Lip}}$ . For any initial condition  $(\theta_0, X_0)$  such that  $\mathbb{E}[|\theta_0|^2 + |X_0|^2] < \infty$ , we have for any  $T \geq 0$

$$\mathbb{E} \left[ \sup_{t \in [0, T]} (\|\theta_{\lambda, t} - \theta_t\|^2 + \|\mathbf{X}_{\lambda, t} - \mathbf{X}_t\|^2) \right] \leq (\lambda^2 \|\nabla U\|_{\text{Lip}}^4 C_T + \|\nabla U\|_{\text{Lip}}^2 \mathcal{O}(\lambda^4)) T \exp(2\|\nabla U\|_{\text{Lip}}^2 T),$$

where  $C_T := \sup_{t \leq T} \mathbb{E}[|\theta_{\lambda, t}|^2 + |\mathbf{X}_{\lambda, t}|^2] < \infty$ . It follows that, as  $\lambda \rightarrow 0$ , (47) converges to (49) in  $\mathbb{L}^2$ .

*Proof.* For any  $t \geq 0$ , we have

$$\begin{aligned} \theta_t &= \theta_0 + \int_0^t \left[ - \int \nabla_{\theta} U(\theta_s, x) q_s(x) dx \right] ds, \\ \mathbf{X}_t &= X_0 - \int_0^t \nabla_x U(\theta_s, \mathbf{X}_s) ds + \sqrt{2} \mathbf{B}_t, \end{aligned}$$

and equivalently for  $\theta_{\lambda, t}, \mathbf{X}_{\lambda, t}$ . We first observe that

$$\begin{aligned} \|\theta_{\lambda, t} - \theta_t\|^2 &= \left\| \int_0^t \left[ \int \nabla_{\theta} U^{\lambda}(\theta_{\lambda, s}, x) q_{\lambda, s}(x) dx - \int \nabla_{\theta} U(\theta_s, x) q_s(x) dx \right] ds \right\|^2 \\ &= \left\| \int_0^t \mathbb{E} \left[ \nabla_{\theta} U^{\lambda}(\theta_{\lambda, s}, \mathbf{X}_{\lambda, s}) - \nabla_{\theta} U(\theta_s, \mathbf{X}_s) \right] ds \right\|^2 \\ &\leq \mathbb{E} \left[ \left\| \int_0^t [\nabla_{\theta} U^{\lambda}(\theta_{\lambda, s}, \mathbf{X}_{\lambda, s}) - \nabla_{\theta} U(\theta_s, \mathbf{X}_s)] ds \right\|^2 \right], \end{aligned}$$

and

$$\mathbb{E} [\|\mathbf{X}_{\lambda, t} - \mathbf{X}_t\|^2] = \mathbb{E} \left[ \left\| \int_0^t [\nabla_x U(\theta_s, \mathbf{X}_s) - \nabla_x U^{\lambda}(\theta_{\lambda, s}, \mathbf{X}_{\lambda, s})] ds \right\|^2 \right].$$

Combining the above we obtain

$$\begin{aligned} \mathbb{E} \left[ \sup_{s \in [0, t]} \|\theta_{\lambda, s} - \theta_s\|^2 + \mathbb{E} [\|\mathbf{X}_{\lambda, s} - \mathbf{X}_s\|^2] \right] &\leq \mathbb{E} \left[ \int_0^t \|\nabla U(\theta_s, \mathbf{X}_s) - \nabla U^{\lambda}(\theta_{\lambda, s}, \mathbf{X}_{\lambda, s})\|^2 ds \right] \\ &\leq 2\mathbb{E} \left[ \int_0^t \|\nabla U(\theta_s, \mathbf{X}_s) - \nabla U(\theta_{\lambda, s}, \mathbf{X}_{\lambda, s})\|^2 ds \right] \\ &\quad + 2\mathbb{E} \left[ \int_0^t \|\nabla U(\theta_{\lambda, s}, \mathbf{X}_{\lambda, s}) - \nabla U^{\lambda}(\theta_{\lambda, s}, \mathbf{X}_{\lambda, s})\|^2 ds \right] \\ &\leq 2\|\nabla U\|_{\text{Lip}}^2 \int_0^t (\|\theta_{\lambda, s} - \theta_s\|^2 + \mathbb{E} [\|\mathbf{X}_{\lambda, s} - \mathbf{X}_s\|^2]) ds \\ &\quad + 2\mathbb{E} \left[ \int_0^t \|\nabla U(\theta_{\lambda, s}, \mathbf{X}_{\lambda, s}) - \nabla U^{\lambda}(\theta_{\lambda, s}, \mathbf{X}_{\lambda, s})\|^2 ds \right]. \end{aligned}$$

In the case in which  $\nabla U$  is Lipschitz continuous, we further have that  $\nabla U^{\lambda}(v) = \nabla U(\text{prox}_U^{\lambda}(v))$  for  $v = (\theta, x)$  [Pereyra, 2016, Section 2], and we have

$$\|\nabla U(v) - \nabla U^{\lambda}(v)\| = \|\nabla U(v) - \nabla U(\text{prox}_U^{\lambda}(v))\| \leq \|\nabla U\|_{\text{Lip}} \|v - \text{prox}_U^{\lambda}(v)\|.$$

Recalling that, since  $U$  is gradient Lipschitz,  $\text{prox}_U^{\lambda}(v) = v - \lambda \nabla U(v) + \mathcal{O}(\lambda^2)$  [Parikh and Boyd, 2014, Section 3.3], we further have that

$$\begin{aligned} \|\nabla U(v) - \nabla U^{\lambda}(v)\| &\leq \|\nabla U\|_{\text{Lip}} (\lambda \|\nabla U(v)\| + \mathcal{O}(\lambda^2)) \\ &\leq \|\nabla U\|_{\text{Lip}} (\lambda \|\nabla U\|_{\text{Lip}} (1 + \|v\|) + \mathcal{O}(\lambda^2)), \end{aligned} \tag{50}$$

and we can bound

$$\begin{aligned} &\mathbb{E} \left[ \int_0^t \|\nabla U(\theta_{\lambda, s}, \mathbf{X}_{\lambda, s}) - \nabla U^{\lambda}(\theta_{\lambda, s}, \mathbf{X}_{\lambda, s})\|^2 ds \right] \\ &\leq \lambda^2 \|\nabla U\|_{\text{Lip}}^4 \int_0^t \mathbb{E} [1 + \|(\theta_{\lambda, s}, \mathbf{X}_{\lambda, s})\|^2] ds + \|\nabla U\|_{\text{Lip}}^2 \mathcal{O}(\lambda^4) t \\ &\leq \lambda^2 \|\nabla U\|_{\text{Lip}}^4 C_T t + \|\nabla U\|_{\text{Lip}}^2 \mathcal{O}(\lambda^4) t \end{aligned}$$



with  $C_T$  given in the statement of the result.

Let us denote by  $h(t) = \sup_{s \in [0, t]} \|\theta_{\lambda, s} - \theta_s\|^2 + \mathbb{E}[\|\mathbf{X}_{\lambda, s} - \mathbf{X}_s\|^2]$ . Then, using the bounds above we have that

$$h(t) \leq 2\|\nabla U\|_{\text{Lip}}^2 \int_0^t h(s) ds + (\lambda^2 \|\nabla U\|_{\text{Lip}}^4 C_T + \|\nabla U\|_{\text{Lip}}^2 \mathcal{O}(\lambda^4)) t.$$

Using Gronwall's inequality we obtain

$$h(t) \leq (\lambda^2 \|\nabla U\|_{\text{Lip}}^4 C_T + \|\nabla U\|_{\text{Lip}}^2 \mathcal{O}(\lambda^4)) t \exp(2\|\nabla U\|_{\text{Lip}}^2 t),$$

from which the result follows.  $\square$

## D Experiments Details

### D.1 Derivation of the proximal operators

#### D.1.1 Laplace prior with unknown mean $\theta$

We recall that using a Laplace prior  $g_2(\theta, x) = \sum_{i=1}^{d_x} |x_i - \theta|$ .

$$\text{prox}_{g_2}^\lambda(\theta, x) = \arg \min_{(u_0, u)} h(u_0, u) = \arg \min_{(u_0, u)} \{g_2(u_0, u) + \|(u_0, u) - (\theta, x)\|^2 / (2\lambda)\}.$$

The first order optimality condition is given by

$$0 \in \partial g_2(u_0, u) + \nabla(\|(u_0, u) - (\theta, x)\|^2 / (2\lambda)).$$

We recall that  $\phi \in \mathbb{R}^d$  is a subdifferential of the  $\ell^1$ -norm at  $x \in \mathbb{R}^d$  if and only if  $\phi_i(x) = \text{sign}(x_i)$  if  $x_i \neq 0$  and  $|\phi_i(x)| \leq 1$  otherwise [Parikh and Boyd, 2014].

Let us define the set  $D = \{i \in \{1, \dots, d_x\} | u_i - u_0 = 0\}$ . Then, the first order optimality condition becomes

$$\begin{aligned} 0 \in & \left\{ -\sum_{i \notin D} t_i - \sum_{i \notin D} \text{sign}(u_i - u_0) + (u_0 - \theta)/\lambda \mid |t_i| \leq 1 \right\} \\ & \begin{cases} 0 \in \{t_i + \frac{u_i - x_i}{\lambda} \mid |t_i| \leq 1\} & \text{if } i \in D \\ 0 = \text{sign}(u_i - u_0) + (u_i - x_i)/\lambda & \text{if } i \notin D \end{cases} \end{aligned}$$

Reordering terms, we get

$$u_0 \in \left\{ \theta + \lambda \left( \sum_{i \notin D} t_i - \sum_{i \notin D} \text{sign}(u_i - u_0) \right) \mid |t_i| \leq 1 \right\}, \quad (51)$$

$$\begin{cases} u_i \in \{x_i - \lambda t_i \mid |t_i| \leq 1\} & \text{if } i \in D, \\ u_i = x_i - \lambda \text{sign}(u_i - \theta) & \text{if } i \notin D. \end{cases} \quad (52)$$

Assuming that  $D = \emptyset$ , the previous system of equations can be solved iteratively using a fixed point algorithm.

Alternatively, for a lower computational cost we can obtain an approximate solution by setting  $u_0 = \theta$  in (52)

$$\begin{cases} u_i \in \{x_i - \lambda t_i \mid |t_i| \leq 1\} & \text{if } i \in D, \\ u_i = x_i - \lambda \text{sign}(u_i - \theta) & \text{if } i \notin D. \end{cases}$$

which is solved applying the soft-thresholding operator

$$u_i = \theta + [x_i - \theta - \lambda \text{sign}(x_i - \theta)] \mathbb{1}_{\{|x_i - \theta| \geq \lambda\}}.$$

Using these  $u_i$ 's, taking  $u_0 = \theta$  in the right-hand side of (51) and assuming  $D = \emptyset$ , we obtain

$$u_0 = \theta + \lambda \sum_{i=1}^{d_x} \text{sign}(u_i - \theta).$$

### D.1.2 Laplace prior with unknown scale $e^{2\theta}$

For the Bayesian neural network experiment we consider a Laplace prior with zero mean and unknown scale parameterised by  $e^{2\theta}$  (which ensures that the scale is positive), we have  $g_2(\theta, x) = 2d_x\alpha + \sum_i |x_i|e^{-2\alpha}$ . Its proximal operator is given by

$$\text{prox}_{g_2}^\lambda(\theta, x) = \arg \min_{(u_0, u)} h(u_0, u), \quad h(u_0, u) = 2u_0d_x + \sum_i |u_i|e^{-2u_0} + \|(u_0, u) - (\theta, x)\|^2/(2\lambda).$$

The optimality condition is given by

$$0 \in \partial(2u_0d_x + \sum_i |u_i|e^{-2u_0}) + \nabla(\|(u_0, u) - (\theta, x)\|^2/(2\lambda)),$$

which provides the following system of equations

$$\begin{aligned} 0 &= 2d_x - 2e^{-2u_0} \sum_{i=1}^{d_x} |u_i| + \frac{1}{\lambda}(u_0 - \theta), \\ \begin{cases} 0 \in \{e^{-2u_0}t_i + (u_i - x_i)/\lambda \mid |t_i| \leq 1\} & \text{if } u_i = 0, \\ 0 = e^{-2u_0} \text{sign}(u_i) + (u_i - x_i)/\lambda & \text{if } u_i \neq 0. \end{cases} \end{aligned}$$

Reordering terms, we get

$$u_0 = \theta - 2\lambda d_x + 2\lambda e^{-2u_0} \sum_i |u_i| \tag{53}$$

$$\begin{cases} u_i \in \{x_i - \lambda e^{-2u_0}t_i \mid |t_i| \leq 1\} & \text{if } u_i = 0, \\ u_i = x_i - \lambda e^{-2u_0} \text{sign}(u_i) & \text{if } u_i \neq 0. \end{cases} \tag{54}$$

This system of equations can be solved using an iterative solver, however this will incur in a high computational cost. Therefore, we opt for the following approximation of (54), where we set  $u_0 = \theta$ ,

$$\begin{cases} u_i \in \{x_i - \lambda e^{-2\theta}t_i \mid |t_i| \leq 1\} & \text{if } u_i = 0, \\ u_i = x_i - \lambda e^{-2\theta} \text{sign}(u_i) & \text{if } u_i \neq 0. \end{cases} \tag{55}$$

The solution of (55) is

$$u_i \approx [x_i - \lambda e^{-2\theta} \text{sign}(x_i)] \mathbb{1}\{|x_i| \geq \lambda e^{-2\theta}\}.$$

Using these  $u_i$ 's together with the Lambert  $W$  function, the solution of (53) is given by

$$u_0 \approx \theta - 2\lambda d_x + \frac{1}{2}W(4\lambda e^{-2\theta} \sum_i |u_i|).$$

### D.1.3 Uniform prior

We recall that using a uniform prior

$$g_2(\theta, x) = d_x \log(2\theta) + \sum_{i=1}^{d_x} \iota_{[-\theta, \theta]}(x_i),$$

where  $\iota_{\mathcal{K}}$  is the convex indicator of  $\mathcal{K}$  defined by  $\iota_{\mathcal{K}}(x) = 0$  if  $x \in \mathcal{K}$  and  $\iota_{\mathcal{K}}(x) = \infty$  otherwise. In this case, the proximal operator satisfies

$$\begin{aligned} \text{prox}_{g_2}^\lambda(\theta, x) &= \arg \min_{(u_0, u)} \{g_2(u_0, u) + \|(u_0, u) - (\theta, x)\|^2/(2\lambda)\} \\ &= \arg \min_{\substack{(u_0, u) \\ |u_i| \leq u_0}} \{d_x \log(2u_0) + \|(u_0, u) - (\theta, x)\|^2/(2\lambda)\}. \end{aligned}$$

We can obtain an approximate solution by deriving the first order conditions for  $u_i$  with  $i = 0, 1, \dots, d_x$  and combining them with the constraint  $|u_i| \leq u_0$ :

$$\begin{aligned} u_0 &= \begin{cases} \frac{\theta + \sqrt{\theta^2 - 4\lambda d_x}}{2} & \text{if } \theta^2 \geq 4\lambda d_x, \\ \max_i |x_i| & \text{otherwise,} \end{cases} \\ u_i &= \text{sign}(x_i) \cdot \min\{|x_i|, |u_0|\}. \end{aligned}$$

### D.1.4 Approximation for PIPULA and PPGD

In PIPULA and PPGD, we need to compute the proximal operator of  $U = g_1 + g_2$  which is usually not available in closed form. Since  $\gamma$  is normally set to a small enough value, we follow Pereyra [2016] and approximate the proximity map of  $U$  as

$$\begin{aligned}\text{prox}_U^\gamma(v) &= \arg \min_{v'} \{g_1(v') + g_2(v') + \|v' - v\|^2 / (2\gamma)\} \\ &\approx \arg \min_{v'} \{g_1(v) + (v' - v)^\top \nabla g_1(v) + g_2(v') + \|v' - v\|^2 / (2\gamma)\} \\ &\approx \arg \min_{v'} \{g_2(v') + \|v' - v + 2\gamma \nabla g_1^\top(v)\|^2 / (2\gamma)\} \\ &\approx \text{prox}_{g_2}^\gamma(v + 2\gamma \nabla g_1^\top(v)),\end{aligned}$$

where  $v = (\theta, x)$ ,  $v' = (\theta', x')$ .

## D.2 Bayesian logistic regression

**Dataset** We create a synthetic dataset by first fixing the value of  $\theta$  and sampling the latent variable  $x \in \mathbb{R}^{50}$  from the corresponding prior. We then sample the 900 observations from a Bernoulli distribution with parameter  $s(v_j^\top x)$ , where  $s$  is the logistic function and the entries of the covariates  $v_j$  are drawn from a uniform distribution  $\mathcal{U}(-1, 1)$ . The true value of  $\theta$  is set to  $\theta = -4$  for the Laplace prior and  $\theta = 1.5$  for the uniform one.

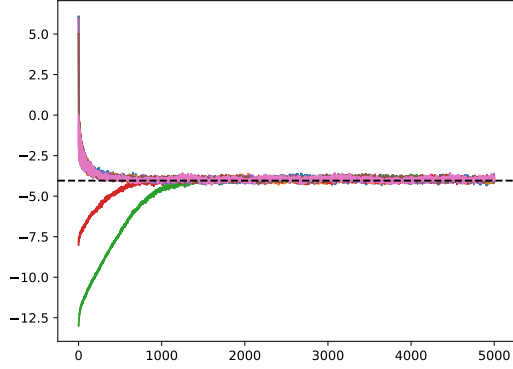
**Implementation details.** The  $x$ -gradients of  $g_1$  can be computed analytically. To choose the optimal values of  $\gamma$  and  $\lambda$  for the different implementations, we perform a grid search in the range  $[5 \times 10^{-4}, 0.5]$ . The selected optimal values are displayed in Table 7. We note that in PIPGLA the optimal values for  $\lambda, \gamma$  turn out to be when  $\lambda = \gamma$ .

Table 7: Optimal hyperparameters for Bayesian logistic regression example. Recall that for PPGD and PIPULA we only have the  $\gamma$  parameter since we set  $\lambda = \gamma$ .

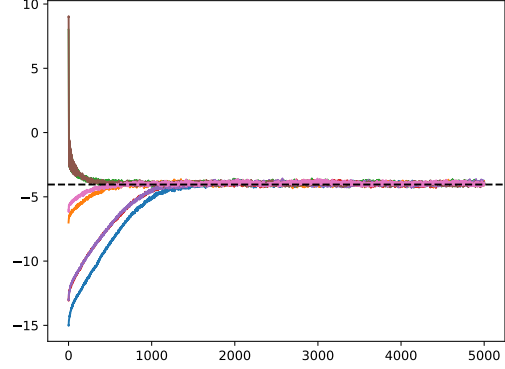
| Algorithm | Approx./Iterative | $\gamma$ |       | $\lambda$ |      |
|-----------|-------------------|----------|-------|-----------|------|
|           |                   | Laplace  | Unif  | Laplace   | Unif |
| PPGD      | Approx            | 0.1      | 0.03  | —         | —    |
|           | Iterative         | 0.06     | —     | —         | —    |
| PIPULA    | Approx            | 0.06     | 0.03  | —         | —    |
|           | Iterative         | 0.06     | —     | —         | —    |
| MYPGD     | Approx            | 0.05     | 0.001 | 0.25      | 0.01 |
|           | Iterative         | 0.05     | —     | 0.005     | —    |
| MYIPLA    | Approx            | 0.05     | 0.001 | 0.35      | 0.01 |
|           | Iterative         | 0.05     | —     | 0.005     | —    |
| PIPGLA    | Approx            | 0.01     | 0.02  | 0.01      | 0.02 |
|           | Iterative         | 0.01     | —     | 0.01      | —    |

**Results** Figure 3 shows the  $\theta$ -iterates obtained with MYIPLA and PIPGLA starting from 7 different initial values  $\theta_0$  and using the approximate solver for  $\text{prox}_{g_2}^\lambda$  with  $g_2(\theta, x) = \sum_{i=1}^{d_x} |x_i - \theta|$  and an iterative procedure using 40 iterations in each step. We observe that the iterative solver results in a slightly slower convergence to stationarity, but overall the two sets of algorithms converge to the same true value of  $\theta$ . We also observe that the convergence to stationarity for PIPGLA is much slower compared to MYIPLA. However, if we increase the value of  $\gamma$  in the hope of faster convergence, the iterates either do not converge to the true value or the standard deviation is significantly larger. For all algorithms considered, approximate solvers are 25% faster than iterative solvers (see Table 2).

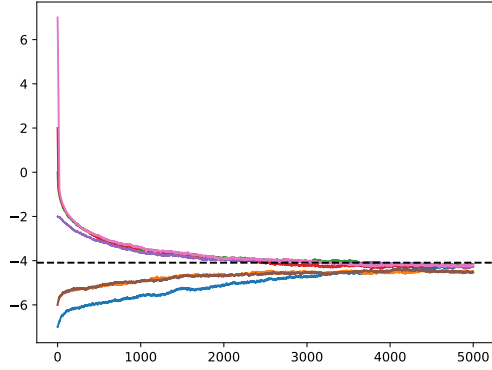
We also compare the results for the Uniform prior, in this case we only use the approximate proximity map (Figure 4).



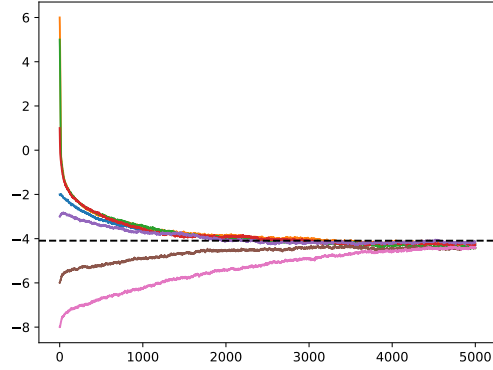
(a) MYIPLA, approximated  $\text{prox}_{g_2}^\lambda$ .



(b) MYIPLA, iterative solver for  $\text{prox}_{g_2}^\lambda$ .

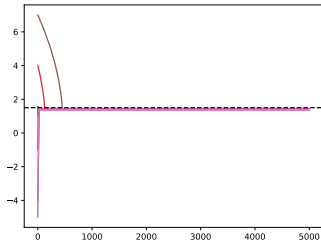


(c) PIPGLA ( $\lambda = \gamma$ ), approximated  $\text{prox}_{g_2}^\lambda$ .

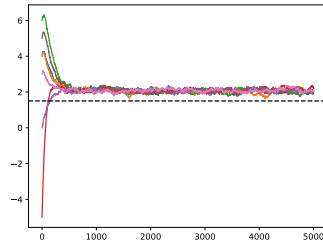


(d) PIPGLA ( $\lambda = \gamma$ ), iterative solver for  $\text{prox}_{g_2}^\lambda$ .

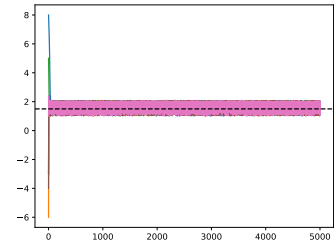
Figure 3: Bayesian logistic regression with isotropic Laplace priors on the regression weights  $\prod_i \text{Laplace}(x_i|\theta, 1)$ , with true  $\theta = -4$ . Each plot shows the  $\theta$ -iterates for 7 different starting points.



(a) MYPGD.



(b) MYIPLA.



(c) PIPGLA.

Figure 4: Bayesian logistic regression with isotropic uniform priors on the regression weights  $\prod_i \mathcal{U}(x_i|-\theta, \theta)$ , with true  $\theta = 1.5$ . The plot displays the  $\theta$ -iterates for 7 randomly chosen starting points.

Table 8: Bayesian logistic regression for Laplace and uniform priors. Normalised MSE (NMSE) for the last iterate of  $\theta$  (*last*) and the posterior mean after discarding a burn-in of 1500 samples (*avg*). Each different algorithm is run 500 times for different starting points using 50 particles and 5000. NMSEs are averaged over the 500 replicates. The second column indicates whether the proximal map is calculated approximately or iteratively, using 40 steps in each iteration. For the uniform prior case we have not implemented the iterative method.

| Algorithm | Approx/   | Laplace                           |                                   | Uniform                           |                                   |
|-----------|-----------|-----------------------------------|-----------------------------------|-----------------------------------|-----------------------------------|
|           | Iterative | NMSE last(%)                      | NMSE avg(%)                       | NMSE last(%)                      | NMSE avg(%)                       |
| PPGD      | Approx    | $14.70 \pm 4.42$                  | $16.73 \pm 0.83$                  | $3.63 \pm 4.93$                   | <b><math>0.11 \pm 0.04</math></b> |
|           | Iterative | $19.04 \pm 1.34$                  | $18.66 \pm 0.60$                  | —                                 | —                                 |
| PIPULA    | Approx    | $12.18 \pm 1.62$                  | $12.34 \pm 0.82$                  | $4.71 \pm 6.02$                   | $0.12 \pm 0.01$                   |
|           | Iterative | $19.22 \pm 1.28$                  | $18.63 \pm 0.79$                  | —                                 | —                                 |
| MYPGD     | Approx    | $6.09 \pm 0.34$                   | $4.94 \pm 0.51$                   | <b><math>0.60 \pm 0.23</math></b> | $0.60 \pm 0.02$                   |
|           | Iterative | $4.44 \pm 1.40$                   | $4.33 \pm 0.59$                   | —                                 | —                                 |
| MYIPLA    | Approx    | $4.42 \pm 1.32$                   | $4.31 \pm 0.67$                   | $15.26 \pm 4.44$                  | $16.01 \pm 2.01$                  |
|           | Iterative | $4.67 \pm 1.60$                   | $4.45 \pm 0.42$                   | —                                 | —                                 |
| PIPGLA    | Approx    | $2.30 \pm 0.58$                   | $2.45 \pm 0.94$                   | $6.83 \pm 3.97$                   | $4.22 \pm 0.07$                   |
|           | Iterative | <b><math>2.02 \pm 0.54</math></b> | <b><math>2.03 \pm 0.88</math></b> | —                                 | —                                 |

Since all the algorithms considered aim at estimating the parameter  $\theta$  by sampling from a distribution which concentrates around  $\theta^*$ , we compare the estimators of  $\theta^*$  obtained by using only the last iterate  $\theta_{K+1}^N$  and averaging over a number of iterates. We compare the normalised MSE (NMSE) for  $\theta$  for the estimator obtained by averaging the  $\theta$ -iterates after discarding a burn-in of 1500 samples (column named *avg*) against using the last  $\theta$  of the chain (column *last*). The results are in agreement, with the NMSE for the averaged estimator having lower variance in most settings (Table 8).

### D.3 Bayesian neural network

**Dataset.** We use the MNIST dataset. Features are normalised so that each pixel has mean zero and unit standard deviation across the dataset. We split the dataset into 80/20 training and testing sets.

**Proximal operator of  $g_2$ .** As  $g_2$  can be expressed as  $g_2(\theta, x) = g_2(\alpha, w) + g_2(\beta, v)$ , we can compute their proximal operators separately. It is sufficient to calculate the proximal operator for  $g_2(w, \alpha)$  since it is equivalent to that of  $g_2(v, \beta)$ . To do so, we have that

$$\text{prox}_{g_2}^\lambda(\alpha, w) = \arg \min_{(u_0, u)} h(u_0, u), \quad h(u_0, u) = 2u_0 d_w + \sum_i |u_i| e^{-2u_0} + \|(u_0, u) - (\alpha, w)\|^2 / (2\lambda),$$

whose approximate solution is calculated in Section D.1.2.

**Implementation details.** For the  $x$ -gradients of  $g_1$ , we use JAX’s grad function (implementing a version of autograd). Plugging the expressions above in the corresponding equations, we can implement the proposed algorithms. However, due to the high dimensionality of the latent variables, we stabilise the algorithm using the heuristics discussed in Section 2 of Kuntz et al. [2023]. This simply entails dividing the gradients and proximal mapping terms of the updates of  $\alpha$  and  $\beta$  by  $d_w$  and  $d_v$ . We then set  $\gamma = 0.05$  and  $\lambda = 0.5$  which ensures that the algorithms are not close to losing stability. In addition, the weights of the network are initialised according to the assumed prior. This is done by setting each weight to  $\pm a \log u$  where  $u \sim \mathcal{U}(0, 1)$ , the sign is chosen uniformly at random and  $a > 0$  is interpreted as the average initial size of the weights. Williams [1995] suggests setting  $a = 1/\sqrt{2m}$  for  $w$  and  $a = 1.6/\sqrt{2m}$  for  $v$ , where  $m$  is the fan-in of the destination unit.

**Predictive performance metrics.** To allow comparison, we use the same performance metrics as in Kuntz et al. [2023]. We include their presentation of this metrics for completeness.

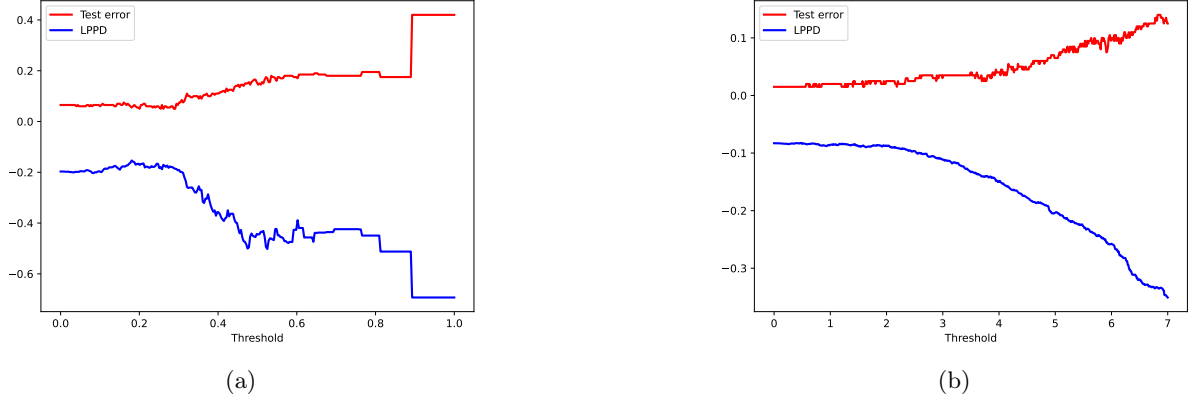


Figure 5: Evolution of the performance metrics when weights below a certain threshold are set to zero, when particles are averaged before (a) or after (b) computing the performance.

Given a new feature vector  $\hat{f}$ , the posterior predictive distribution for a label  $\hat{l}$  associated with the marginal likelihood maximiser  $\hat{\theta}_*$  is given by

$$p_{\hat{\theta}_*}(\hat{l}|\hat{f}, \mathcal{Y}_{\text{train}}) = \int p(\hat{l}|\hat{f}, x) p_{\hat{\theta}_*}(x|\mathcal{Y}_{\text{train}}) dx.$$

As  $p_{\hat{\theta}_*}(x|\mathcal{Y}_{\text{train}})$  is unknown, we approximate it with the empirical distribution of the final particle cloud  $q = N^{-1} \sum_{i=1}^N \delta_{X_K^i}$ , leading to

$$p_{\hat{\theta}_*}(\hat{l}|\hat{f}, \mathcal{Y}_{\text{train}}) \approx \int p(\hat{l}|\hat{f}, x) q(dx) = \frac{1}{N} \sum_{i=1}^N p(\hat{l}|\hat{f}, X_K^i) =: g(\hat{l}|\hat{f}).$$

The metrics considered to evaluate the approximation of the predictive power are the average classification error over the test set  $\mathcal{Y}_{\text{test}}$ , i.e.

$$\text{Error} := \frac{1}{|\mathcal{Y}_{\text{test}}|} \sum_{(f, l) \in \mathcal{Y}_{\text{test}}} \mathbf{1}\{l = \hat{l}(f)\}, \quad \text{where } \hat{l}(f) := \arg \max_i g(\hat{l}|\hat{f}),$$

and the log pointwise predictive density (LPD, Vehtari et al. [2017])

$$\text{LPD} := \frac{1}{|\mathcal{Y}_{\text{test}}|} \sum_{(f, l) \in \mathcal{Y}_{\text{test}}} \log(g(l|f)).$$

Under the assumption that data is drawn independently from  $p(dl, df)$ , we have the following approximation for large test data sets,

$$\begin{aligned} \text{LPD} &\approx \int \log(g(l|f)) p(dl, df) = \int \left[ \int \log\left(\frac{g(l|f)}{p(l|f)}\right) p(dl|df) \right] p(df) + \int \log(p(l|f)) p(df) \\ &= - \int \text{KL}(g(\cdot|f) \| p(\cdot|f)) p(df) + \int \log(p(l|f)) p(df). \end{aligned}$$

This means that the larger the LPD is, the smaller the mean KL divergence between our classifier  $g(l|f)$  and the optimal classifier  $p(l|f)$ .

**Results.** We have analysed the sparsity of the weights from the final particle cloud for MYIPLA. Figure 5 shows how the performance metrics evolve when weights below a certain threshold are set to zero, when particles are averaged before (5a) or after (5b) computing the performance.

Once we have set the weights of the matrix below a certain threshold to zero, it is necessary to explore the dead units. These are hidden units all of whose input or output weights are zero [Williams, 1995]. In both cases, the unit is redundant and it can be eliminated to obtain a functionally equivalent network architecture, we will call this new effective weight matrix  $w_{\text{pruned}}$ .

The occupancy ratio of a weight matrix  $w$  [Marinó et al., 2023] is defined as  $\psi = \text{size}(w_{\text{pruned}}) / \text{size}(w)$ , where size denotes the memory size. The inverse of  $\psi$  is the compression ratio. We compute the occupancy ratio of the

weight matrix for both the hidden and output layer for different values of the pruning threshold. We do this for each particle of the final cloud and obtain the average as well as for the averaged final particle cloud, results are shown in Figure 6.

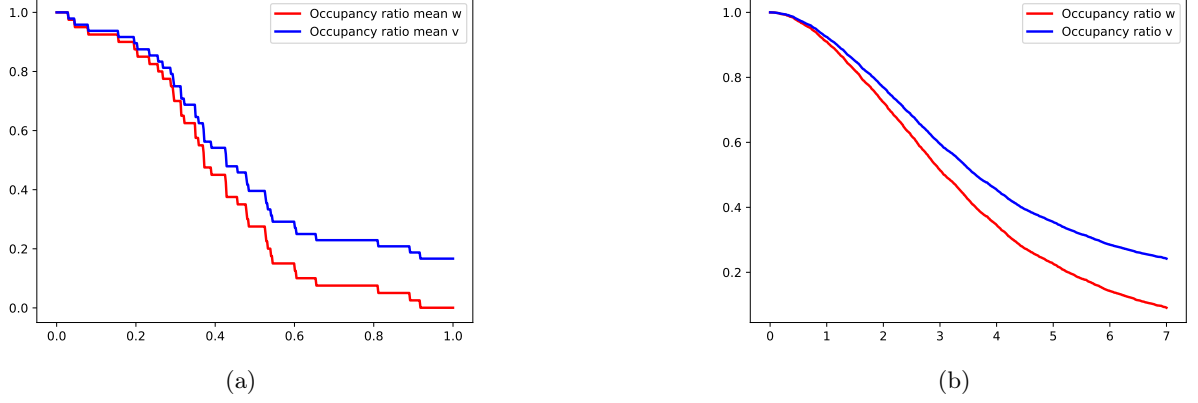


Figure 6: Occupancy ratio for the weights matrices of the hidden and output layers as a function of the pruning threshold, when particles are averaged before (a) or after (b) computing the occupancy ratio.

## D.4 Sparse matrix completion

### D.4.1 Example 1

**Dataset.** To obtain each of the matrices  $X^l$  we generate two integers  $a, b \in [-3, 3]$ , then

$$X_{i,j}^l = \begin{cases} a + b + \varepsilon & \text{if } i \bmod 2 = 0, j \bmod 2 = 0 \\ -a + b + \varepsilon & \text{if } i \bmod 2 = 1, j \bmod 2 = 0 \\ a - b + \varepsilon & \text{if } i \bmod 2 = 0, j \bmod 2 = 1 \\ -a - b + \varepsilon & \text{if } i \bmod 2 = 1, j \bmod 2 = 1 \end{cases}$$

where  $\varepsilon \sim N(0, 10^{-2})$ . Each entry from the resulting  $Y^l$  is observed with a probability of 0.5.

**Proximal operator of  $g_2$ .** Recall that  $g_2(\theta, \Phi, X)$  is of the form

$$g_2(\theta, \Phi, X) = -\log(C(\theta)) + e^{-\theta} \sum_l \|X^l\|_{\text{tr}}.$$

Due to the difficulty of calculating  $C(\theta)$  we assume that it is approximately constant  $C(\theta) \approx C$ . Thus, it is not necessary to take it into account when deriving the proximal operator.

To compute the proximal map, we first observe that if  $\theta, \Phi$  are known, then by Cai et al. [2010] (Theorem 2.1)

$$\text{prox}_{g_2}^\lambda(X^l) = \arg \min_Z \{e^{-\theta} \|Z\|_{\text{tr}} + \frac{1}{2\lambda} \|X^l - Z\|_F^2\} = S_{e^{-\theta}\lambda}(X^l) := U \Sigma_{e^{-\theta}\lambda} V^T,$$

where  $X = U \Sigma V^T$  is the SVD, and  $\Sigma_\beta$  is diagonal with entries  $(\Sigma_\beta)_{ii} = \max\{\Sigma_{ii} - \beta, 0\}$ . Based on this, we calculate

$$\text{prox}_{g_2}^\lambda(\theta, \Phi, X) = \arg \min_{(\alpha, \Gamma, Z)} \{e^{-\alpha} \sum_l \|Z^l\|_{\text{tr}} + \frac{1}{2\lambda} (\|\theta - \alpha\|^2 + \|\Phi - \Gamma\|_F^2 + \sum_k \|X^l - Z^l\|_F^2)\}.$$

The minimisers  $(\alpha, \Gamma, Z)$  satisfy the following system of equations

$$\Gamma = \Phi,$$

$$\alpha = \theta + \lambda e^{-\alpha} \sum_l \|S_{e^{-\alpha}\lambda}(X^l)\|_{\text{tr}} \implies (\alpha - \theta) e^{\alpha - \theta} = \lambda e^{-\theta} \sum_l \|S_{e^{-\alpha}\lambda}(X^l)\|_{\text{tr}}, \quad (56)$$

$$Z^l = S_{\lambda e^{-\alpha}}(X^l). \quad (57)$$

Solving this system is complicated due to the dependence between  $\alpha$  and  $Z$  and using an iterative solver can be computationally burdensome. Therefore, we have decided to approximate (56) by

$$(\alpha - \theta)e^{\alpha - \theta} \approx \lambda e^{-\theta} \sum_l \|S_{e^{-\theta}\lambda}(X^l)\|_{\text{tr}} \implies \alpha \approx \theta + W(\lambda e^{-\theta} \sum_l \|S_{e^{-\theta}\lambda}(X^l)\|_{\text{tr}}).$$

Substituting this value of  $\alpha$  into (57), we obtain

$$Z^l \approx S_{e^{-\alpha}\lambda}(X^l).$$

**Implementation.** To stabilise the implementation of MYIPLA, we have divided the gradients and proximal mapping term of the updates of  $\theta$  and  $\Phi$  by the dimension of the tensor  $(Y^1, \dots, Y^L)$ , that is,  $m \times n \times L$ . We then set  $\gamma = 0.05$  and  $\lambda = 0.35$ .

**Results.** The evolution of the relative error of the missing entries of the tensor  $(Y^1, \dots, Y^L)$  across steps is shown in Figure 7. Figure 8 displays the errors of the entries of  $Y^l$  for a randomly chosen  $l$  and a randomly chosen particle of the final cloud.

#### D.4.2 Example 2

**Dataset.** The entries of  $\Phi$  are obtained from a  $N(\theta, \sigma^2)$ , where  $\sigma = 0.25$  and  $\theta = 1.4$  for the experiment in the main text. The matrix  $X$  is generated in the same way as the  $X^l$  matrices in Example 1. Similarly, each entry of  $Y$  is observed with a probability 0.5.

**Proximal operator of  $g_2$ .** Recall that  $g_2(\xi, \theta, X, \Phi)$  is of the form

$$g_2(\xi, \theta, X, \Phi) = -\log(C(\xi)) + e^{-\xi} \|X\|_{\text{tr}}.$$

As in Example 1, due to the difficulty of calculating  $C(\xi)$  we assume that it is approximately constant  $C(\xi) \approx C$ . Therefore, it is not necessary to take it into account when deriving the proximal operator, which is given by

$$\text{prox}_{g_2}^\lambda(\xi, \theta, X, \Phi) = \arg \min_{(\alpha, \delta, Z, \Gamma)} \{e^{-\alpha} \|Z\|_{\text{tr}} + \frac{1}{2\lambda} (\|\xi - \alpha\|^2 + \|\theta - \delta\|^2 + \|X - Z\|_F^2 + \|\Phi - \Gamma\|_F^2)\}.$$

The minimisers  $(\alpha, \delta, Z, \Gamma)$  satisfy the following system of equations

$$\begin{aligned} \delta &= \theta, \quad \Gamma = \Phi, \\ \alpha &= \xi + \lambda e^{-\alpha} \|S_{e^{-\alpha}\lambda}(X)\|_{\text{tr}} \implies (\alpha - \xi)e^{\alpha - \xi} = \lambda e^{-\xi} \|S_{e^{-\alpha}\lambda}(X)\|_{\text{tr}}, \end{aligned} \tag{58}$$

$$Z = S_{e^{-\alpha}\lambda}(X). \tag{59}$$

To avoid the computational cost of solving (58)-(59) using an iterative solver, we approximate (58) by

$$(\alpha - \xi)e^{\alpha - \xi} \approx \lambda e^{-\xi} \|S_{e^{-\xi}\lambda}(X)\|_{\text{tr}} \implies \alpha \approx \xi + W(\lambda e^{-\xi} \|S_{e^{-\xi}\lambda}(X)\|_{\text{tr}}).$$

Substituting this  $\alpha$  in (59), we obtain

$$Z \approx S_{e^{-\alpha}\lambda}(X).$$

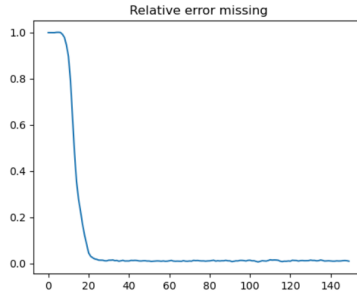


Figure 7: Relative error of the missing entries of the tensor  $(Y^1, \dots, Y^L)$  across steps.



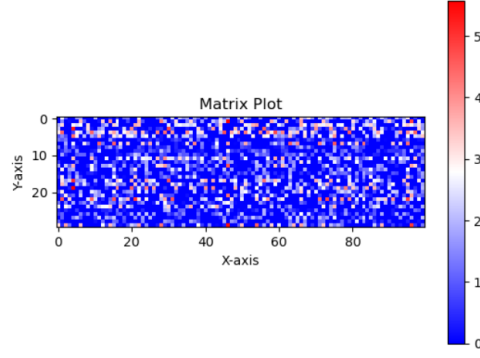


Figure 8: Errors of the entries of  $Y^l$  for a randomly chosen  $l$  and a randomly chosen particle of the final cloud.

**Implementation.** To stabilise the implementation of MYIPLA, we have divided the gradients and proximal mapping term of the updates of  $\xi$  and  $\theta$  by the dimension of the tensor  $X$  ( $d_x = r \times n$ ) and  $\Phi$  ( $d_\Phi = m \times r$ ), respectively. We then set  $\gamma = 0.05$  and  $\lambda = 0.35$ .

**Results.** The relative error of the missing entries of the matrix  $Y$  and the average relative error of the particle cloud  $\Phi_l^1, \dots, \Phi_l^N$  are plotted across steps in Figure 9.

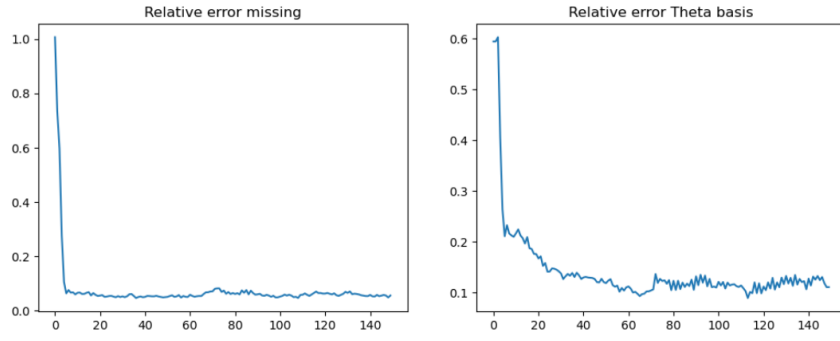


Figure 9: Performance measures across steps.